



MINIMALLY INVASIVE SURGERY AND INTERVENTIONAL TECHNIQUES  
DEPARTMENT OF BIOMECHANICAL ENGINEERING  
DELFT UNIVERSITY OF TECHNOLOGY

# A STEERABLE STYLET FOR THE TRANSJUGULAR INTRAHEPATIC PORTOSYSTEMIC SHUNT PROCEDURE



D.P. VAN DUIJN [#4003616]

Supervisor:  
Dr.ir. N.J. van de Berg [TU Delft]

Committee:  
Dr. J.J. van den Dobbelen [TU Delft]  
Dr.ir. N.J. van de Berg [TU Delft]  
Dr.ir. I. Apachitei [TU Delft]

MARCH 16, 2019



## Preface

This thesis is about a new design for a stylet used in the Transjugular Intrahepatic Portosystemic Shunt (TIPS) procedure. In comparison to the original used stylet, this design is able to steer in one plane. This ability facilitates the TIPS procedure, with as goal to reduce the complexity of the intrahepatic puncture between the portal vein and hepatic vein.

This thesis is written as graduation project of the Master BioMechanical Engineering at Delft University of Technology, where I followed the track BioMechanical Design with the specialization BioInspired Technology.

The interest for medical instruments was raised at the end of my Bachelors after several knee operations due to injuries which were performed minimally invasive. After an internship at DEAM B.V., a company in Amsterdam which is specialized in medical steerable instruments, I was convinced the subject for my graduation project had to do with designing or improving medical instruments.

I did this project with great pleasure and am glad that I was able to make a prototype of a new steerable instrument. The design of the prototype was motivated by a steerable ablation needle. With some adjustments and improvements in the design, the steering mechanism was useful for the TIPS stylet. I hope this design will be further investigated so it become useful for the TIPS procedures, or will contribute in improvements of multiple other medical instruments.

I got the opportunity to do this graduation project thanks to my supervisor Nick J. van de Berg. He came up with this topic and together we searched for the right research question. Beside this, Nick supported me from begin to end with meetings every two weeks, help or information when needed and put me in touch with interventional radiologists.

Finally, I want to thank my parents and girlfriend in particular. In some periods the project did not go smoothly, design errors occur or results were disappointing wherefore my motivation disappeared quickly. I have managed to bring this project to a successful end through their confidence and motivating conversations.

The committee members for my graduation were:

Dr. J.J. van den Dobbelen [TU Delft]

Dr.ir. N.J. van de Berg [TU Delft]

Dr.ir. I. Apachitei [TU Delft]

Enjoy reading this graduation project.

Daan van Duijn  
#4003616

Delft, The Netherlands  
March 16, 2019

## Abstract

In recent years, more and more medical operations are done minimally invasive. Intervention radiology is a medical specialty which uses minimally invasive techniques to diagnose, or treat diseases. Instruments like needles and catheters are used by radiologists to enter the network of veins and arteries guided by image modalities. A complex treatment in the interventional radiology is the Transjugular Intrahepatic Portosystemic Shunt (TIPS) procedure. This treatment is developed for people who suffer from liver cirrhosis which are not eligible for liver transplantation. The problem which arise with a liver affected by cirrhosis is that it can not transmit enough blood. Without transplantation or a treatment this will eventually lead to death. During the TIPS procedure a connection is made between the right hepatic and the portal vein by a shunt. As a result, blood pressure reduction in the portal system since the blood can flow back to the right atrium of the heart, bypassing the liver.

The hardest part in a TIPS procedure is the intrahepatic puncture between the hepatic and portal vein. The interventional radiologist tries to enter the portal vein by puncturing a small stylet from the hepatic vein through the liver tissue. Due to cirrhosis the liver tissue is very stiff and stylet deflection will occur. To reduce the uncertainty of entering the portal vein, this thesis is focused on designing a stylet that is more stiff and able to steer. It is expected that the complexity of the procedure will be reduced and a higher hit rate to enter the portal vein will be achieved.

The prototype of the steerable stylet has been evaluated through various experiments, a visibility test and with procedures in a test liver model. During these experiments the steering characteristics, the stiffness of the stylet, the maximum lateral forces exerted by the tip while steering, the influence of the stylet orientation and the visibility are obtained. Afterwards, an evaluation was done in a liver model, made of PVA, to determine whether the stylet is capable to reduce the complexity of the intrahepatic puncture step in the TIPS procedure.

With the prototype made in this graduation project, based on a steerable ablation needle, the complexity of the TIPS procedure is not reduced yet. The steerable stylet was not able to enter the portal vein. It was already hard to enter the right hepatic vein since the pre-bent stiffening cannula was adapted with a smaller angle which was necessary since the steerable stylet was too stiff to push through the pre-bent angle. According to this prototype, possibilities are shown to use a mechanical steering mechanism in instruments with a long thin shaft. The transmission in combination with the joint mechanisms fits within 1.3mm diameter, was able to bridge 60cm from distal end to proximal end and had only 4 components, the stylet, the rigid cannula, the key to fix the stylet to the rigid cannula and the transmission. By translating the stylet in a push or pull direction relative to the rigid cannula, steering angles could be achieved. With further research and development this steering mechanism must be able to steer the required amount of degrees without any extra components, is well visible with ultrasound, and is good resistant against lateral forces.

# Contents

<b>Abstract</b>	<b>ii</b>
<b>List of Abbreviations</b>	<b>v</b>
<b>List of Definitions</b>	<b>v</b>
<b>1 Clinical Introduction</b>	<b>1</b>
1.1 Interventional Radiology . . . . .	1
1.2 Liver Function . . . . .	1
1.2.1 Veins in and around the Liver . . . . .	2
1.3 Material to Mimic Liver Tissue . . . . .	3
1.3.1 Water-Based Phantoms . . . . .	3
1.3.2 Oil-Based Phantoms . . . . .	3
1.4 Liver Cirrhosis . . . . .	4
1.4.1 Cause . . . . .	4
1.4.2 Diagnosis . . . . .	4
1.4.3 Treatment . . . . .	5
1.4.4 Complications . . . . .	7
1.4.5 Clinical Outcome . . . . .	7
1.5 Problem Statement . . . . .	8
1.6 Research Question . . . . .	8
1.7 Objective and Approach . . . . .	8
1.8 Thesis Outline . . . . .	9
<b>2 Steerable Instruments</b>	<b>10</b>
2.1 Technical Introduction . . . . .	10
2.1.1 Joint Mechanisms . . . . .	10
2.1.2 Steering Technique . . . . .	12
2.1.3 Stylet Materials . . . . .	13
2.1.4 Actuator Mechanisms . . . . .	14
2.1.5 Transmission . . . . .	14
2.1.6 Visibility of the Tip . . . . .	15
2.2 Design Criteria . . . . .	15
2.2.1 Mechanical Requirements . . . . .	15
2.2.2 Medical Requirements . . . . .	18
2.2.3 Conclusion . . . . .	19
<b>3 Concept and Prototyping</b>	<b>20</b>
3.1 Concept Generation . . . . .	20
3.1.1 Joint Mechanism . . . . .	21
3.1.2 Transmission . . . . .	21
3.1.3 Actuator . . . . .	24
3.1.4 Handle . . . . .	24
3.1.5 Additional Requirements . . . . .	24
3.1.6 Final Concept . . . . .	25
3.2 Prototyping . . . . .	26
3.2.1 Manufacturing . . . . .	26
3.2.2 Prototype . . . . .	26
<b>4 Evaluation</b>	<b>27</b>
4.1 Mechanical Characteristics . . . . .	27
4.1.1 Methods . . . . .	28
4.1.2 Results . . . . .	30
4.1.3 Discussion . . . . .	30
4.1.4 Conclusion . . . . .	32
4.2 Visibility in Ultrasound . . . . .	33

4.2.1	Methods . . . . .	33
4.2.2	Results . . . . .	34
4.2.3	Discussion . . . . .	35
4.2.4	Conclusion . . . . .	35
4.3	Liver Model . . . . .	36
4.3.1	Evaluation Method . . . . .	36
4.3.2	Results . . . . .	37
4.3.3	Discussion . . . . .	37
4.3.4	Conclusion . . . . .	38
<b>5</b>	<b>Discussion</b>	<b>39</b>
5.1	The TIPS Stylet . . . . .	39
5.2	Experiments . . . . .	39
5.3	Visibility . . . . .	40
5.4	Liver Model . . . . .	40
5.5	Recommendations . . . . .	41
<b>6</b>	<b>Conclusion</b>	<b>42</b>
6.1	Liver Model . . . . .	42
6.2	The TIPS Stylet . . . . .	42
	<b>References</b>	<b>42</b>
	<b>Appendices</b>	<b>46</b>
<b>A</b>	<b>TIPS: The Procedure Step-by-Step</b>	<b>48</b>
<b>B</b>	<b>How to: Assembling the TIPS Stylet</b>	<b>50</b>
<b>C</b>	<b>How to: Remove Stylet from Rigid Cannula</b>	<b>52</b>
<b>D</b>	<b>Test Model for the TIPS Procedure</b>	<b>53</b>
<b>E</b>	<b>Experimental Setup</b>	
	Measuring Steering Angles, Joint Stiffness and Maximum Transverse Forces	59
<b>F</b>	<b>Data from Experiments</b>	<b>67</b>

## List of Abbreviations

<b>IR:</b>	Interventional Radiologist
<b>TIPS:</b>	Transjugular Intrahepatic Portosystemic Shunt
<b>PSPG:</b>	Portosystemic Pressure Gradient
<b>HV:</b>	Hepatic Vein
<b>RHV:</b>	Right Hepatic Vein
<b>PV:</b>	Portal Vein
<b>RPV:</b>	Right Portal Vein
<b>DoF:</b>	Degrees of Freedom
<b>RoM:</b>	Range of Motion
<b>PVA:</b>	Poly Vinyl Alcohol
<b>HE:</b>	Hepatic Encephalopathy
<b>RUPS:</b>	Rösch-Uchida Transjugular Liver Access Set
<b>ESLD:</b>	End Stage Liver Disease
<b>CAD:</b>	Computer Aided Design

## List of Definitions

<b>Dorsal:</b>	Dorsal movements refers to movements in the direction to the back of the human body.
<b>Ventral:</b>	Ventral movements refers to movements in the direction to the front of the human body.
<b>Posterior:</b>	Posterior refers to what is to the back of the subject.
<b>Anterior:</b>	Anterior refers to what is in front of the subject.
<b>Superior:</b>	Superior refers to what is above the subject.
<b>Inferior:</b>	Inferior refers to what is below the subject.
<b>Sagittal:</b>	The sagittal plane is a vertical plane that divides the body in a right and left part.
<b>Coronal:</b>	The coronal plane is a vertical plane that divides the body into a ventral and dorsal part.
<b>Distal End:</b>	In an anatomical way the term distal is used to describe a part that is distant from the main mass of the body. In a needle it refers to the tip, the part what is the most distant from the surgeon/radiologist.
<b>Proximal End:</b>	In an anatomical way the term proximal is used to describe a part that is close by the main mass of the body. In a needle it refers to the handle, the part what is close by the surgeon/radiologist.

*”If it is not working after 5 minutes of trying,  
either change the catheter or change the hands.”*

*—Dr. Josef Rösch—*



# 1 | Clinical Introduction

These days, minimally invasive surgery is becoming increasingly popular among surgeons and radiologists. A reason for this is due to the fact that only a few small incisions and trocars are needed to do surgeries or diagnoses. Compared to traditional open surgery, minimally invasive surgery reduces recovery time, risk of infections, pain for the patient, hospital stay, physical trauma, damage to the surrounding muscles and blood loss [1, 2, 3].

## 1.1 | Interventional Radiology

The department of interventional radiology uses minimally invasive, image guided procedures to diagnose and treat diseases of nearly every organic system [4]. Compared to minimally invasive surgery, where the size of instruments and incisions lies between 5 - 12 mm [5], the incisions and instruments in interventional radiology are even smaller. The biggest diameter in this thesis, according to the Transjugular Intrahepatic Portosystemic Shunt (TIPS) procedure, comes from a 9Fr introducer sheath (3mm) [6].

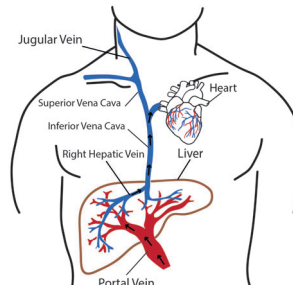
For using the network of veins and arteries, small incisions in the skin are needed to enter existing paths, e.g. veins. The interventional radiologist (IR) is able to approach almost every organ with instruments through this network. Due to this, such procedures are less invasive and complicated compared to minimally invasive surgeries, where instruments are inserted through anatomical openings or through the skin into the body cavity to reach the desired location [7].

Visualization during interventional procedures is done by: ultrasound, X-ray fluoroscopy, magnetic resonance imaging (MRI), computed tomography (CT) scans or a combination. With these imaging methods, the IR is able to guide instruments precisely to the diseased organ or desired area while observing the monitors to validate the position and orientation of the instrument.

One of the most complex procedures within interventional radiology is the TIPS procedure. Normally, blood from the stomach, spleen, intestines, pancreas and gallbladder (gastrointestinal tract) come together into the portal system, where the blood drains through the portal vein (PV) into the liver. The liver processes this blood, nutrients will be stored and the blood is detoxified before it returns into the systemic blood circulation.

Due to liver cirrhosis, the liver is not able to process the blood from the gastrointestinal tract quick enough. This results into high blood pres-

sure inside the portal system, also known as portal hypertension. Portal hypertension can be treated with a liver transplantation or with the TIPS procedure. In Figure 1.1 relevant veins for the TIPS procedure are shown.



**Figure 1.1:** The human anatomy with relevant veins for the TIPS procedure. The procedure path exist of: the jugular vein, superior vena cava, inferior vena cava, the right hepatic vein and the portal vein. The arrows indicates the normal blood flow for a healthy liver.

## 1.2 | Liver Function

In the blood circulation, the liver functions as a transition station between the digestive tract and the large circulation. The digestive tract consists of the gastrointestinal tract and the accessory organs of digestion. Because of its location, the liver fulfills a metabolic function with respect to the food components derived from the environment, processed in the gastrointestinal tract.

Besides its function as a transition station, other important tasks for the liver are absorbing usable components from the blood and eliminating useless and potentially harmful components [8]. In addition, the liver regulates the supply of glucose and lipids that the body uses as fuel. A healthy liver is therefore able to fight infections and blood clotting. Besides this, the liver is able to make digestive juices, provides energy for the body and processes medicines, food and alcohol.

Normally, blood from the gastrointestinal tract flows from the intestines through the PV into the liver. As the PV passes through the liver, it breaks up into increasingly smaller branches. The tiniest branches are called sinusoids because of their structure. Those branches are in close contact with the liver cells, which allows them to remove and add substances to the blood. The blood is detoxified and nutrients will be stored after which the blood is collected in increasingly larger branches. These branches eventually come together into the hepatic vein (HV). This HV returns the blood to the right atrium of the heart, where the blood can be used again in the systemic circulation.

### 1.2.1 | Veins in and around the Liver

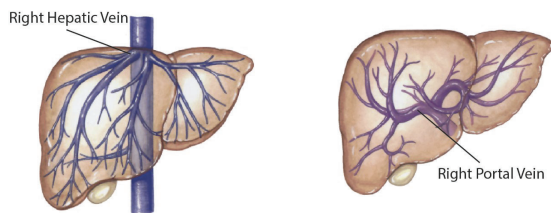
This section will discuss the veins and their function in and around the liver which are important for the TIPS procedure. The branches of the HV and the PV are already explained, where they ensure that the blood flows through the liver. For the TIPS procedure the following veins are also of interest: the jugular vein, superior vena cava and inferior vena cava.

#### Hepatic Vein

The left, middle and right HV can be distinguished. The right hepatic vein (RHV) leads to the inferior vena cava independently, where the middle and left HV form a common trunk before it leads into the inferior vena cava. The TIPS procedure is usually performed through the RHV because it leads directly from the inferior vena cava. Besides this, it is the largest of the three hepatic veins, with a diameter of approximate 1cm [9]. Figure 1.2a represents a schematic overview of the HV in the liver where the RHV is mentioned.

#### Portal Vein

The other important vein in the liver is the PV, which is approximately 0.8 to 1 cm wide [10]. The vein is a connection between the gastrointestinal tract and the liver. Within the liver, the PV splits first into a right and left vein before it splits into smaller branches to supply the right and left lobes of the liver [10]. Figure 1.2b represents a schematic overview of the PV where the right portal vein (RPV) is denoted.



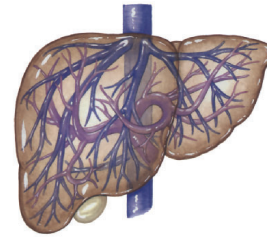
(a) The HV splits in the right, middle and left vein inside the liver.

(b) The PV splits in the right and left vein when it is inside the liver.

**Figure 1.2:** Schematic overview of the HV and PV and its branches in the liver. Reprinted from Jeanne LaBerge [10].

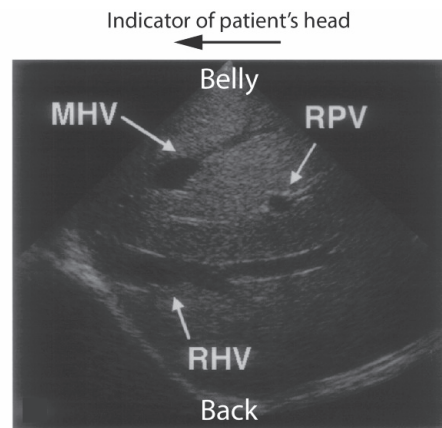
#### Portal and Hepatic Veins

The branches of the hepatic and portal veins are entangled inside the liver, which is represented by Figure 1.3. The intrahepatic puncture during the TIPS procedure is preferably performed from the RHV to the RPV because these veins have both a bigger diameter than the others, and maintains most consistent their positions [10].



**Figure 1.3:** Schematic overview of the HV and PV and their branches entangled. Reprinted from Jeanne LaBerge [10].

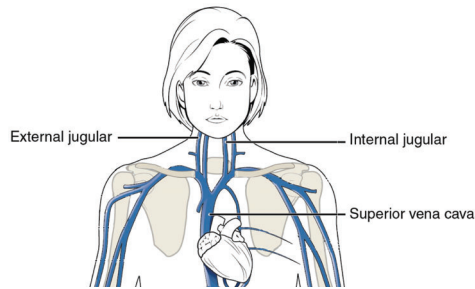
The anatomic basis for performing the TIPS procedure is the assumption that the RHV is located superior and posterior to the PV bifurcation [11]. Going further into the RHV it receives branches anteriorly and posteriorly. The point where the RHV is as close as possible to the PV, is a few centimeters dorsal to the bifurcation of the PV. The positions of the RHV to the RPV are well illustrated on a sagittal sonography in Figure 1.4. When puncturing from the RHV to the RPV, the stylet should be directed ventrally [10].



**Figure 1.4:** A sagittal ultrasound image of the middle hepatic vein, RHV and PV. This section view shows that the RHV is dorsal to the RPV. Reprinted from Jeanne LaBerge [10].

#### Jugular Vein

The jugular vein is the largest vein in the neck [12]. Both sides of the neck contains an internal and external jugular vein. These veins drain blood from the brain, face and neck, back to the heart via the superior vena cava. The left internal vein is generally smaller than the right internal jugular vein [12]. Figure 1.5 represents an overview of the jugular veins and the superior vena cava. The right internal jugular vein is bigger than the left internal jugular vein, easier to find, and is in one line with the superior and inferior vena cava towards the liver wherefore it is used for the TIPS procedure.



**Figure 1.5:** A schematic overview of the jugular veins and the superior vena cava.

### Superior and Inferior Vena Cava

The inferior vena cava is the largest vein in the body, directly connected to the superior vena cava, which is the second largest. These veins collect the deoxygenated blood from veins serving the tissue. The superior vena cava drains blood from the veins in the upper body (above the heart), where the inferior vena cava drains blood inferior to the heart. Both veins return the blood to the right atrium of the heart [13]. The diameter of the veins vary between 0,46 and 2,26 cm [9]. Due to the low pressure exerted by venous blood the walls are very thin.

The superior and inferior vena cava connects the jugular vein to the HV in the liver, during a TIPS procedure the instruments go through the following veins to enter the liver: internal jugular vein, superior vena cava, inferior vena cava and HV.

## 1.3 | Material to Mimic Liver Tissue

For a wide range of materials, research is done to mimic human tissue. Researchers studied whether materials have the same textural and/or imaging properties as real tissue. During the TIPS procedure, ultrasound and CT are important imaging modalities. A method for finding a good material to mimic the tissue is elastography. Elastography is an imaging modality for soft tissue that maps elastic properties and stiffness. Typical tissue options, with elastographic properties similar to liver tissue, are water-based and oil-based phantoms.

### 1.3.1 | Water-Based Phantoms

Since water is the main component of living soft tissue, water-based materials are usually good choices for the fabrication of tissue mimicking phantoms [14]. In these phantoms, water is the solvent and can be mixed either with a natural polymer (e.g. gelatin) or a synthetic polymer (e.g. poly vinyl alcohol). By adding very small particles to the mixture, scatterers, it increases scatter for ultrasound imaging and becomes better visible.

Gelatin gels can provide a wide range of tissue stiffness. Since the composition of these gels can be changed independently, it is easy to control the gel its stiffness, sound speed, absorption, and scattering [15]. This gives the opportunity to make samples with different characteristics.

Another water-based material is Poly Vinyl Alcohol (PVA). PVA is a synthetic polymer with comparable ultrasound imaging properties to real tissue [16]. The composition of the material is made of PVA grains mixed in water. After it is mixed, a freeze-thaw process takes place. The ratio of the mixture and the amount of freeze-thaw cycles will affect the stiffness of the material.

A third water-based gel is Polyacrylamide. Datla et al.[17] did a research to polyacrylamide gel to mimic both mechanical properties as thermal damage. Since more steerable needles are developed with nitinol, which will shrink or stretch when heated, it is important that thermal damage in tissue will be tested. As a conclusion of Datla et al. [17] polyacrylamide gel can be made with different elastic modulus where it is possible to meet the mechanical properties of real tissue. Also the heating damage of heated nitinol falls within the range of real tissue, tested for the prostate.

### 1.3.2 | Oil-Based Phantoms

Mimicking soft human tissue can also be done with oil-in-gelatin dispersions [18]. An advantage of oil-in-gelatin mixtures is that the dielectric properties can be changed simply by varying the volume per cent of oil.

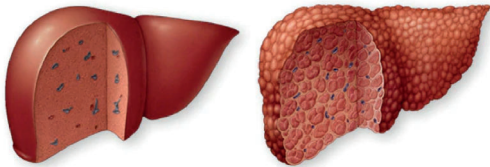
Nowadays, polysaccharides are often used as soft tissue mimicking material with same electromagnetic properties. Unfortunately, this material is difficult to handle (they must be in airtight containers or need special holders), is non-durable (parameters change over time) and is mechanically sensitive [19]. Zivkovic et al.[19] made a new composite material containing calcium alginate microspheres incorporated into an epoxy matrix, which overcome the restricting factors. This new composite material is a good alternative for the polysaccharides sample.

Paraffin-gel waxes are new oil-based materials for mimicking human tissue. Vieira et al.[20] studied these waxes and are investigated as new soft tissue mimicking materials for ultrasound guided breast biopsy training [20]. As result, the sample meets values for the speed of sound (acoustic

properties), attenuation and young's modulus (mechanical properties) compared to real soft tissue.

### 1.4 | Liver Cirrhosis

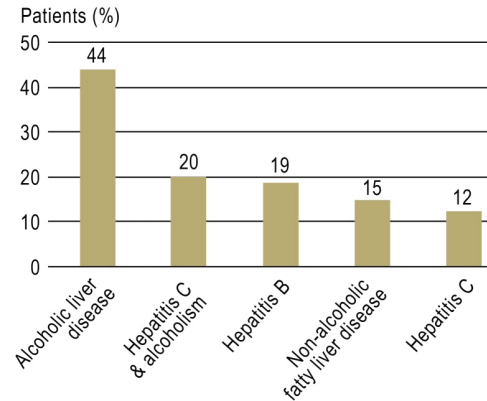
A liver which is not working optimally, is not able to process all the blood from the gastrointestinal tract. This may result into an increased blood pressure in the PV. Due to the high blood pressure, fluid builds up in the abdomen, which causes pressure pain around the liver and massive bleeding. This phenomenon is called portal hypertension. Portal hypertension is a consequence of a scarred liver, also known as liver cirrhosis. Cirrhosis is a complication of liver fibrosis, a disease that involves loss of liver cells and irreversible scarring of the liver. In cirrhosis, the connection between blood and the branches of the PV are destroyed. Even though the newly formed or surviving liver cells may still be able to process and remove components from the blood, they do not have the normal, intimate connection with the blood. Besides this, the scarring within the cirrhotic liver obstructs the normal blood flow through the liver and to its liver cells [21]. A liver with cirrhosis develops scar tissue inside and around the liver. Figure 1.6 shows the difference between a healthy liver and a liver with cirrhosis.



**Figure 1.6:** At the left a healthy liver with normal tissue. At the right a liver with cirrhosis, where scar tissue will replace the normal liver tissue. Reprinted from [www.mayoclinic.org](http://www.mayoclinic.org) [22].

#### 1.4.1 | Cause

Among the many liver disorders that can lead to cirrhosis, some progress rapidly (years) and others more slowly (decades). Cirrhosis is often a consequence of fatty liver disease due to alcoholism, hepatitis B, hepatitis C or by nonalcoholic fat accumulating in the liver [8]. Cirrhosis is more common by persons with overweight or smokers [23]. Figure 1.7 represents the percentages of newly diagnosed liver diseases caused by alcohol abuse, hepatitis B or hepatitis C. These values are from a private clinic in the USA, measured in 2008.



**Figure 1.7:** Percentages of liver cirrhosis by newly diagnosed liver diseases. Values from a private clinic in the USA (2008). Reprinted from Wiegand et al. [23].

#### 1.4.2 | Diagnosis

The development of liver cirrhosis occurs in four different stages as shown in Table 1.1. Due to the large reserve capacity of the liver, liver diseases often only cause problems if it has advanced to stage 3 or 4. By then it is already too late for a treatment. Unfortunately, in the first two stages it is hard to determine whether there is an onset of liver cirrhosis. The healthy part of the liver works hard and is often able to completely substitute its diseased counterpart, patients will not have any complaints.

**Table 1.1:** The four stages of liver disease

Stage	Liver disease
1	Inflammation
2	Fibrosis
3	Cirrhosis
4	End stage liver disease (ESLD)

In **stage 1**, inflammation of the liver can cause abdominal pains as the body tries to fight the infection or irritation. This first stage can be caused by excessive alcohol consumption, hepatitis B, hepatitis C or nonalcoholic fatty liver disease, as mentioned in chapter 1.4.1. Alcohol abuse is the toughest one, since it directly injures the cells in the liver.

If this inflammation is not treated, it can lead to liver damage and permanent scarring. The liver comes into **stage 2**, also known as fibrosis. At this stage, liver cells attempt to repair themselves, but may result in scar tissue [24]. This scarring begins to block the normal blood flow inside the liver. Until here, it is still possible to treat the liver in order to establish full recovery.

Untreated liver fibrosis may lead to a permanently damaged liver. At this moment, the disease has advanced into **stage 3**. The liver gets stuck in a continuous cycle in which it tries to repair the damaged liver cells, which causes the scar tissue to be more significant. This advanced fibrosis leads to cirrhosis. The scar tissue is developed in such an advanced stage that it cannot be cured. Treatments include liver transplantation, delaying or preventing the progression of further scarring. Because of the scar tissue inside the liver, it is not able to perform its tasks properly. Portal hypertension will be diagnosed. The blood flow from the gastrointestinal tract will not be processed quick enough. The blood in the PV will build up, the body responds by making new veins, named collateral vessels, to ensure that the blood flows from the gastrointestinal tract back to the heart, bypass the liver. Failing of the collateral vessels due to increased blood pressure in the PV, can lead to internal bleedings (variceal bleeding). Besides this, it can also cause an abnormal amount of fluid in the abdomen [25]. From this stage, the fluid build up in the abdomen is visible and pressure pain around the liver can be felt.

People with cirrhosis who have signs of the previous complications may develop end-stage liver disease (ESLD), **stage 4**. In this last stage, multiple symptoms arise. Besides the fluid build up in the abdomen, the legs of the patient may swell. In addition, yellow discoloration of the skin and eyes can be detected, bruises are quickly visible, the skin is itchy and will bleed easily, the patient will feel nauseous and has no appetite. The best treatment at this stage is liver transplantation [21]. If this is not possible an alternative treatment is the TIPS procedure.

### 1.4.3 | Treatment

Waiting lists for liver transplantation are often extensive. Even if a liver is available, there is always the risk that the transplanted liver will not be accepted by the body. The alternative treatment for ESLD is the TIPS procedure.

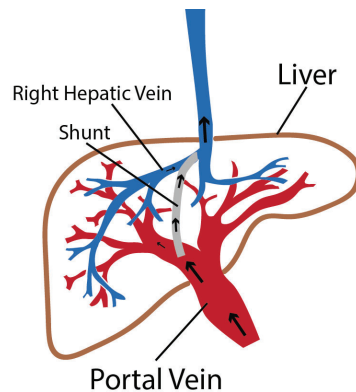
The concept of the TIPS procedure was developed in the late 1960s and resulted from inadvertent access to intrahepatic portal venous branches during transjugular cholangiography [26]. In this operation, a shunt was placed between the HV and PV for a brief duration. However, surgeons concluded that other material may enable the shunt to stay for a longer period. In the mid 1980s, metallic expandable shunts were introduced. This improvement allowed surgeons, when performing

the TIPS procedure, to insert shunts that would hold for a longer time period. Since the late 1990s the TIPS procedure has become well accepted as a minimally invasive treatment for complications of portal hypertension [26] (liver cirrhosis).

The TIPS procedure is performed by an IR in order to decompress the high blood pressure in the portal system of the liver, caused by cirrhosis. Since curative therapy for ESLD is liver transplantation, management of the disease becomes very important, particularly if a patient is on an active waiting list [27]. The blood pressure in the portal system is decompressed by making a connection between the RHV and the RPV with a stilet. Nowadays, two 'access sets' are available for this procedure, the Rösch-Uchida Transjugular Liver Access Set (RUPS) and the Ring Transjugular Liver Access Set (RING). Both methods and sets are from Cook Medical ©. This thesis will focus on the method with the RUPS access set since the RING set does not use a stilet for the intrahepatic puncture.

In order to decide if a patient needs a TIPS procedure, the IR use a portosystemic pressure gradient (PSPG) to determine if there is portal hypertension. The IR measures the pressure in the PV and in the inferior vena cava. In theory, there is portal hypertension if the PSPG is greater than 6 mm HG. Bleeding complications of portal hypertension usually occurs only when the PSPG exceeds 10 mm HG [26]. To decide whether the IR will perform a TIPS procedure he will briefly consult with his colleagues about the PSPG value and the health of the patient.

If there is decided to do the procedure the IR makes a small incision in the neck to enter the jugular vein. From there, it is possible to access the RHV with long thin catheters. By first making a connection between the veins in the liver with a stilet, a self expandable shunt can be placed in order to preserve this connection. Figure 1.8 shows the liver after a TIPS procedure. The shunt is placed between the RHV and the PV in order to let the blood flow from the intestine through the shunt to the hepatic vein. From this point, the blood is redirected back into the systemic circulation avoiding the liver, which reduces the pressure.



**Figure 1.8:** A schematic liver where a TIPS procedure is performed. Blood flows through the placed shunt from the PV to the HV, into the systemic circulation, back to the heart.

### Procedure

First of all, the pressure is measured in the PV by inserting a 21G needle directly through the skin into the PV. The IR uses ultrasound visualization to locate the needle and check if it is in the PV. Once in place, a guidewire is placed through the needle to assist the positioning of a 4Fr catheter. Through this catheter the IR is able to measure the pressure with a special instrument. After the measurement an angiographic catheter is placed through the 4Fr catheter. With this angiographic catheter, the IR can inject contrast liquid, which is visible on CT scans, into the veins. From the CT scans it becomes clear for the IR where the veins and all its branches are located. This imaging modality is known as fluoroscopy.

Secondly, the IR makes an incision in the neck to enter the jugular vein with a 17G needle. An introducer sheet with 10Fr Dilator and guidewire (Figure 1.9, item 6), are inserted through the jugular vein into the inferior vena cava. The IR will again measure the pressure, but now in the HV to define the PSPG value of the patient.

If a TIPS procedure must be performed, the IR uses the introducer sheet which is still in the inferior vena cava, without the 10Fr Dilator. An overview of the RHV and its branches are obtained by using fluoroscopy again. An angiographic catheter, with an angle of 30 degrees, is placed through the sheet into the RHV. After fluoroscopy took place and CT scans are made the catheter is retracted from the body. A 14G stiffening cannula with a 10Fr catheter (Figure 1.9, item 3 & 4), will be pushed through the introducer sheet. Since the stiffening cannula has an angle of 30 degrees in the

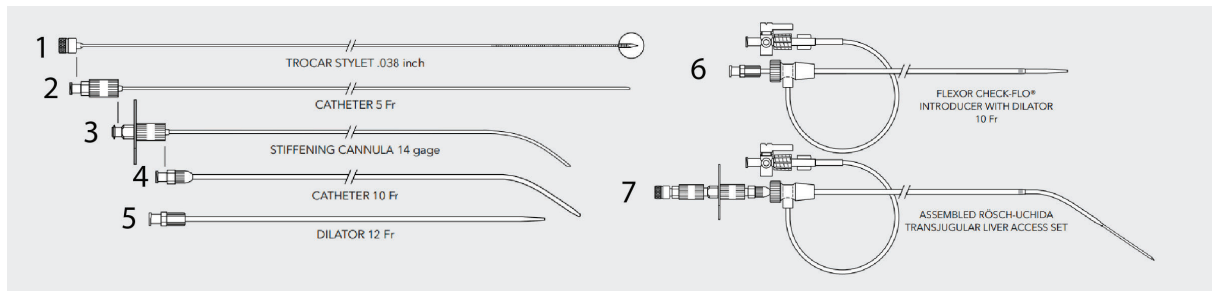
tip, the IR is able to enter the RHV by maneuver the 10Fr catheter.

Since the angiographic catheter from the first steps is still in the PV, the IR can again apply fluoroscopy to get an overview in one scan of the stiffening cannula and the branches of the PV. Unfortunately, CT scans give only a 2D image as result. As described in Chapter 1.2.1, the RHV is located dorsal relative to the PV. The IR rotates the stiffening cannula in the direction (ventrally) of the PV. How far the cannula must be orientated ventrally is determined experimentally and on experience since this is not visible on the 2D CT scan. Next, a stylet with a 5Fr Catheter (Figure 1.9, item 1 & 2) will go through the stiffening cannula to perform the intrahepatic puncture to the PV.

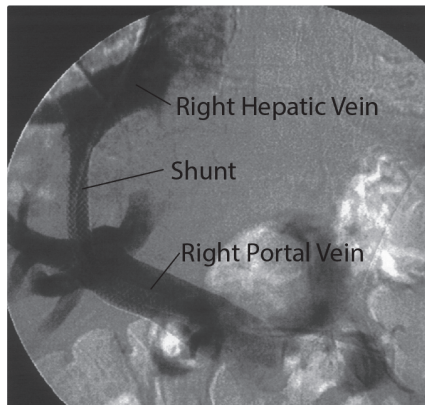
On CT scans, in combination with the fluoroscopy, the IR can check whether the stylet is punctured into the PV. If so, the stylet will be taken out, while the 5Fr catheter stays in the PV. A syringe with contrast liquid is connected to this 5Fr catheter. First, the syringe is pulled vacuum by applying suction. If blood flows into the syringe, the IR knows that he punctured directly in the PV. If not, it is most likely that the stylet has passed through the PV. The IR will then pull back the syringe, including the 5Fr catheter, under a vacuum conditions until blood enters the syringe. If blood is visible, the IR injects the contrast liquid. With new CT scans the IR checks whether the 5Fr catheter is actually in the PV.

The syringe will be removed and a guidewire will go through the 5Fr catheter into the PV. The 5Fr catheter will be pulled back, the 10Fr catheter, which was still in the inferior vena cava, will push through the liver tissue into the PV, guided by the guidewire. A self-expandable shunt will be placed over the guidewire and inside the 10Fr catheter. The shunt is placed in the liver where it makes the connection between the RHV and the PV. The guidewire and catheter are pulled back. Now, only the self-expandable shunt is in the liver. After the shunt is expanded, the pressure is measured in the RHV and PV again to check if the PSPG is decreased.

All steps of the TIPS procedure, with the used imaging method and instruments, are elaborated in Appendix A. Figure 1.10 shows, on a CT scan, the result of a TIPS procedure. A shunt is placed between the RHV to the RPV to decrease the pressure in the portal system.



**Figure 1.9:** Needles and catheters used for the TIPS procedure according to the RUPS method. All catheters and needles are assembled together in item 7. Reprinted from the instructions of Medical Cook © [6].



**Figure 1.10:** A coronal CT scan of the liver after a TIPS procedure. A shunt connect the right hepatic vein with the portal vein to reduce the pressure in the portal system. Reprinted from Jeanne LaBerge [10].

#### 1.4.4 | Complications

Although the TIPS procedure reduces the pressure in the portal system, it also brings potential risks. For instance, the diverted blood flow may worsen the liver function and increases the risk of the brain swelling (hepatic encephalopathy)[28, 29], which is the most common complication. In a study from Zhao et al. [29], 30.6% of the 183 patients got hepatic encephalopathy (HE) within 5 years. Other patients got complications such as suffering from recurrent or emerging gastrointestinal bleeding (27.9%), recurrent or emerging refractory ascites or hydrothorax (12%).

HE is a result caused by liver dysfunction. Toxins, like ammonia, stay in the blood. The best characterized neurotoxin linked to HE is ammonia, the primary source of ammonia is the gastrointestinal tract [30]. Normally, the liver converts the ammonia into glutamine and prevents an entry to the systemic circulation. After a TIPS procedure the blood will bypass the liver, there is no decreased metabolism of ammonia and it will enter the systemic circulation. Ammonia, and other toxins, will be build up in the brain, which can cause mental confusion, personality changes, memory loss, and sleepiness.

A treatment against HE is to revise or block the shunt, so no blood will bypass the liver. For patients with liver cirrhosis this is not an option because they either suffer from portal hypertension or from HE. Alternative treatments are given by Andres T. Blei [31] by decreasing the nitrogenous load from the gut, improve the extra-intestinal elimination or to counteract abnormalities of central neurotransmission.

#### 1.4.5 | Clinical Outcome

In this section only direct clinical outcomes are discussed. It is difficult to compare outcomes over several years, as patients are on waiting lists for liver transplantation or may die due to other consequences.

Although it is a challenging procedure, the success rate of the TIPS procedure is very high. The success rate in a study of Zhao et al. [29] was 95.7%. The procedure was performed at 191 patients where the success rate was measured directly after.

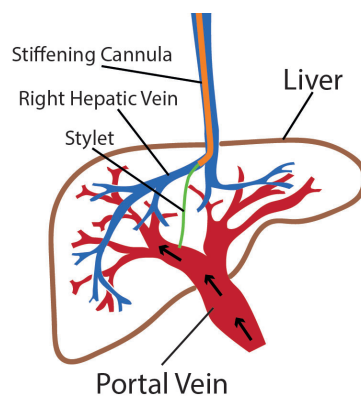
In a study done by Heinzow et al. [32], the TIPS procedure was performed at 81 patients divided in two groups. A first group of 54 patients with liver cirrhosis including variceal bleeding, and a second group of 27 patients with cirrhosis and refractory ascites. After the TIPS procedure, which was successful at every patient, the average PSPG significantly decreased from  $23.4 \pm 5.3$  to  $11.8 \pm 4.0$  mm Hg in the first group versus  $22.1 \pm 5.5$  to  $11.7 \pm 4.2$  mm HG in the second group ( $p = 0.001$ ).

Han et al. [33] did a study for a group of 38 patients, a success rate was achieved of 96.6%. TIPS were successfully placed in 36 patients. Measuring the pressure afterwards concludes that the PSPG was significantly decreased from  $15.5 \pm 6.3$  to  $7.8 \pm 4.1$  mm Hg ( $p < 0.01$ ).

Finally, Keller et al. [26] did a research to available TIPS results since the late 1990s. As a result, from the late 1990s till 2016 the technical success rate of performing the TIPS procedure with skilled hands was 97.3%. From all the procedures which were measured the rate of fatal procedural complications was low (2.2%).

### 1.5 | Problem Statement

Even though the TIPS procedure has proven to be very effective, especially when people are not eligible for a liver transplantation, the procedure is still complex. During the procedure multiple catheters, needles and sleeves are inserted and retracted. The most important step is the intrahepatic puncture, where the stylet is pushed through the RHV into the RPV. A schematic view of the intrahepatic puncture can be seen in Figure 1.11.



**Figure 1.11:** The intrahepatic puncture between the RHV and RPV with the stylet. In green the stylet, in orange the stiffening cannula (item 1 and 3 in Figure 1.9).

The orientation of the veins and its branches in the liver is an important issue since they are not located at the same place for every patient. In order to locate the instruments and veins, 2D imaging methods are used. With these methods, radiologists have difficulties with pointing the pre-bent stiffening cannula ventrally into the direction of the RPV. Even when the orientation of the pre-bent stiffening cannula is correct, the IR rarely pushes the stylet from the RHV directly into the PV. This problem occurs due to the stiff tissue of the sick liver, wherefore deflection of the stylet can occur. Because of this deflection, it sometimes occurs that the intrahepatic puncture step has to be repeated multiple times before entering the RPV.

Improving the stylet with a steerable tip can help the IR to reduce the complexity of the procedure. When the stylet is able to steer in liver tissue,

deflections can be prevented by adjusting the tip, and a wider range of motion (RoM) to adjust the stylet into the desired direction can be achieved. These both advantages will reduce the uncertainty to enter the PV.

Another problem concerning the TIPS-procedure is the lack of available realistic test models. The orientation of the stiffening cannula during the intrahepatic puncture step is orientated mostly on experience. Due to ethical and practical issues, it is not feasible for new IRs to test on biological tissues like real livers. For the TIPS procedure one test/training model from Cook Medical © was found. In this model, the veins and liver tissue are made of a material which do not correspond to real tissue. With a more realistic test model new IRs can train the procedure to become comfortable with it. Besides this, with a good model an IR is also able to test and train with the steerable stylet to see if the complexity of the procedure will be reduced. For a good model the HV and PV must be integrated and the material must mimic liver tissue.

### 1.6 | Research Question

The goal of this thesis is to reduce the complexity of the intrahepatic puncture step during the TIPS procedure to increase the hit rate to enter the portal vein. To reach this goal this thesis is focused on designing a steerable stylet which is used for the intrahepatic puncturing step. The following research question is formulated.

Research Question:

*”Will the hit rate increase to enter the portal vein during a TIPS procedure by using a steerable stylet for the intrahepatic puncture?”*

### 1.7 | Objective and Approach

To find an answer on this research question, some sub question have to be answered first. A possible problem by making the tip steerable is the stiffness of the stylet. If it loses its stiffness because of a flexible tip, it will cause even more uncontrollable deflections of the stylet during the intrahepatic puncture. A sub question to answer is: ”Is the steerable stylet stiff enough to puncture through liver tissue?”



Besides this, the desired RoM is important to know. Therefore, the position of the portal vein relative to the right hepatic vein is important to know. The second sub question is: "What is the desired range of motion in the steerable stylet before it has an advantage over the original stylet?"

To approach this sub questions, and the research question, a new design for a steerable stylet is discussed and made. With a stylet with steerable tip, the IR has more freedom, can more easily orientate the stylet to the PV and is able to prevent deflection during the intrahepatic puncture. These benefits will contribute to a better hit ratio. Secondly, a test model is build to test and train the TIPS procedure with the new designed steerable stylet. The hit rate of the setup with the steerable stylet will be compared with the original setup.

Before a new design can be made for the steerable stylet, the complexity of the TIPS procedure must be fully comprehend. Information from literature was found, ordered and discussed. All different steps of the treatment were closely investigated. A step-by-step plan with the required instruments and visualization methods are described in Appendix A. This plan is developed by watching instruction movies of the supplier (Cook Medical ©), reading articles, interviewing an IR and attending two TIPS procedures. The literature has established a set of criteria and requirements which are taken into account by designing the new steerable stylet and test model.

In order for the test model to be appropriate, it has to contain the relevant veins which will be approached during the TIPS procedure. To make the test model as realistic as possible, it is necessary that the material mimic liver tissue and the stylet does not follow previous punctured tracks. Since the puncturing is mainly done in the liver part, this part must be made easily replaceable. And since a liver with cirrhosis is stiffer than a healthy liver, it is desired that the IR can test needles and stylets in livers with different characteristics. In order to find specific characteristics for liver tissue existing literature was closely studied.

In the end, after designing the steerable stylet and test model, experiments were done with the original and the steerable stylet to compare their characteristics. To find answers on the sub questions, experiments are done to compare the maximum steering angle, the joint stiffness characteristics, the maximum force exerted by the tip and the visibility of the steerable stylet in relation to the

original one. Since the pre-bent stiffening cannula influences the stylet, experiments are done in combination with and without the stiffening cannula. For the visibility, experiments are done with a test setup including an ultrasound device where the visibility of the tip and shaft of the stylet is tested in different angles. Finally, a conclusion is drawn whether the steerable stylet is able to increase the hit ratio during the intrahepatic puncture. If so, it will reduce the overall complexity of the procedure and the procedure time. To validate this, the TIPS procedure will be executed by IRs on the test model with the steerable stylet.

## 1.8 | Thesis Outline

This thesis contains the following chapters:

- Chapter 1: Clinical Introduction. Introduction about what this thesis is about, what the TIPS procedure is, the research goal and how this goal is approached.
- Chapter 2: Technical Introduction. What kind of research is already done on steerable instruments. What kind of joint mechanisms, actuation types and materials are normally used for steerable instruments. This chapter ends with design criteria for the steerable stylet.
- Chapter 3: Concept and Prototyping. A few concepts are worked out with criteria points in mind. All sub parts are discussed to motivate design choices and the first part will be closed with a final concept. In the second part of this chapter the prototyping phase will be discussed.
- Chapter 4: Evaluation. The prototype is encountered in a few experiments to evaluate if the steerable stylet reduces the complexity of the current TIPS procedure. For every experiments a small conclusion is drawn.
- Chapter 5: Discussion. The pro's and cons of the steerable stylet will be discussed. Which improvements are needed before it can be used by interventional radiologists, and what were the limitations during the experiments, and how can they improved? In the end recommendations for further research are given in order to the problems which arose during this graduation project.
- Chapter 6: Conclusion. The research question will be answered. By looking at the results from the experiments, an overall conclusion can be drawn about the steerable stylet.

## 2 | Steerable Instruments

### 2.1 | Technical Introduction

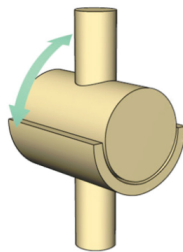
To provide the best steerable solution to reduce the complexity of the TIPS procedure, this section contains a technical introduction for different joint mechanisms, steering techniques, materials, actuation types, transmissions and visibility properties found in literature for needles.

#### 2.1.1 | Joint Mechanisms

A mechanism can be described as a mechanical device, an assemblage of links connected to each other by joints, in such a way the links are allowed to move in a controlled relative motion [5]. In order to achieve a steerable output from a simple input, multiple mechanical components will interact together in the distal end, actuated at the proximal end. Medical steerable instruments often have small diameters, which makes the steering mechanisms complex.

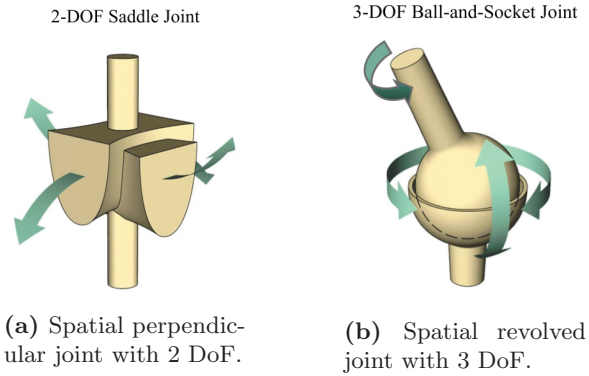
Mechanisms for steerable instruments can be divided in two movement categories, planar (2D) or spatial (3D) [34]. The principle of the planar joint is a mechanism which allows a rotational movement in one plane (2D), in other words, it has one degree of freedom (DoF). An example of a planar joint is shown in Figure 2.1.

1-DOF Revolute joint



**Figure 2.1:** Example of a planar joint with 1 DoF. Reprinted from David Kelly [35].

A spatial joint is a geometrical extension of the planar joint which can be divided in spatial perpendicular and spatial revolved mechanisms. The spatial perpendicular mechanisms is limited in two-planes, it allows two rotational movements in two perpendicular planes (2 DoF). The spatial revolved mechanism allows, next to the two rotational movements, also a rotational movement around a third axis (3 DoF). How these movements are made depends on the mechanism. Figure 2.2 shows examples of both spatial mechanisms, with their rotational movements indicated and DoF denoted.



(a) Spatial perpendicular joint with 2 DoF.

(b) Spatial revolved joint with 3 DoF.

**Figure 2.2:** A representation of both spatial joint mechanisms. Reprinted from David Kelly [35].

Next to the rotational movement, joint mechanisms can also be divided in how the rotational movement is established. Options for these movements are rolling, sliding, a combination of both or by deforming material (compliant). An overview of joint mechanism examples are shown in Table 2.1.

#### Rolling Joints

Rolling joints consist of two or multiple interfacing halves. During the rotational motion the halves will roll against each other, around a shared contact point. These halves will rotate with respect to each other along a trajectory defined by their curvature. Because the contact area between the halves is very small, such mechanism will slip quickly. A bending movement for a planar rolling joint is represent in Figure 2.3. Perpendicular rolling joints consists of a combination of two planar rolling joint aligned perpendicular to each other, wherefore the mechanisms can rotate around two axes.



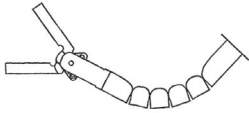
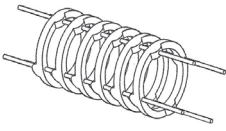
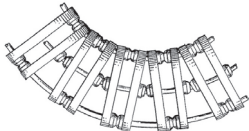
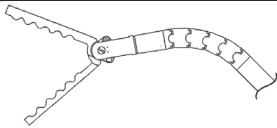



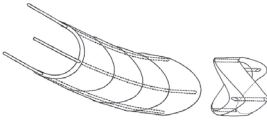

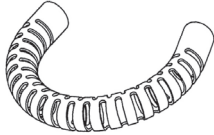
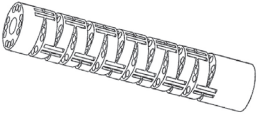
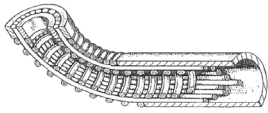
(a) Two halves in a parallel state.

(b) Two halves after a rotational movement.

**Figure 2.3:** Overview of the rotational movement for a rolling joint mechanisms.

Because of the translation on a small surface during the rotational movement, the rolling joint halves are susceptible to transverse and axial split, or even worse, a disconnection between the halves can occur. To prevent slip, physical features such as gears or belts can be used. To prevent split, additional constraints e.g., stops or driving cables must be applied [34]. In general, this mechanism is not torsional stiff and needs adjustments before it can be used properly as a steering mechanism.

**Table 2.1:** Examples of joint mechanisms ordered by mechanism type and rotation movement.  
Reprinted from Jelinek et al. [34]

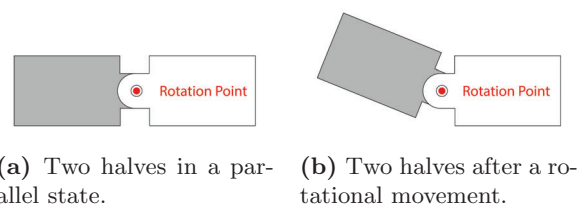
Mechanism \ Movement	Planar	Spatial Perpendicular	Spatial Revolved
<b>Rolling</b>	 Patented by Parrot et al. [36]	 Patented by Banik et al. [37]	 Patented by Allred and Bingham [38].
<b>Sliding</b>	 Patented by Stroup and Deptala [39]	 Patented by Marczyk et al. [40]	 Patented by Banik et al. [37]
<b>Rolling Sliding</b>	 Patented by Menn [41]	 Patented by Saadat et al. [42]	 Patented by Boury [43]
<b>Compliant</b>	 Patented by Stone et al. [44]	 Patented by Dewaele et al. [45]	 Patented by Breedveld and Scheltes [46]

### Sliding Joints

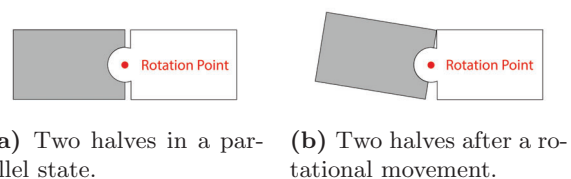
The working principle of the sliding joint looks similar to the rolling joint. However, the halves of the sliding joint have a perfect geometry. The rotational movement is made about a fixed point which can be given by a pin, pivot or a protrusion in one half. Sliding joints can be divided by hinged and curved joints. Sliding hinged joints are connected by, for example, a pin, and will rotate around this connection. An advantage is that it is compact and has a big range of motion, especially compared to the sliding curved joints where the halves work with at one side a protrusion and the other side a notch, a kind of puzzle pieces which yield for a smooth bending. The rotation will follow the curvature, but since the protrusion has to fit in the notch there is not much space to rotate. The range of motion of single sliding curved joints are very low.

Figure 2.4 and 2.5 shows rotational movements for a planar hinged and planar curved sliding joint. The planar hinged mechanism got his fixed rota-

tion point by a pin with a big range of motion. The rotation of the planar curved mechanisms will follow the curvature of the pieces with a very low range of motion.



**Figure 2.4:** Overview of the rotational movement for a planar hinged sliding joint mechanisms.



**Figure 2.5:** Overview of the rotational movement for a planar curved sliding joint mechanisms.

Because of the fixed rotational point both curved and hinged joint mechanisms are good resistant against transverse split. If the pin in the hinged mechanisms is locked, extra constraints are added. The hinged joint will then prevent axial split and the torsional stiffness will increase. Extra constraints for the curved sliding mechanisms depends on the design. If there are not constraint to prevent axial split, it is possible that the two halves are separated from each other by an axial force.

### Rolling Sliding Joint

This joint type is a combination of the rolling and sliding joint where the halves have the possibility to roll and to slide against each other. The joints looks similar to sliding curved joints, only with looser constraints. More specific, the joint motion can involve the combination of partial rolling and sliding at the same time, first rolling then sliding, or just sliding itself [34]. Rotations and translations can be done simultaneously or sequentially.

The halves of these joint mechanisms have a shared contact point but no fixed rotation point. During a rotational movement the halves will rotate around the contact point when this contact point slides along the curvature of the halves. In general, these mechanisms are more susceptible to axial split, transverse split, and to axial spin then the rolling or sliding mechanisms. But again, the design of such joint mechanisms can decide the amount of extra constraints. By designing more constraints the mechanism will be better resistant against the split and spin problems, but will give also more friction during the rotational movement.



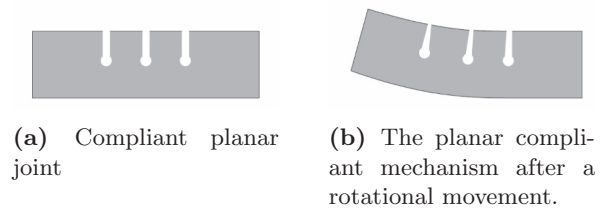
(a) Two halves in a parallel state. (b) Two halves after a rotational movement.

**Figure 2.6:** Overview of the rotational movement for a planar rolling sliding joint mechanisms.

### Compliant Joints

Compliant mechanisms are flexible, monolithic structures, in which the deflection of designated flexible members, so-called flexure hinges [47], transmit force, motion, and energy. These joints get their functional properties by a single piece of material. For a compliant joint mechanism material is removed in such a way that a flexible part is created with the desired properties. Figure 2.7 shows a planar compliant joint. This mechanism

can rotate in the plane perpendicular to the plane where material is removed as shown in Figure 2.7b.



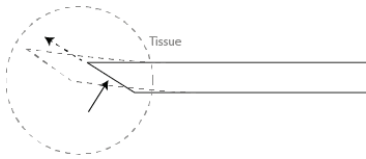
**Figure 2.7:** Overview of the rotational movement of a compliant joint mechanisms.

The characteristics of the mechanism depends on the dimensions of the flexural part and material properties, such as stiffness and yield stress. These dimensions and material properties will have an influence on the range of motion, and the resistance against torsional, axial and lateral forces [34]. In general, a big advantage of compliant mechanisms is that it is made out of one piece of material. More constraints are directly into the mechanism compared to the other mechanisms wherefore it is generally better resistant to the torsional, axial and lateral forces.

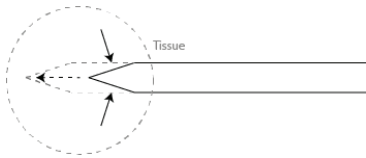
#### 2.1.2 | Steering Technique

Steerable mechanisms can also be classified by their steering technique. A division is made between the active and passive steering techniques. Bending forces during passive needle insertion are a direct result of the interaction between tissue and the tip. Some surgeons use the flexibility of a bevel tip needle during insertion to increase maneuverability and refer to it as passive needle steering.

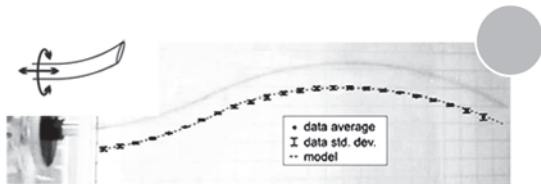
Passive steering technique depends on the behaviour of the needle, the tip shape and the properties of the inhomogeneous tissue. Figure 2.8 shows the forces on the needle during puncturing. In case of the bevel tip, the forces on the tip caused by the tissue, are asymmetric and will deflect the needle. In combination with rotating the needle entirely, the passive steering technique can be used to steer the needle in the desired direction. Figure 2.10 shows a curved operation path, made with a bevel tip needle. Symmetric tip shapes, e.g. conical or triangular, exerts the forces while puncturing equally as shown in Figure 2.9. As a result, symmetrical tips cannot be used for the passive steering technique.



**Figure 2.8:** The bevel-tip needle exerts forces asymmetrically. Cutting tissue occurs at an offset angle.



**Figure 2.9:** The conical tip (symmetrical) exerts forces from the tissue equally.



**Figure 2.10:** A curved operation path, steered with a passive steering technique by puncturing and rotating the entire needle with bevel tip. Reprinted from Webster et al. [48].

Active steering can already be applied before there is any interaction between the tip and tissue [49]. With this technique, it is potential to achieve a higher accuracy and precision to reach the operation target compared to rigid straight needles [50]. Besides this, active steering technique can be used with all kind of tip shapes, will not be influenced by the inhomogeneous tissue and is easier to control for the surgeons the passive steering. Active steering techniques can be divided in two types regarding how the steering mechanism is induced, *pre-defined* or *on demand* [50]. Pre-defined needles are already bent to the desired angle before they have any interaction with tissue. On demand steering needles have the possibility to change the steering angle anytime by an actuation which can be controlled by a controller or human hand, in fee air or when the tip is in tissue.

### 2.1.3 | Stylet Materials

The material choice for the stylet will decide some characteristics of the stylet, which will influence the behaviour during a puncture. Connecticut Hypodermics Inc. [51] is a company which is specialized in making stylets and uses the following materials in their stylets: 304 Stainless Steel, Type 316 Stainless Steel, Inconel 625 and Nitinol.

### 304 Stainless Steel

For needle applications 403 stainless steel is the most common and widely accepted material. It is available in different ranges of hardness and tensile strength. Besides this, a range of choices to finish the surface of the inner and outer diameter is available. A silicone or polytetrafluoroethylene (PTFE) coating can easily be added to the stylet to reduce the friction force during insertion. For better echogenic, the ability to bounce an echo, the tip area of the stylet can be improved with a special echogenic coating.

### 316 Stainless Steel

Type 316 stainless steel has almost the same properties as 304 stainless steel but differs in composition. 304 Stainless Steel contains 18% chromium and 8% nickel while 316 contains 16% chromium, 10% nickel and 2% molybdenum [52]. The molybdenum helps to resist against corrosion. Since 316 stainless steel is more expensive it will only be used in stylets for applications with higher corrosion potential.

### Inconel 625

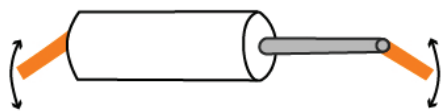
Inconel 625 is also a nickel-chromium-molybdenum alloy and can be used for stylets if corrosion still occur by stylets made of 316 stainless steel. Compared to 316 stainless steel, inconel contains more percentage molybdenum (8 - 10%) and is therefore a perfect alloy which is oxidation and corrosion resistant [53]. Inconel is used for instruments in highly corrosive applications.

### Nitinol

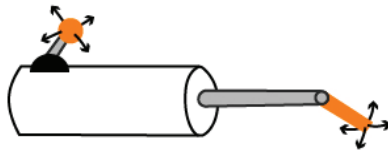
Lastly, there is nitinol, a super elastic shape memory material which contains approximately 50% nickel and 50% titanium [54]. For most engineering materials, load increases in a linear relationship with the deflection or stretching within the material. Nitinol responds different, large strains can be accommodated on loading, or recovered on unloading, with only a small change in stress [55, 56, 54]. This characteristic makes nitinol super elastic, it has the ability to withstand and recover larger deforming stresses than normal engineering materials. Next to this, nitinol is a shape memory alloy. During manufacturing of nitinol, a heat treatment to 450-550 °C for 1-5 minutes can be done where it is clamped in a custom shape, this process is called shape training [55]. Nitinol remembers the shape during the heat treatment, if it is heated afterwards above the transformation temperature range, it is able to recover to its memorized shape.

### 2.1.4 | Actuator Mechanisms

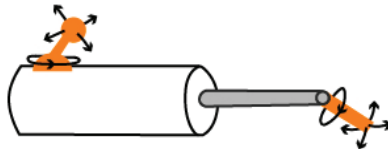
The actuation for a steerable joint in an on demand steering technique takes place at the proximal end, and can be done in various ways. The greatest influence on the actuator choice are the necessary DoF for the steering part. More DoF will result in a more complex actuator mechanism. The most obvious and natural solution for an actuator is with a rotational movement since also a rotation takes place at the distal end. By making a translation movement at the proximal end, for example by pressing a button, it will be difficult for the surgeon or IR to properly estimate the orientation of the steering mechanism. Figure 2.11 represents three schematic examples for actuator mechanisms with different DoF, all with a rotational movement at the proximal end.



(a) A planar movement with 1 degree of freedom. Actuation by a lever.



(b) A spatial perpendicular mechanism with 2 degrees of freedom. Actuation by a joystick.



(c) A revolved spatial mechanism with 3 degrees of freedom. Actuation by a joystick which is also able to rotate around its own axis.

**Figure 2.11:** Three examples of actuation types which represents different DoF. (a) 1 DoF. (b) 2 DoF. (c) 3 DoF.

Figure 2.11a shows a planar movement, a rotation in one plane. A simple lever at the proximal end can achieve a same movement at the distal end. Spatial mechanism can be actuated by, for example, a joystick as represented in Figure 2.11b. With this joystick movements can be made in the sagittal plane, for a front and back movement, and the transverse plane, for a movement to the left and right. These movements in the actuator will make the same rotational movements in the distal end by using a more complex transmission and joint mechanism. Lastly, Figure 2.11c represents an actuator

mechanism with 3 DoF. This principle works the same as the spatial mechanisms with a joystick but can also rotate the joystick on itself. Such mechanisms are known as a spatial perpendicular system, which is able to realize a 3 DoF movement, but is also very complex.

### 2.1.5 | Transmission

To achieve a rotational movements in the distal end, a transmission between the actuator and joint mechanism is needed. Some joint mechanisms needs a translation movement seized in the joint, where others needs a rotational movement in the joint. Typical transmission options for engineering are mechanisms like gears, cables, rods or the use of energy sources for a thermal actuation, like heat.

Where gears in mechanical designs are often used to generate a transmission from rotation to rotation, or from rotation to translation using a worm gear, the decision to opt for gears in the medical world is not self-evident. Gear transmissions are susceptible for friction, slip and wear. Especially if they are scaled down to small sizes what is often a requirement in medical applications, especially for medical instruments.

#### Thermal

As described in Chapter 2.1.3 there are shape memory alloys like nitinol, which can recover the memorized shape when heated above the transformation temperature. Using this characteristic, a thermal transmission can be created for medical applications. By heating up the nitinol it becomes possible to make a rotational movement in the distal end when the memorized shape was in an angle. It become also possible to achieve a translation if nitinol wires were stretched during the shape training. Heating it up will create a small translation movement since it remembers its stretched shape.

#### Cables and Rods

Cables can be used to create a mechanism with a translation as transmission. This can be achieved, for example, by pull a cable (translation), or by rolling up a cable (rotation). A disadvantage of cables is that a push translation is not feasible, only pull movements can be performed. A planar rotation in the tip of an instrument which must be able to rotate to both sides can be achieved by implementing two cables in the design. Each cable can be pulled, so a steering movement can be made in both directions.

Rods does not have this problem, both push and pull translations can be created with one single

rod. Unfortunately, with a rod it is not possible to get a translation directly from a rotation. To convert a rotation an intermediate step has to be made. If this intermediate step is done properly, a push or even a pull translation can be achieved from a rotational movement. For example, a joint mechanisms with a fixed rotation point given by a hinge is able to rotate by a push or pull translation if a rod is connected to the tip with a hinged spacer.

### 2.1.6 | Visibility of the Tip

Before the TIPS procedure is performed, scans are made of the patients body with computer tomografie (CT) or magnetic resonance imaging (MRI) imaging scans. The used method depends on the health of the patient and whether he/she has metals in the body that can be attracted by the MRI. Both imaging methods will make a body scan which can be divided in layers. The radiologist can scroll through the layers to see specific areas of the body. If there is liver cirrhosis, or the beginning of a disease, it can be seen from the scans. If the liver has already cirrhosis, fluid will be visible around it.

During the TIPS procedure the IR is guided by ultrasound, CT scans and fluoroscopy, as described in chapter 1.4.3. During the procedure it is important that the veins of the human body are visible, which is done with fluoroscopy. On the other hand, the tip of the stylet must be visible on the scans in order to locate the stylet and to check its orientation for the intrahepatic puncture. To increase the hit rate during the intrahepatic puncture, the visibility of the tip inside the veins of the human body is an important criteria to take into account.

Nowadays, a lot of developments aim to increase the visibility by enhancing the imaging methods or the reflection properties of the needles [57]. Van de Berg et al. [57] did a study to the visibility of different needles by doing experiments with needles punctured into a PVA sample. While the sample rotated around a fixed ultrasound probe, pictures could be captured from different angles inside the PVA. As result, a standardized set of reflection conditions for the comparative analysis of the needle echogenicity where needles with flat surfaces in the tip or kerfed patterns in the shaft were the best visible. By using this experimental setup and the already know standardized set and graphs, a conclusion about the visibility of the steerable stylet can be derived if it is at least as good visible as other common needles.

## 2.2 | Design Criteria

Problems like sterilization, re-usability, ease of use, human errors and costs are known for medical instruments. Needles for interventional procedures will cause even more problems like: imaging limitations, needle deflection, target uncertainty, tissue deformation, registration error and, in the case of hand-held needles, the surgeon's hand-eye coordination [58, 59].

The complexity of the TIPS procedure, especially for the intrahepatic puncture, is largely due to problems as described above. In order to reduce this problems, this chapter will discuss all sub components and their criteria before a design for the steerable stylet is made. The requirements of the design can be divided in *Mechanical Requirements* and *Medical Requirements*.

### 2.2.1 | Mechanical Requirements

The mechanical requirements that the steerable stylet must meet can be subdivided into: steering technique, number of parts, degrees of freedom, joint mechanism, actuator mechanism, transmission and material choice.

#### Steering Technique

As described in Chapter 2.1.2 there are two sorts of steering techniques; passive and active. Since the goal of this thesis is to increase the hit rate to enter the portal vein during a TIPS procedure, where image limitations are already a problem, it will not be a good choice to apply a passive steering technique. It would become very hard for the IR to make a ventral steering curve performing the intrahepatic puncture, guided by 2D image modalities.

A pre-bent active steering technique is already be applied by entering the RHV with the pre-bent 14G stiffening cannula. Using another pre-bent active steering technique for the stylet brings some disadvantages. Firstly, it will decrease the ability to push the stylet through the 14G stiffness cannula, because the stylet is already bent before it enters the stiffening cannula. And secondly, the stiffening cannula is directed towards the RHV when it is inserted. If the stylet is pushed through, it has a very small space to orientate ventrally in the direction of the PV for the intrahepatic puncture.

The on-demand active steering technique, on the other hand, is very interesting to look at. If the stylet gets the possibility to steer when needed,

the stylet can first be pushed through the stiffening cannula before a steering movement is accomplished. When the RHV is entered by the stiffening cannula, the stylet can directly pushed against the wall of the RHV. The IR can steer the tip of the stiffening cannula ventrally, in the direction of the portal vein. The stylet can be punctured through the liver tissue. If needed, it would be possible to steer by to correct the puncturing path.

### Minimum Number of Parts

Another criteria point is the complexity of the mechanism. In general, complex steering mechanisms need more space and have often not the ability and feasibility to minimize. In order to keep the stylet with the same diameter (0.9652mm), less parts are desired. Complexity also bring more costs of manufacturing based on the increased number of parts, the time spent in arriving at a suitable design, and will be more sensitive for damage. The design of the steerable mechanism must contain as less parts as possible while it is still able to minimize and achieve the desired steering possibilities.

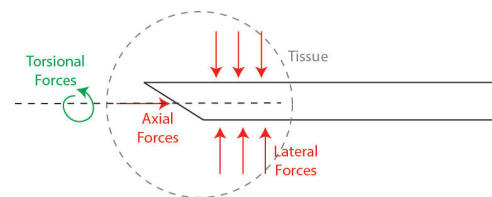
### Degrees of Freedom

During a TIPS procedure the IR turns the stiffening cannula first into the RHV. Afterwards, the stiffening cannula will be rotated ventrally as far as possible into the direction of the PV, guided by the fluoroscopy. By making this movement, the IR ensures that the distal end of the stiffening cannula is in one plane with the PV, obliquely forward with respect to the HV. For improving the certainty to enter the PV the stylet must have the ability to steer in that plane. Since the mechanism must as simple as possible and only a steering movement in one plane is required, a 1 DoF planar joint mechanism is sufficient to facilitate the procedure.

### Joint Mechanism

In Chapter 2.1.1 the rolling, sliding, rolling sliding and compliant mechanisms are discussed. The DoF for a mechanism is easy to define since these will depend whether a mechanism is planar, spatial perpendicular or spatial revolved. To decide whether the rotation point is fixed or not, depends mainly on the joint type, which is explained in chapter 2.1.1. To determine the RoM for the different steerable joint mechanisms, available steerable instruments are studied. In this case, the RoM is often found by laparoscopic instruments since these are much more common on the medical market. A disadvantage of these instruments is the larger diameter which is around 5 mm. To reduce the complexity and sensitivity of the steering joint

mechanism, the minimum number of parts which are needed to realize a steering movement are important to know as well. Lastly, a distinction is made between the different stiffness characteristics for the joint mechanisms. Chapter 2.1.1 already discussed the torsional stiffness, the transverse split and axial split for different joint types a bit. The torsional stiffness will define how good a mechanism is resistant against torsional forces. The sensitivity for transverse and axial split in a mechanism, which can be caused by axial and lateral forces, is described with the lateral and axial stiffness. How stiffer the mechanisms, how better the resistance. Figure 2.12 represents the axial, lateral and the torsional forces which will act on the stylet during insertion into tissue. Unfortunately, it is hard to find values for those forces and stiffness characteristics in literature or patents. To define the characteristics a classification is used which is made in another literature study [60]. The stiffness of the different mechanisms are ordered as in Table 2.2.



**Figure 2.12:** A representation of the axial, lateral and torsional forces on a needle.

**Table 2.2:** Classification to define the stiffness and resistance against the axial, lateral and torsional forces.

Classification	Description
A	High stiffness, good resistance against forces.
B	Medium stiffness, some resistance against forces (not as high as A).
C	Low stiffness, forces have influence on the accuracy of the mechanism.

In Table 2.3 all different joint types are listed with their characteristics. However, a side note has to be made. The results of Table 2.3 are based on existing medical research papers and patents till October 2017. Even though the most recent literature has been taken into account by then, it is possible due to the quick development of technology that the results could be outdated.

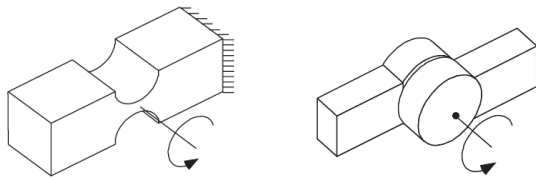
From Table 2.3 and the literature from chapter 2.1.1 the complaint joint has the best resistance against the torsional, lateral and axial forces, immediately followed by the planar sliding hinged



**Table 2.3:** Joint Mechanisms and their characteristics

Joint type	Movement	DoF	Range of Motion [degrees]	Fixed Rotation Point	Characteristics			Minimum Diameter [mm]	Minimum Steerable # Parts
					Torsional Stiffness	Lateral Stiffness	Axial Stiffness		
<b>Rolling</b>	Planar	1	100 [36]	No	B	B	C	5.0 [36]	2
	Perpendicular	2	180 [37]	No	C	B	C	12.88 [37]	3
	Revolved	3	40 [38]	No	C	C	C	9.5 [38]	3
<b>Sliding Curved</b>	Planar	1	180 [39, 61]	Yes	A	B	B	5.5 [39]	2
	Perpendicular	2	180 [62, 40]	Yes	A	B	B	5.0 [62]	2
	Revolved	3	180 [63, 64]	Yes	B	B	B	2	2
<b>Sliding Hinged</b>	Planar	1	>180	Yes	A	B	A	2.0 [65] 8.0 [67]	3
	Perpendicular	2	180 [66]	Yes	A	B	A	6.3 [68]	4
<b>Rolling Sliding</b>	Planar	1	180	No	B	B	C	4.0 [69]	2
	Perpendicular	2	180	No	B	B	C	16.00 [42]	3
	Revolved	3	180	No	C	C	C	3	3
<b>Compliant</b>	Planar	1	180 [70] 15-45 [71, 72]	Yes	A	A	A	0.36 [70]	1
	Perpendicular	2	90 [73, 74] 60 [75]	Yes	A	A	A	5.0 [73, 75]	1
	Revolved	3	90 [76]	Yes	B	B	B	1.0 [46]	1

joint. Figure 2.13 represents a planar compliant and a planar sliding hinged joint. The compliant mechanisms have the ability to be miniaturized and can be injection-molded out of one piece of material. It can easily be fabricated as a monolithic structure due to its hinge-less nature in design. Due to this advantages, less parts are required compared to traditional joints. Besides this, compliant mechanisms compared to rigid body systems connected by a conventional pin joint, are potentially more accurate, better scalable, cleaner, less noisy and more cost saving in manufacturing and maintenance [47].

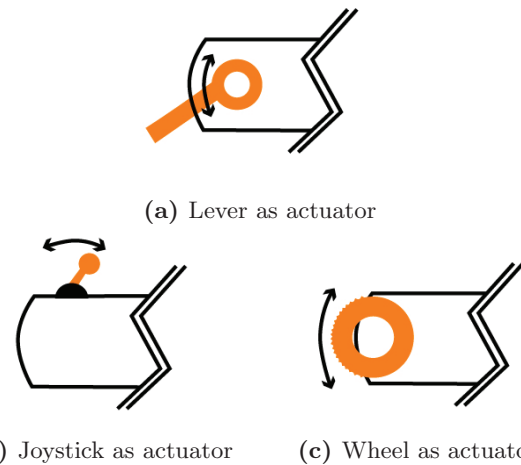


(a) Compliant conventional flexure (b) Standard revolute joint

**Figure 2.13:** In (a) a compliant conventional flexure with the same rotation possibilities as a sliding hinged joint, represented in (b). The sliding hinge joint contains a higher RoM, but need more parts to create the rotational movement. Reprinted from Speich et al. [77].

### Actuator Mechanism

For making the actuator mechanism as simple as possible for the IR, only the necessary movement is recommended. As describe above, a planar (1 DoF) movement in the tip of the stylet is desired in order to improve the procedure. As described in section 2.1.4 the most obvious solution for the actuator is to use a rotational movement so the IR can properly estimate the orientation of the stylet. Pressing or pulling a button will not feel as a natural movement for a rotation in the tip. A rotational movement as actuator is desired, this will be feel more natural and is easier to control for the IR. A 1 DoF movement can be made with a simple lever, a joystick or a wheel as shown in Figure 2.14.



(a) Lever as actuator (b) Joystick as actuator (c) Wheel as actuator

**Figure 2.14:** Overview of three different planar actuator mechanisms with a rotational movement.

### Transmission

The transmission is a challenge since the stylet may not differ much from the current stylet. If it is made with a bigger diameter, it will no longer fit through the 5Fr catheter and the stiffening cannula, other instruments must then be adapted as well. The current stylet has a diameter of 0.9652 mm and is 62.5 cm long. First of all, since the stylet is that long, a rotational movement as transmission from the proximal to distal end is not possible. The steering movement from the proximal end must be transmitted to the joint mechanism by a translation. Since the actuator creates a rotational movement an internal intermediate step is needed to make a translation from the rotation given by the actuator. This intermediate step will require some extra space in the handle of the stylet.

To create the translation, gears are not a suitable transmission due to the small teeth. A lot of slip will occur so it becomes hard to make a precise and accurate movement. As a requirement the stylet have to steer in one plane to both sides, even when it is in tissue. The transmission can be done by cables, nitinol or rods. For the transmission with cables or nitinol at least two cables or wires must be attached from the proximal end to the distal end which will take some space around the stylet. The principle with rods can make a rotation to both sides with only a push or pull translation. Such principle is already applied in a thin steerable ablation needle designed by Nick J. van de Berg [78]. The stylet is covered within a thin rigid cannula. The front of the stylet consists of two parts that meet in the tip. The rigid cannula ensures that one side is fixed just in front of the steering mechanism. By pushing or pulling the non-fixed half of the stylet, a rotation in the tip can be achieved. Also with the rod principle some extra space around the stylet is needed since an extra rigid cannula is required to fix one of the halves of the stylet.

As a result, cables, heated nitinol or the push and pull principle can be all working in the new design. Since all three principles needed some extra space around the stylet, it must become clear during the concept generation which principle suits the best to keep the diameter of the stylet as small as possible.

### Material

More and more steerable instruments are available onto the market for interventional radiology [79, 70, 80] where a lot of this instruments use a compliant mechanism with the super elastic nitinol

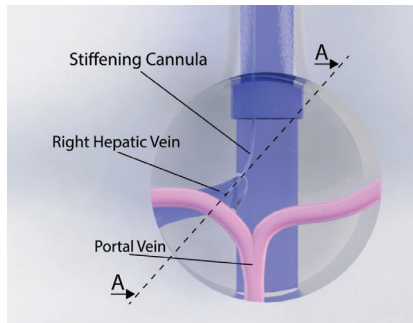
as material. As discussed in section **Joint Mechanism**, the compliant joint is the best solution. A compliant mechanism uses the deformation of the material as steering mechanism. Nitinol is super elastic and has the ability to withstand and recover large deformation stresses which makes it the best choice for the joint mechanism.

### 2.2.2 | Medical Requirements

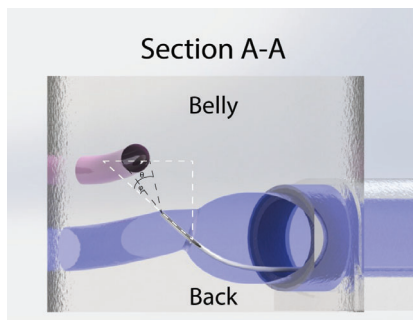
Important medical requirements for the new design of the steerable stylet are the desired RoM and visibility. In order to reduce the intrahepatic step, it has been decided that the stylet must have the RoM so it is able to enter the PV even if the stiffening cannula is pressed against the side of the RHV by making steering movements. Besides this, the stylet must be good visible with ultrasound and CT scans. The requirements must meet at least the visibility abilities of the original stylet.

### Range of Motion

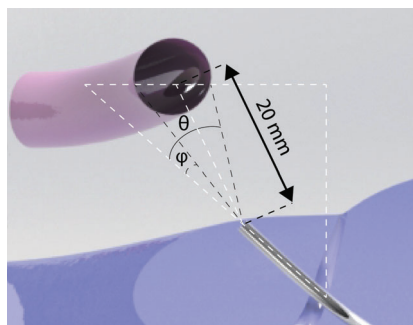
It is hard to determine the desired RoM from literature. As described in chapter 2.2.1 a one plane (planar) steering movement facilitates the procedure. Some dimensions and angles are measured from the test model for the TIPS procedure of Cook Medical©. By reproducing this test model in a 3D computer aided design (CAD) model, the angles and distances between the veins inside the test model could be measured. Figure 2.15 represents a top view of the reproduction of the liver where the RHV, RPV and stiffening cannula are visible. The stiffening cannula is orientated from the RHV to the PV. Figure 2.16 shows a section view where the section is made in the plane parallel to the stiffening cannula. This plane is difficult to define since every liver looks slightly different, and the cannula will be pressed a bit into the liver tissue when it is orientated in the direction of the PV. Figure 2.17 is zoomed in on the angles that are found from the section view. These values gives an indication for the required steering angle to enter the PV after the stylet comes out the stiffening cannula, even from the side of the RHV. As a result, a minimum angle of 10 degrees ( $\phi$ ) is found and a maximum angle of 35 degrees ( $\theta$ ). The IR tries to position the stiffening cannula so the stylet can enter the portal vein without any steering movements. The RoM for the new steerable stylet is set to cover the entire diameter of the RPV. The proposed RoM is  $\theta - \phi = 25$  degrees. If the stiffening cannula is orientated correctly, the stylet can be pushed though the tissue without any steering movements. If the stiffening cannula is orientated to the side of the RHV, like in Figure 2.17, 25 degrees RoM should be still enough to enter the PV.



**Figure 2.15:** A top view of the reproduced liver model of Cook Medical ©. In blue the RHV, in pink the PV.



**Figure 2.16:** A section view of the liver model in the plane parallel to the cannula. Angles are derived for the stylet in order to enter the RPV.



**Figure 2.17:** The angles and distances between the stiffening cannula and the RPV.

### Visibility Requirements

For reducing the effort, and increasing the hit rate during the TIPS procedure, visibility of the instruments are important to take into account. Before the intrahepatic puncture is performed, the stiffening cannula and stylet are located in the RHV where the tip is orientated in the direction of the PV. The IR checks the orientation guided by ultrasound. During the intrahepatic puncture step

the IR follows the tip with ultrasound and makes the veins visible with fluoroscopy and CT scans.

The visibility of the tip and the shaft for both stylet and stiffening cannula with ultrasound are important. As a conclusion in the article of Van de Berg et al. [57], shafts with kerfed-patterns, a 18G trocar needle tip and a 22G chiba needle tip (with flat surfaces) had the best outcomes. For the steerable stylet a compliant or a sliding hinged joint mechanism will be used. Both mechanism contains some cut-outs, or exists of multiple components, the shaft visibility of these mechanisms will be better than the original stylet since kerfed-patterns are included. Besides this, tip shapes with flat surfaces scores the best for the visibility in the article. Therefore, flat surfaces in the tip are desired. Visibility tests will be done with the prototype as described in the article to conclude visibility characteristics of the steerable stylet.

### 2.2.3 | Conclusion

All positive outcomes from this chapter are listed in Table 2.4. Some parts or characteristics for the design are already fixed since one positive option was left. The steerable stylet is able to reduce the complexity of the procedure if it is able to steer in one plane wherefore a planar movement with 1 DOF is necessary. Because these steering mechanisms need fewer parts, it is also better resistant against any damage, it is cheaper to produce and easier to replace parts if necessary. As steering technique, active on-demand is chosen because the stylet first has to pass through a pre-bent cannula. With the pre-bent active technique this will not be possible. Using the passive steering technique it is possible to go through the cannula but it will be difficult to estimate how the stylet will react due to the inhomogeneous stiff liver tissue in the diseased liver. The material of the steerable stylet will be the super elastic material nitinol. The material in the steering mechanism is able to bend without any fatigue in the material. For the joint mechanism, the actuator and transmission more options are found as good results. For these options a choice will be made during the creation of the concept.

**Table 2.4:** Properties and characteristics for a suitable steerable stylet for the TIPS procedure

Joint Type	Movement	Technique	DoF	RoM	Actuator	Transmission	Material
Compliant	Planar	Active	1	25°	Lever	Cables	Nitinol
Sliding Hinged		on-demand			Joystick Wheel	Heated Nitinol Rod (Push/Pull)	

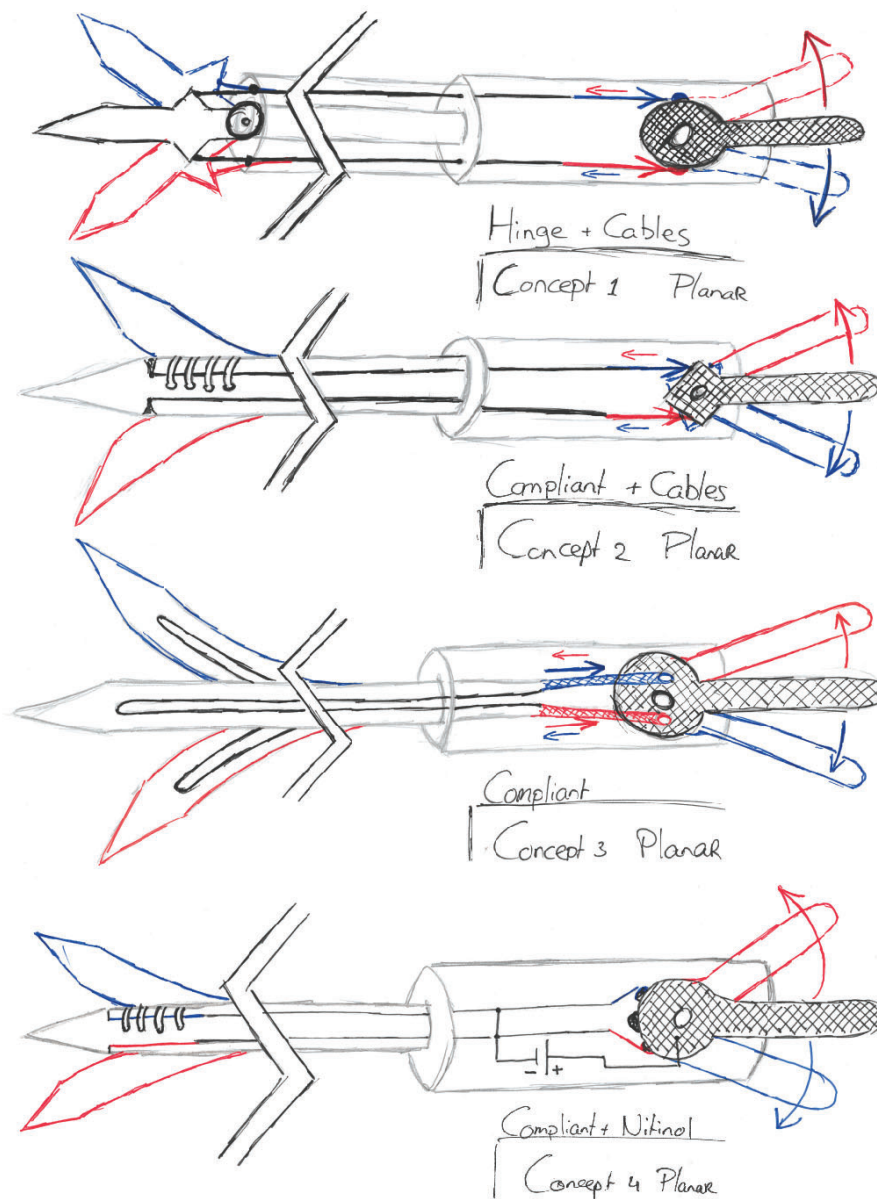
### 3 | Concept and Prototyping

This chapter discusses the concept and prototype of the steerable stilet for the TIPS procedure, build up from the outcomes from Table 2.4.

#### 3.1 | Concept Generation

Based on Chapter 2.2.3, as well as the ablation needle previously developed by Nick J. van de Berg [78], four stilet concepts were derived, as shown in Figure 3.1. These concepts translates the design of the ablation needle to the application of TIPS procedures, taking into account the increased length

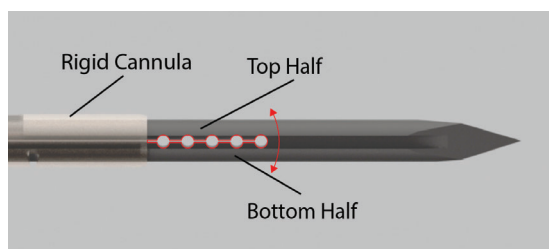
of the shaft. The four concepts vary in terms of the joint mechanism and transmission, whereas other components, including the actuator and transmission translator, have been purposely kept close to the starting point, the ablation needle. In order to create the best final concept, the concept generation is split up in sections for the joint mechanism (distal end), the transmission and the handle (proximal end). All components will be briefly discussed to make the steerable stilet feasible.



**Figure 3.1:** Four different drawings of concepts for the steerable stilet. All four are planar mechanisms actuated by a lever. As transmission the cables, heated nitinol and push and pull principles are drawn. For the joint mechanisms there are three compliant systems and one with the sliding hinged principle.

### 3.1.1 | Joint Mechanism

The two suitable joint mechanisms for the final design are the compliant and the sliding hinged joint mechanisms as concluded from Chapter 2.2.1. The stylet can have a maximum diameter of 0.9652 mm to fit within the 5Fr Catheter used in the TIPS procedure. To achieve this, it is desirable that the steering mechanism is well scalable and consist of as few components as possible. The sliding hinged joint consists of two halves that are connected to each other by a pin. If it must fit within the same diameter, these parts become very small and fragile. The pin for example, should be no longer than 0.9 mm. The goal is to design a robust steerable stylet that is rigid enough to puncture through tissue without a chance that something breaks. A compliant mechanism can be extracted from one piece of material, less components are needed, it is less fragile and better scalable. The steerable ablation needle also contains a compliant steering mechanism, a schematic overview of the mechanism is represented in Figure 3.2. Since this compliant steering mechanism works well in the ablation needle, and stays within the maximum diameter, there is chosen to reproduce the same steering mechanism in the steerable TIPS stylet. The rotation is created around the round holes in the mechanism. The choice for 5 holes is reproduced from the ablation needle. Another option was to choose for only a slit in the material, the rotational movement will also work then but only more force would be required and the material in the slit will have more pull and push tensions, resulting in the risk of breakage in the material. Because of the round holes, less force is needed and the material has more surface that can absorb the tensile and pushing stresses, wherefore the stresses will be better distributed.



**Figure 3.2:** A schematic overview of the compliant joint mechanism for the steerable stylet. The red lines represents the material surface which handle the push and pull stresses during rotation.

### 3.1.2 | Transmission

The rotational movement, created by the actuator in the handle, is transformed to a translation in the handle. This translation will eventually actu-

ate the joint mechanism, where the translation is transformed in a rotation again. The three suitable transmission principles are thermal energy (heated nitinol), cables and rods. The working principles of these transmission are already discussed in Chapter 2.1.5.

An example for a transmission with thermal energy would be nitinol wires which will be heated by an energy source. This principle could work if the actuator can activate an electric pulse. This electric pulse can heat the nitinol wires wherefore they are able to make a steering movement due to the shape memory characteristics. Such transmission will be an electrical system which can be powered by a battery or AC power. A disadvantage of the battery is the limited lifetime and extra check before the procedure can be performed. Even when the battery is made replaceable, the battery can run out during a procedure. Power supply via AC power ensures that a wire is attached to the stylet. Extra wires in an operation room are not desirable since the IR can stay behind, or are in the way when the IR tries to move the actuator to steer. To make the design simple, robust with as few components as possible which can be easily replaced a mechanical transmission is desired.

### Mechanical Transmissions

A mechanical solution for the transmission can be done with cables or by one or multiple rods. Since a planar movement is desired to both sides, a transmission with cables contains at least two cables. These are necessary on both sides of the steering mechanism since a cable can only provide a push translation. The cables can be placed inside or outside the stylet. By making the cables inside the stylet, the stylet must be made hollow, which is hard for this long shaft and small diameter. Besides this, a hollow stylet will affect the stiffness and the cables must be very thin to fit into the hollow stylet.

A second option with cables is to place them on the outside of the stylet. A prerequisite is that the cables must be protected otherwise they can bring damage to the surrounding tissue during the procedure. This protection can be done by the stiffening cannula, as designed in the sketch of the hinge joint mechanism with cables in Figure 3.1, or by another tube or sleeve. In the tip the cables must be attached to the joint mechanism. For a design with the cables on the outside the rotation point must still fall within the stiffening cannula, otherwise still damage to surrounding tissue will be caused by the cables during the intrahepatic

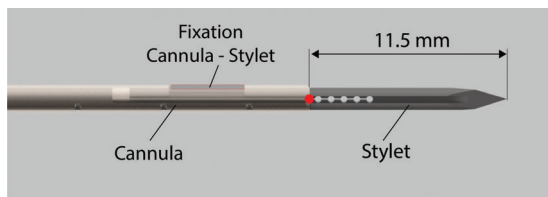
puncture. If the rotation point still falls within the stiffening cannula there arise some limitations for the RoM of the joint mechanism.

Another mechanical option is a transmission with a rod, translations can be created by pushing or pulling the rod. This principle is also used in the steerable ablation needle where it contains almost the same diameter as the original stylet used in the TIPS procedure. Another advantage of this transmission is that a compliant joint mechanisms is combined within the transmission, wherefore even less components have to be used. In the front of the stylet two halves comes together where a top half and a bottom half can translate along each other. One of the two halves is fixed to the rigid cannula around, the other half will make a pull or push translation in order to get the steering movement. Figure 3.2 shows the joint mechanism within the top and bottom half of the transmission.

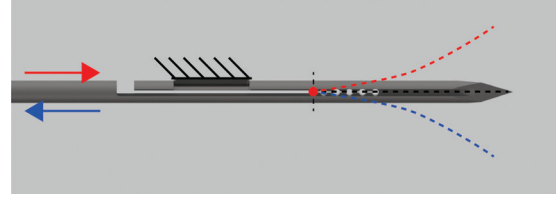
The rod transmission mechanism gets the preference since it is able to work within a small diameter wherefore the problem to keep the same small diameter is solved. A disadvantage of this principle is that an outer rigid cannula is necessary to let the steering mechanism work. Now, a 5Fr catheter is around the original stylet (item 2, Figure 1.9) during the TIPS procedure. The rigid cannula in the design of the ablation needle stays within this 5Fr diameter. With some adjustments in the setup it must be able to replace the 5Fr catheter with the rigid cannula. With these opportunities and the fact that this principle contains less parts, the rod transmission is the best solution for the final design.

### Translation Transmitter

Figure 3.3 shows the tip of the steerable ablation needle with the rigid cannula around. The rotation point, directly after the cannula (red dot) and the fixation are indicated. Figure 3.4 represents only the stylet (without rigid cannula) where the working principle is depicted if a push (red) or pull (blue) force is exerted, while one side is fixed.



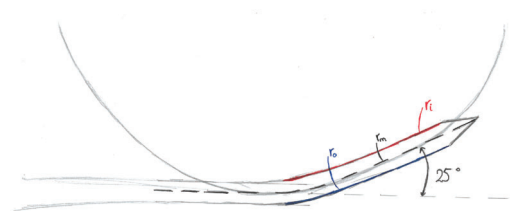
**Figure 3.3:** Final concept of the transmission where the joint mechanism and transmission are combined.



**Figure 3.4:** Working principle of the push/pull transmission where one side is fixed. The red lines indicates a push translation. The blue lines a pull translation.

The aim of the transmitter is to transmit a translation from the handle to the joint mechanism which will eventually create the steering angle. This section contains equations to define the translation in millimeters to achieve the proposed 25° steering angle in the tip.

The distance between the rotation point till the tip is 11.5 mm, copied from the ablation needle. To find the required translation first the radius of the middle line ( $r_m$ ) must be calculated. This will be done on the basis of the length of the middle line ( $l_m$ ), which is 11.5 mm. Since the diameter of the stylet is known, also the inner ( $r_i$ ) and outer ( $r_o$ ) radius can be calculated. Now, the length of the inner ( $l_i$ ) and outer ( $l_o$ ) line can be calculated for only the part of the circumference for 25 degrees. The translation can then be defined by the difference in length between the outer and inner line. In Figure 3.5 a sketch of the stylet is shown as clarification in a 25° steered configuration. The middle, inner and outer lines are denoted. The translation is calculated by the difference in length of the blue ( $r_o$ ) and red line ( $r_i$ ).



**Figure 3.5:** This sketch represents the steering angle of 25 degrees of the stylet. The needed radius of the inner circle ( $r_i$ ) in red, the middle circle ( $r_m$ ) in black and the outer line ( $r_o$ ) in blue are denoted.

Circumference circle:

$$CC = 2 \cdot \pi \cdot r_m \quad (3.1)$$

Length of the middle line  $l_m$  (25° of the circumference for the middle circle):

$$l_m = \frac{2 \cdot \pi \cdot r_m}{360/25} \quad (3.2)$$

The length of  $l_m = 11.5$  mm as known from the design so the radius  $r_m$  can be calculated.

$$11.5 = \frac{2 \cdot \pi \cdot r_m}{14.4} \quad (3.3)$$

$$r_m = \frac{11.5 \cdot 14.4}{2 \cdot \pi} \quad (3.4)$$

$$r_m = 26.356 \text{ mm} \quad (3.5)$$

The stylet has a diameter of 0.9652 mm, a radius of 0.4826 mm. With the radius of the inner and outer circle, the inner ( $l_i$ ) and outer ( $l_o$ ) line length of the 25° part of the circumference can be calculated.

$$r_i = 26.356 - 0.4826 = 25.8734 \text{ mm} \quad (3.6)$$

$$r_o = 26.356 + 0.4826 = 26.8386 \text{ mm} \quad (3.7)$$

$$l_i = \frac{2 \cdot \pi \cdot r_i}{14.4} \quad (3.8)$$

$$l_i = 11.289 \text{ mm} \quad (3.9)$$

$$l_o = \frac{2 \cdot \pi \cdot r_o}{14.4} \quad (3.10)$$

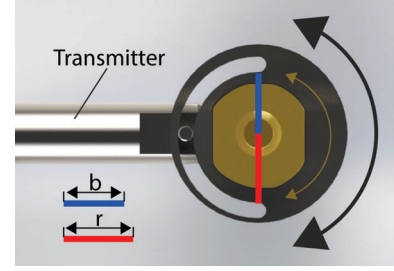
$$l_o = 11.710 \text{ mm} \quad (3.11)$$

This will result in a push or a pull translation of:

$$T = l_o - l_i = 0.421 \text{ mm} \quad (3.12)$$

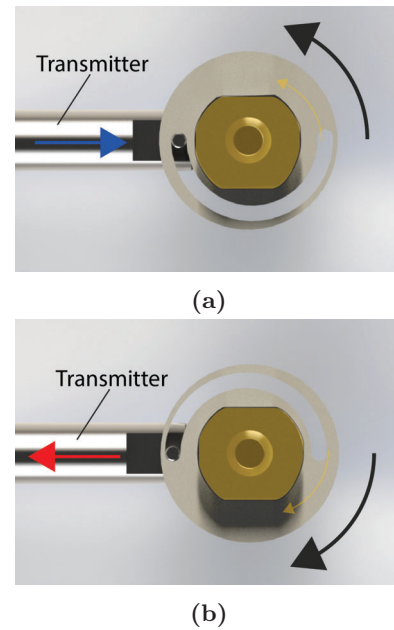
As a result, the translation of the transmitter must be 0.421 mm to make the proposed 25° steering angle in the tip. If the non-fixed side of the tip is pushed 0.421 mm, the tip will steer 25° upwards (red), as shown in Figure 3.4. By pulling it 0.421 mm it makes a rotation downwards (blue).

The mechanism to create a translation from a rotation is also reproduced from the ablation needle with some small adjustments. The rotational movement created in the actuator will be converted to a translation by using a wheel with an asymmetric circular slot (the spiral). A pin connects the transmitter to the circular groove. Figure 3.6 shows the mechanism where the asymmetric groove is in his zero degree angle state. The arrows represents the possibilities for the rotation movement given by the actuator. The distance from the middle point to the asymmetric groove is given by the red and blue line. The difference between those lines is two times the translation for the pull or for the push movement. Since this movement is 0.421 mm, the difference between the blue and red line is  $2 \cdot 0.421 \text{ mm} = 0.842 \text{ mm}$ .



**Figure 3.6:** The asymmetric groove at the unsteered configuration. Since the distance between the red and blue line are different, a pull or push translation can be created in the transmitter from a rotation.

Figure 3.7a represents the working principle if the lever is turned up in his maximum configuration. The circular groove will pull on the transmitter. How the joint mechanism in the tip will react depends on which half is fixed in the tip. If the upper half is fixed, the tip of the stylet will steer downwards. If the lower part of the tip is fixed, the tip will steer upwards. Figure 3.7b represents the opposite way when the actuator makes a rotation downwards, a push translation will be created in the transmitter. If the stylet and rigid cannula can be fixed in different orientations relative to the transmitter it gives the opportunity to choose the preferred way to steer the stylet. A push translation by turning up the lever can be result in a steering direction upwards, downwards or even to the left or right side. How the steering mechanism will react depends on the orientation of the fixation.



**Figure 3.7:** The situation of the asymmetric groove when the actuator is rotated upwards in (a) and downwards in (b).

### 3.1.3 | Actuator

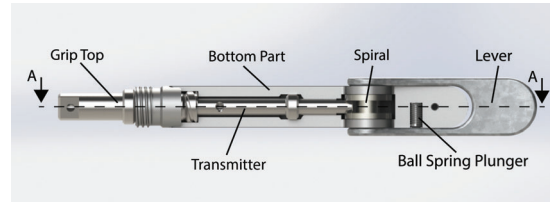
It is important that the actuation in the handle is easy to operate by the IR, where a controllable natural movement is desired. The steerable TIPS stilet will contain a planar steerable mechanism which is enough to fulfill the requirements. From the three options for the actuator which are given in Chapter 2.2.1, the lever gets the preference. This choice is mainly based on the design of the ablation needle where also a lever is used. It is easy to put force on the actuator and the lever will easily stay in the position in which it is turned. This gives an advantage that the steering angle can be adjusted in little steps or completely to its maximum steering angles. The joystick will be more fragile and the actuator will easily turn back to its zero state point if there is no pressure exerted. If the joystick is made on top of the handle like Figure 2.11b, an extra step is needed to create a rotational movement in the translation transmission. If the joystick is made at the end of the handle like the lever the transmission will be work more easily, but it would be hard for the IR to make controllable movements. Using the wheel as actuator, more force from the hand must be exerted on the wheel then the other options. Besides this, it would be hard to let the steering angle constant if the wheel is rotated in a specific position. This can be solved with a button which will fix the wheel or by adding more friction in the actuator. A stop button will require more components in the mechanisms, by adding more friction also more force from the hand is needed to steer the stilet.

### 3.1.4 | Handle

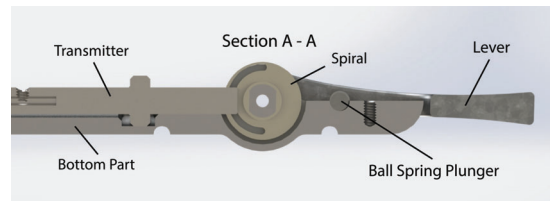
In the handle the translation transmitter and actuator comes together. The lever, as shown in the sketches, will already make a rotational steering movement. This steering movement will corresponds to the steering movement of the tip. To achieve this, the lever must be connected to the spiral, which is able to convert the rotational movement to a translation because of the asymmetric spiral. Since the lever is able to stand in any position, it becomes harder to find the unsteered configuration. To make this easier, a ball spring plunger is included in the design. A spring plunger consist of a bolt with a spring and ball inside, where the ball protrudes for a small part which is able to be pressed inside. The bolt is tightened in the handle. When the lever is at its unsteered configuration the protruding ball will fit exactly in a hole in the lever.

A top view of the final concept of the handle with transmission is shown in Figure 3.8. In this

figure the inside of the handle is visible since the cover is removed. All visible components are denoted. Figure 3.9 shows a section view of line A-A. From this section view the working principle of the transmission with the asymmetric spiral and the ball spring plunger is better visible.



**Figure 3.8:** The final concept of the handle with all sub parts denoted.



**Figure 3.9:** Section view of the final concept of the handle.

### 3.1.5 | Additional Requirements

Before the final design can be completed, there are still a few things that need to be taken into account during the design process. In order to make the procedure look like the procedure as it is performed now, some components have been adapted.

#### Luer Lock

Nowadays, the stilet is connected to the 5Fr catheter with a luer lock. This combination is pushed through the stiffening cannula and connected again with a luer lock (items 1, 2 and 3 in Figure 1.9). In order to keep these procedure steps the same during the procedure, a luer lock has been made in the front of the handle which can connect the stilet to the stiffening cannula. The integrated luer lock in the front is shown in Figure 3.10.

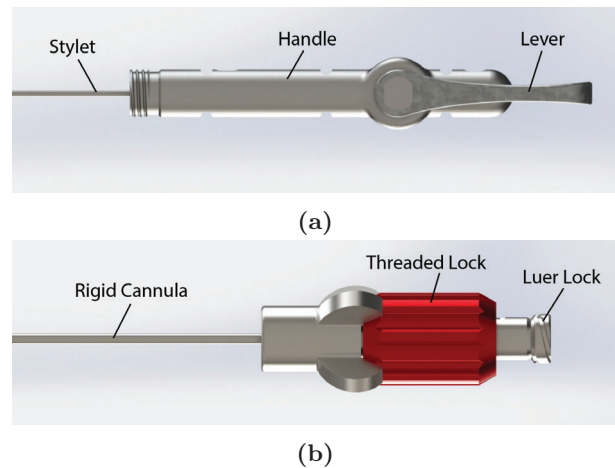




**Figure 3.10:** The luer lock integrated in the handle to connect the stylet with the stiffening cannula.

### Removable

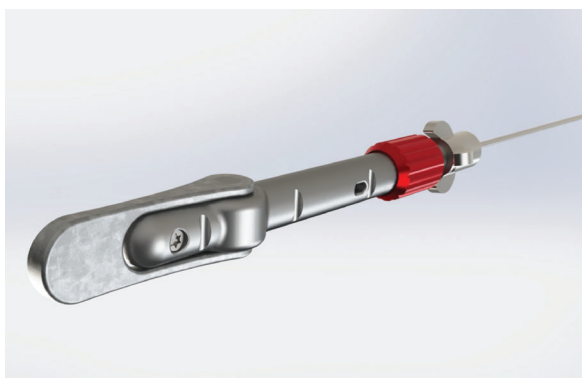
Because the rigid cannula is around the stylet, the 5Fr catheter can no longer be used. The rigid cannula must take care of the function of that catheter. Normally, after the intrahepatic puncture the stylet is removed from the stiffening cannula where the 5Fr catheter remains in the body. A syringe is coupled to this 5Fr catheter by means of a luer lock. A challenge for the new design was to get the stylet out of the body after which the rigid cannula remains with a luer lock connection. This problem has been solved by designing the steerable stylet in two parts as shown in Figure 3.11a and Figure 3.11b. One part can slide over the other, by eventually turning the parts a quarter turn apart, the systems click together and is able to steer. Both parts are coupled and locked by closing the threaded lock. Appendix C explains in more detail how the stylet can be removed from the rigid cannula during the procedure.



**Figure 3.11:** A schematic overview of the both parts. In (a) the part which includes the handle, translation mechanism, lever and stylet. In (b) the second part which can slide over the stylet and can be connected to the first part by turning the parts a quarter turn apart. The parts are connected by tightening the threaded lock.

### 3.1.6 | Final Concept

The final concept for the steerable stylet is represented by Figure 3.12. In Figure 3.12a the concept of the handle is shown with the lever as actuator and the threaded lock (in red) to fix both parts to each other. Figure 3.12b shows the tip of the stylet with the rigid cannula around. A key is attached in this cannula which ensures the fixation in the stylet so that push and pull translations can be performed by the lever. By turning the stylet relative to the rigid cannula a quarter apart the steering mechanism is deactivated and the parts can be disassembled.



(a) The final concept of the handle, with a lever as actuator.



(b) The final concept of the tip, with a compliant joint mechanism.

**Figure 3.12:** An overview of the final concept of the handle and the tip of the new steerable TIPS stylet.

## 3.2 | Prototyping

A prototype is built from the final concept. Construction drawings and CAD models are made for all sub parts in the design. This chapter describe some manufacturing methods and photos from the prototype.

### 3.2.1 | Manufacturing

Most parts for the prototype are manufactured with a 3D printer. For those parts CAD models are made which could be read by the print software. The outside of the handle parts and the threaded lock are printed in metal. The lever, griptop and wheel are printed in plastic. In addition to 3D printing, conventional turning and milling has been used to create the transmission parts and to finish the 3D printed parts. To get the slot with the round holes in the front part of the stylet, wire EDM is used. The rigid cannula around the stylet is a hollow nitinol tube that could be purchased with the right diameter. The key attached to the rigid cannula, through which the stylet can be locked, is also made of nitinol and is fastened by laser welding.

The luer lock in the front wheel of the stylet, to connect to the stiffening cannula, was removed from an old needle and glued back in this prototype. The luer lock inside the handle to connect the syringe is directly 3D printed in the griptop and afterwards processed with a file so the connection fits well.

A manual how to build the TIPS stylet is described in Appendix B.

### 3.2.2 | Prototype

The prototype is represented in Figure 3.13 by 4 different photos. In (a) a close up from the handle, where the red parts are 3D printed in plastic. The silver parts are printed in RVS and finished with turning and milling. In (b) a close up from the tip where the stylet sticks out a little bit from the rigid cannula. In (c) the stylet is disconnected from the rigid cannula by loosening the threaded lock and turning the handle a quarter turn in relation to the stylet. In photo (d) the stylet is totally removed from the rigid cannula.



(a) A close up of the handle of the steerable TIPS stylet.



(b) A close up of the tip of the TIPS stylet with the rigid cannula around.



(c) By loosening the threaded lock and turning the handle a quarter against the front part, the two parts can be disconnected.



(d) The front part of the handle is disconnected. The tip of the stylet is not able to steer since the steering mechanism does not have the fixation of the rigid cannula.

**Figure 3.13:** Photos of the prototype of the new designed steerable TIPS Stylet.

## 4 | Evaluation

To check whether the steerable stylet will reduce the complexity of the TIPS procedure the stylet is subjected to experiments where mechanical and medical characteristics will be evaluated. During the experiments the steerable stylet was used in combination with an adjusted stiffening cannula. This cannula has a pre-bent angle of  $\pm 18^\circ$  instead of the original angle of  $\pm 35^\circ$  because the stylet with rigid cannula was too stiff to make the angle. The following mechanical experiments are done:

- Exp 1: Maximum Steering Angle;
- Exp 2: Joint Stiffness;
- Exp 3: Force Exerted by Tip.

Next to the mechanical experiments, a visibility experiment is done, described in Chapter 4.2, and procedure are done with the stylet in a reproduced liver model, described in Chapter 4.3.

### Maximum Steering Angle

This experiment is performed to conclude whether the steerable stylet is able to steer the proposed  $25^\circ$  in both directions. This amount of degrees is found in Chapter 2.2.2 by looking into a reproduced CAD liver model. With a  $25^\circ$  steering angle the stylet is always able to reach the PV even when the stiffening cannula is orientated a bit to the side of the HV as shown in Figure 2.17.

### Joint Stiffness

This experiment is executed to assess stiffness characteristics of the joint mechanism. Experiments will be done with and without the stiffening cannula, with both orientations of the fixation and

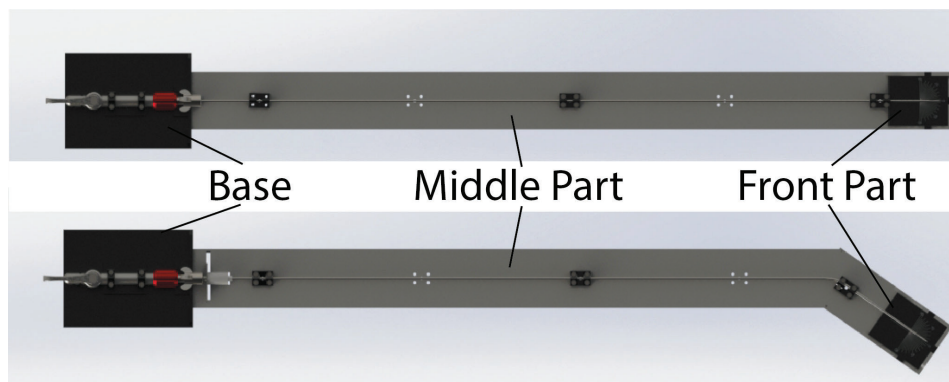
will be compared with the results of the original used stylet with and without stiffening cannula to conclude if the steerable stylet is better resistant against lateral forces during the intrahepatic puncture. With a better resistance, deflection through tissue will occur less quickly. Since the stiffening cannula will hardly bent during a TIPS procedure, the part of interest in the experiments with cannula, is the part of the stylet which sticks out of the cannula.

### Force Exerted by Tip

The third mechanical experiment measures the maximum forces which the tip of the stylet can deliver while making a steering movement (transverse forces). The force is measured while the lever is at its endpoint so the stylet will be in its maximum steering position. The experiments will be performed with and without cannula to see the influence of the stiffening cannula on the strength of the transmission and joint mechanism.

## 4.1 | Mechanical Characteristics

All mechanical experiments are done on a single experimental setup. The parts in the setup can be easily replaced or switched, enabling different experiments can be executed in succession. The experimental setup is discussed in more detail in Appendix E: Experimental Setup. Figure 4.1 shows a topview of both setups. One to evaluate the stylet, whereas the other setup is used to evaluate the stylet in combination with the stiffening cannula with the pre-bent angle in the tip. To get insight of the influences of the stiffening cannula, all experiments are performed on both setups.



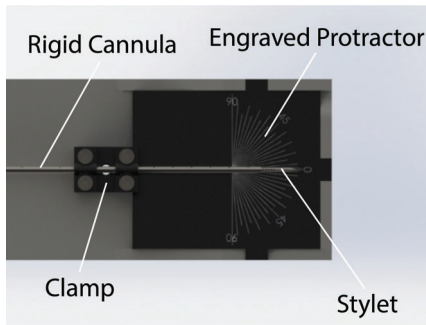
**Figure 4.1:** Schematic top view of both experimental setups for testing the steerable stylet. One setup to evaluate only the stylet, and another setup to evaluate the stylet in combination with the pre-bent stiffening cannula.

4.1.1 | Methods

Maximum Steering Angle

Figure 4.2 shows the frontal end of the setup, including the plate with a protractor engraved on it. This front part can be attached on both experimental setups and is aligned to zero degrees if the stylet is in an unsteered configuration. During the experiments the stylet is steered to the maximum angles in both directions by rotating the lever to its endpoints. The transmitter in the stylet is pushed and pulled with a maximum translation of 0.421 mm. If the stylet is steered in its maximum steering angle the protractor with stylet is photographed from above.

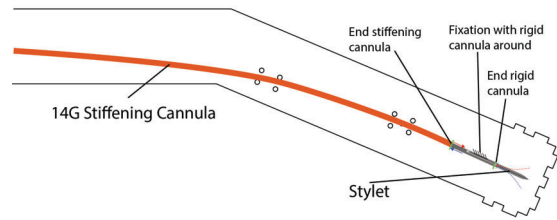
Both translations are executed randomly 5 times (n=5) in both experimental setups, in total 30 photos were taken. The experiments with only the stylet (St) are executed with the fixation to the left side (L). For the experiments with the 14G stiffening cannula (St + Can), a distinction was made for the orientation of the fixation with the rigid cannula. Experiments are done with the fixation to the left side (L) and to right side (R) to see if the orientation relative to the pre-bent stiffening angle will affects the steering angle. A summary for all experimental conditions are given in Table 4.1. Figure E.5c shows the experimental setup with cannula from above with, Figure 4.4 helps to explain the difference between the experimental conditions.



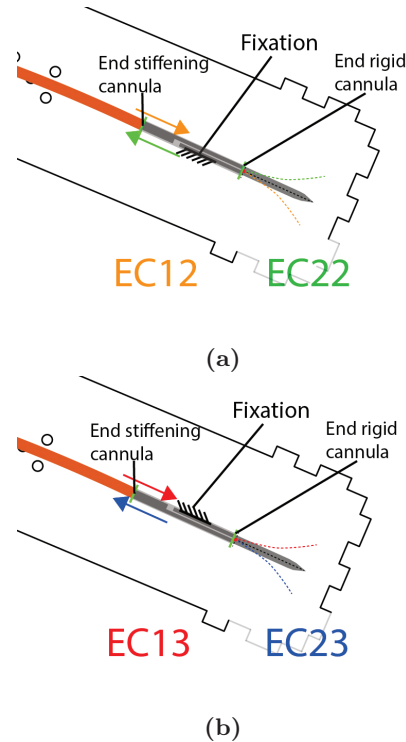
**Figure 4.2:** The front part of the steering angle experiments to define the steering angle of the stylet. The plate contains a protractor engraved on it and can be attached to both experimental setups.

**Table 4.1:** The experimental conditions for the steering angle experiment.

n = 5	L	R	L
	St	St + Can	St + Can
Push	EC11	EC12	EC13
Pull	EC21	EC22	EC23



**Figure 4.3:** The experimental setup with the 14G stiffening cannula.



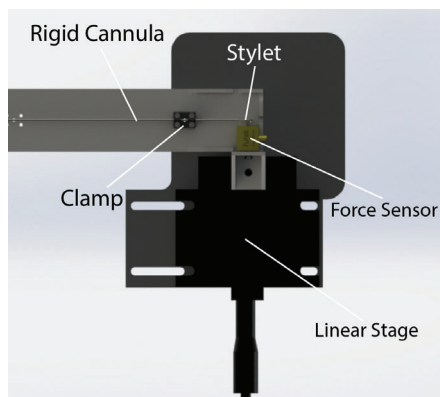
**Figure 4.4:** A schematic overview of the experiments with cannula with the fixation at the right (a) and left (b).

The photos were subsequently analyzed by drawing vector lines for the 0 degrees line, the 90 degree line and the line through the rotation point and the tip of the stylet in Adobe Illustrator. The angles between these vector lines were measured afterwards in Solidworks.

Since not all photos were taking exactly from above an angle error was introduced. The error was found by measuring the angle between the 0 and 90 degrees lines (measured 90 degrees), where after the measured 90 degrees angle was divided by 90. On the basis of this error, it was possible to calculate a better result for the real steering angle between the 0 degrees line and the line from rotation point to the tip by dividing the measured angle by the error.

### Joint Stiffness

The joint stiffness experiments are done with the help of a linear stage and a force sensor. Figure 4.5 shows the front part of the setup, attached to the middle part, with the linear stage and force sensor denoted. In all experiments there is chosen to do the translation in the push direction since it was too hard to clamp the tip of the stylet on to the force sensor for doing experiments in the pull direction. Controllable translations were made with the linear stage, the tip of the stylet was pushed in steps of 0.5 mm while measuring the force with a Futek 2lb (9N) sensor. In combination with a LabJack controller and the software LJStreamM from Labjack the forces were obtained.



**Figure 4.5:** The front part with linear stage and force sensor to find the joint stiffness (displacement-force characteristics) of the stylet.

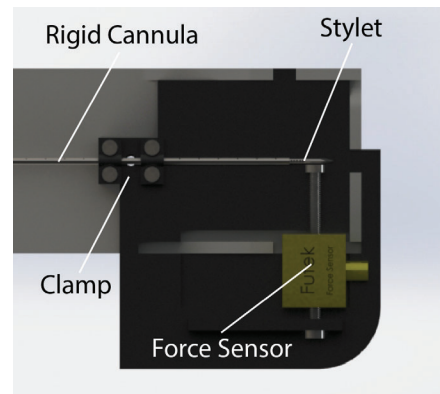
Both experimental setups, with and without stiffening cannula are used for the steerable stylet (SS) and the original stylet (OS). Also in this experiment a distinction was made for the measurements with cannula (C). The push executions are done on both sides of the stylet by rotating the stylet 180°, therefore the fixation is at the left side (L) or at the right side (R). In Appendix E the different setups are shown in more detail. All experiments are done with 5 repetitions ( $n=5$ ) where the tip of the stylet was pushed at least 3 mm away and force measurements were done after each 0.5 mm. Data from the different experimental conditions were obtained as described in Table 4.2, and analyzed afterwards in Microsoft Excel.

**Table 4.2:** Experimental conditions for the joint stiffness experiment. Both original and steerable stylet are tested with and without the stiffening cannula.

$n = 5$	SS	SSC	OS	OSC
L	EC11	EC13		
R	EC21	EC22		
-			EC33	EC34

### Force Exerted by Tip

In this experiment forces exerted by the tip of the steerable stylet are measured while the tip of the stylet was pushed against the Futek 2lb (9N) force sensor. With a LabJack controller and the LJStreamM software from LabJack, continuous measurements of the force sensor were done with a scan rate of 1000 Hertz. The steerable stylet was maximally steered by rotating the lever to its endpoint. The maximum force which was reached during such execution was taking out as value for each test. Figure 4.6 shows the front part of the experimental setup without stiffening cannula where the different components are denoted. The force sensor contains M3 bolts on each side. One is used to fix the sensor to the frontal plate, and the other is used for the alignment with the tip of the stylet. For each experimental condition, the bolt was adjusted to align the bolt until it made contact with the stylet when the stylet was at its unsteered configuration.



**Figure 4.6:** The front part to measure the force exerted by the tip.

In total, four different conditions were tested, with 5 repetitions. A summarize of the experimental conditions is given in Table 4.3. The numbers of the experimental conditions corresponds to the numbers used in experiment 1 and 2. The measured forces were afterwards analyzed in Microsoft Excel.

**Table 4.3:** Experiments to define the forces exerted by the tip of the stylet.

$n = 5$	SS	SSC
R	EC11	EC12
L	EC21	EC23

### 4.1.2 | Results

#### Maximum Steering Angle

The results for each experimental condition were put together in a data set in Microsoft Excel, all separate data from the measurements can be found in Appendix F. Figure 4.7 represents the results of the experiment in bar charts. The used colors for the results corresponds to the colors used in Figure 4.4. Clear differences can be seen in both transmission options, pulled or pushed. In EC11 (only stylet with push transmission) measurements, all results scores lower than average. A big difference can be seen compared to the results of EC21 (only stylet with pull transmission), which reach the biggest steering angles in average. The difference between the average in these both options is 63%.

The big difference between the steering angles for a push and pull transmission decreases in the experiments in which the stiffening cannula was used. The average values of EC12 and EC22 (stylet + cannula, fixation right) have a difference of 14.8%, where the push transmission (EC12) is able to bend further. In the measurements with the fixation to the left side, EC13 and EC23, the average angle during the pull transmission (EC23) is able to steer 13.8% further.

#### Joint Stiffness

All measured data obtained in this experiment are shown in Appendix F: Joint Stiffness. From the average data per experimental condition a line graph is made which is shown in Figure 4.8. An expected linear development can be seen in each condition. The values without cannula (EC11 and EC21) and the values with cannula (EC12 and EC22) are close together, the orientation of the fixation does not influence the characteristics.

The stiffening cannula does influence the joint stiffness. Less force was needed to push the tip 3 mm away for the steerable stylet with cannula (EC13 and EC22) than for the steerable stylet without cannula (EC11 and EC21).

From the results it also becomes clear that the steerable stylet is a lot stiffer than the original stylet according to the needed forces to push the stylet away. Again, the stiffness decreases slightly for the original stylet when it is tested in combination with the stiffening cannula (EC34) relative to the results obtained for the original stylet without cannula (EC33).

#### Force Exerted By Tip

The maximum forces are collected for each experimental condition in Microsoft Excel and plotted in box plots as shown in Figure 4.9. From the figure, EC21 can deliver by far the most force on the force sensor. The lowest measurement in this conditions is still higher than the forces delivered during the other experimental conditions. The medians of the other three conditions are close to each other, only a lot of deviation is visible by EC23. All separated measurements of this experiment can be found in Appendix F.

### 4.1.3 | Discussion

During the maximum steering angle and force exerted by the tip experiments, it sometimes happened that the stylet was not returned fully back to zero degrees when the lever was at its unsteered configuration after an execution. This problem can be caused by hysteresis in the material, friction or inaccurate manufacturing. The stylet is made of nitinol, a shape memory alloy, if the stylet is steered to its maximum angle, there will be some stresses in the joint mechanism. Since these stresses are small the material must be able to bend back to its unsteered configuration. If the stylet returns not directly back it can bend back with some delay due to the hysteresis. Since the stylet did not bend back at all, hysteresis seems unlikely. Another possibility for this problem is friction in the transmission. If the lever goes to the unsteered configuration with friction between the translator and the asymmetric spiral, it can happen that the translator is not rotated back to its unsteered configuration, wherefore the tip of the stylet still is in an angle. Next to the friction, it is also possible that there is a slight clearance between the lever and the transmission, or between the transmission and the fixation at the tip. By returning to the unsteered configuration after a maximum push or pull movement, a slight clearance can cause the stylet to translate the transmission little less far by turning it to zero degrees. To avoid this problem, a check took place after each execution to see if the stylet was at zero degrees. If not, the stylet was steered first to the other side and back. If that still did not work, the stylet was bend back by hand above the zero degree line on the protractor or against the force sensor.

For all experiments it was important to clamp the steerable stylet accurate in the setup so the steering plane was perfectly aligned. Otherwise this could result in small errors. If the stylet does not steer parallel to the protractor in experiment 1, and the photo is taken from above, other values

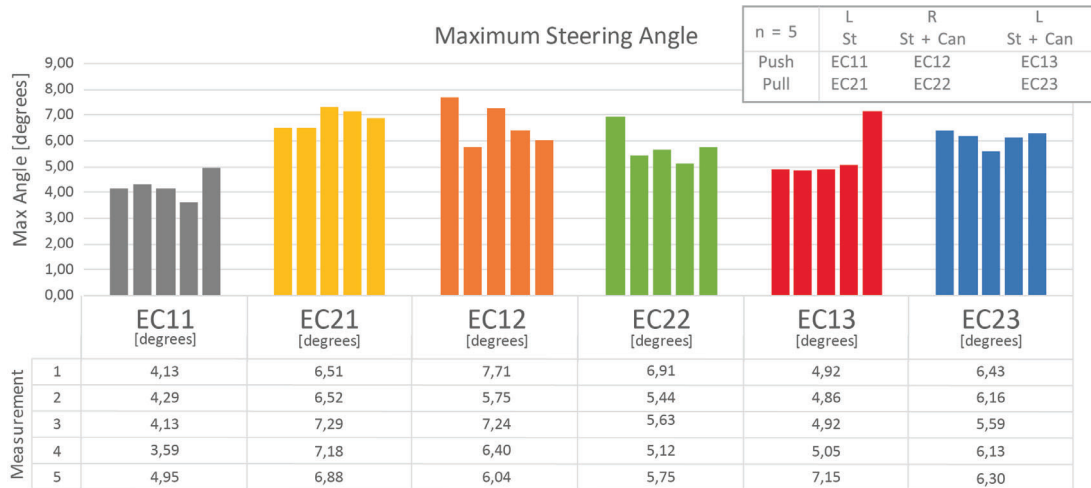


Figure 4.7: The results of the Maximum Steering Angle experiment. All results are shown in bar charts for each experimental condition.

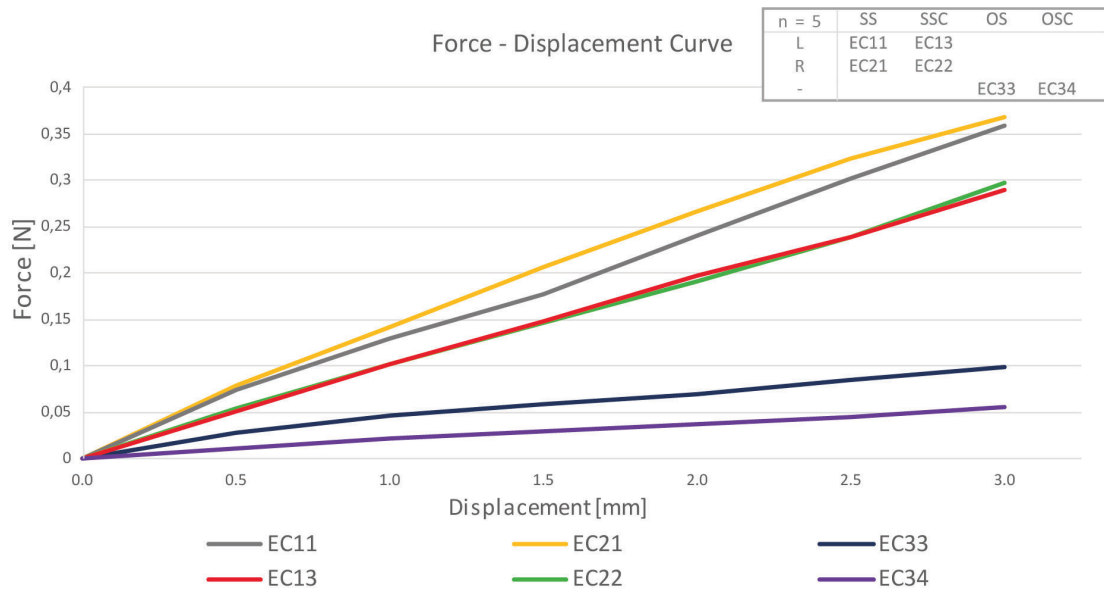


Figure 4.8: The results for the Joint Stiffness experiment. A line is drawn between the measurements after each 0.5 mm. From the lines a linear development is visible for each experimental condition.

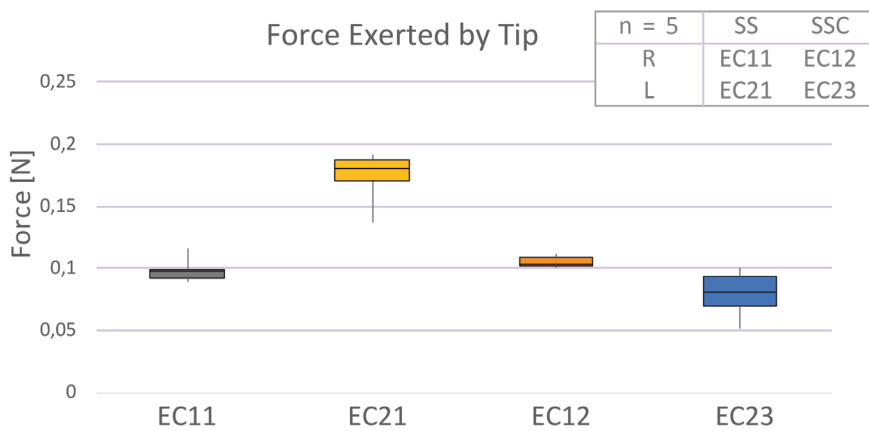


Figure 4.9: The results from the Force Exerted by Tip experiments, depicted in box plots.

are found for the steering angle. In experiment 2 bigger errors will be obtained if the push direction of the linear stage is not parallel to the steering plane, the linear stage will try to push the stylet in a plane where it is not able to steer. As a result, higher forces for the displacement are needed. In experiment 3 the best result will be achieved when the steering plan is perpendicular to the force sensor. If not, the stylet will not steer exactly towards the force sensor wherefore the measured forces will be lower. The handle of the stylet can be clamped in two ways, the lever will be aligned correctly relative to the experimental setup. However, the stylet and cannula can be loosened and turned with respect to the lever, still some steering plane errors could be occur. Before the experiments were executed the stylet was steered to both directions to see by eye if the steering plane was correctly aligned relative to the protractor, the linear stage and the force sensor.

For accurate measurements during experiment 2 and 3, it was important to define the start position of the stylet before measurements were done. This start position was defined with a first non-measured execution where the stylet was straight and made contact with the force sensor. In experiment 2 the linear stage was translated towards the tip of the stylet until there was contact. In experiment 3, the M3 bolt was adjusted until contact between the bolt and stylet was achieved. After each execution for the same experimental conditions, a small check was done to see if the stylet made contact again with the force sensor at its starting point. If not, the stylet was steered to the opposite direction and back, or bend back by hand.

During the executions in experiment 3 the tip was sometimes shifted up or down during the execution. The measurement can be made more accurate by replacing the bolt with another component where the tip of the stylet fits exactly in.

#### 4.1.4 | Conclusion

From experiment 1 it becomes clear that the stylet is able to steer in both directions. The mechanical transmission is a good solution to create a steer movement in the tip, even with the very long distance ( $\pm 60\text{cm}$ ) between the proximal end (actuator) and the distal end (joint mechanism). The stylet is not able to bend the proposed degrees as described in Chapter 2.2.2. From all the measurements the maximum value what is measured was  $7.71^\circ$  instead of the proposed  $25^\circ$ . Small differences are found for the different orientations of the fixation in combination with the stiffening cannula, where it is most striking that the push transmission can steer further with the fixation to the right (EC12) and the pull transmission further with the fixation to the left (EC23). In both orientations the stylet steers further in the same direction of the curve of the pre-bent stiffening cannula.

According to experiment 2 the steerable stylet is much stiffer than the original one wherefore it is better resistant against lateral forces. As a result, the steerable stylet should deflect less quickly if it is punctured through the liver tissue during the TIPS procedure. Since deflection is now a problem during the intrahepatic puncture step, this outcome is positive in order to reduce the complexity of the intrahepatic puncture step.

The steering mechanism is also capable of delivering power during steering. In experiment 3 the transmission mechanism in the shaft was strong enough to transmit the push and pull movements of the translator to the tip where it was able to steer against the force sensor. To conclude if the forces are high enough to be able to steer while the tip is already in tissue, test procedures with a real liver or a representative liver model must be done.

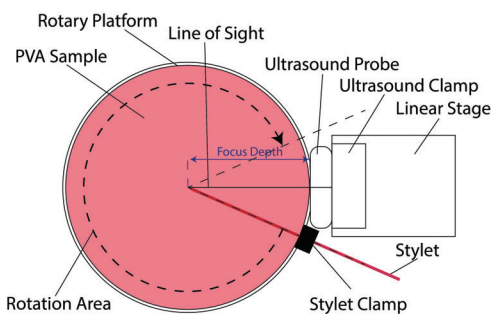


## 4.2 | Visibility in Ultrasound

A fourth experiment is done to check the visibility with ultrasound of the steerable stylet, where the stylet is punctured into a PVA sample. Van de Berg et al. [81] studied visibility and echogenicity characteristics of different stylets. Visibility is the ability to be seen, echogenicity is the ability to generate (sound) reflections [81]. For the steerable stylet, visibility experiments were done on the same setup. A more detailed system description, used materials and how the setup is made, can be found in the article of Van de Berg et al. [81]. The used associated files like the Arduino C and Matlab code, and the CAD models for the 3D printed and laser cut parts can be found on GitHub (<https://github.com/misitlab/needles-in-ultrasound>).

### 4.2.1 | Methods

The setup exists of a rotary platform, a PVA sample, a clamp for the stylets, a fixed ultrasound probe and a monitor. The PVA sample is made with a radius and height of 100 mm, the image of the probe is visible on the monitor and recorded, the rotary platform is driven by a stepper motor connected to an Arduino. During the experiments the stylet is punctured into the PVA sample till a depth of 100 mm, and is clamped. Next, the stylet with sample will be rotated while contacting the ultrasound probe for 310° from  $\pm 25^\circ$  till  $\pm 335^\circ$ . Figure 4.10 shows a schematic topview of the setup with some components denoted.

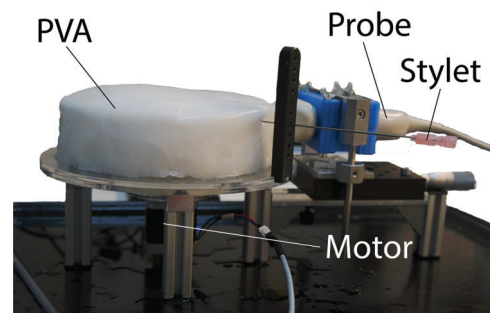


**Figure 4.10:** A schematic topview of the visibility setup. The stylet, punctured in the PVA sample, is rotated around the ultrasound probe. The image of the ultrasound probe is shown on the monitor and recorded.

This experiment is performed with 3 different stylets. A 18G trocar needle, a steerable ablation needle with rigid cannula, and the steerable ablation needle with rigid cannula and a 6F Flexor Ansel Guiding sheath made by Cook Medical ©[82]. The steerable ablation needle contains the same tip and steering mechanism as the steer-

able stylet for the TIPS procedure. Since the shaft of this ablation needle is way shorter ( $\pm 15\text{cm}$ ), it is easier to clamp the needle for this experiment. The shaft of the steerable TIPS stylet is too long to do accurate measurements. During the rotation of the table, many vibrations and deflections will occur in the long rigid cannula and stylet with the chance of damage and influences on the measurements.

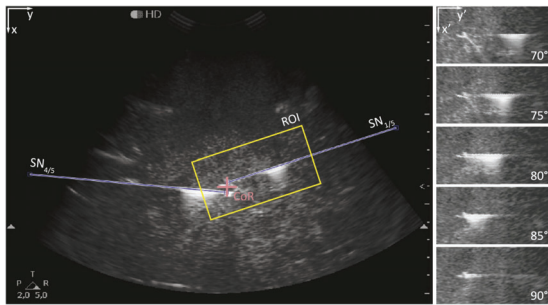
The 18G trocar needle is included in this experiment to compare the obtained results with the results from the article to determine whether the setup is properly reconstructed. The experiment with the extra sheath is done for N.J. van de Berg to see how the visibility of the shaft is influenced by the sheath. Figure 4.11 shows a picture of the setup where the 18G trocar needle is located at its starting position, punctured in the PVA sample.



**Figure 4.11:** A picture during the visibility experiments. Here, the 18G trocar needle is at its starting position of the rotation area.

Each needle is punctured 10 times on different heights in the PVA sample. The PVA sample is rotated while contacting the probe and the image of the probe is recorded. Afterwards, all recorded videos are analyzed in Matlab for  $25^\circ$  to  $180^\circ$  rotation area. The other side from  $180^\circ$  till  $335^\circ$  is assumed as symmetric. Figure 4.12 shows a segmentation step which must be done manually after a video was loaded. This segmentation step was done at one-fifth and four-fifth of the video duration, it enables Matlab to synchronize the video with the angular motion of the needle. Afterwards, Matlab is able to calculate the contrast to noise ratio (CNR), it measures the contrast ratio between the tip (white stripes in Figure 4.12) and the darker area just above the tip for the whole rotation area. For the shaft visibility this analyzing procedure is the same. Besides the visible stylets at one-fifth and four-fifth of the rotation duration, also the region of interest (ROI) and center of rotation (CoR) are denoted. The ROI is given by a filtering algorithm developed by N.J. van de Berg. The average

point of the tip during the rotation is mentioned as the CoR. The article of Van de Berg et al. [81] can be consulted for a detailed explanation.



**Figure 4.12:** The manual segmentation step analyzing the videos in Matlab. The manual input is given by  $SN_{1/5}$  and  $SN_{4/5}$ , the endpoints of the line over the styllet are set by hand. The CoR is the average point where the tip is rotation around. The ROI is given by a filtering algorithm. Reprinted from Van de Berg et al.[81].

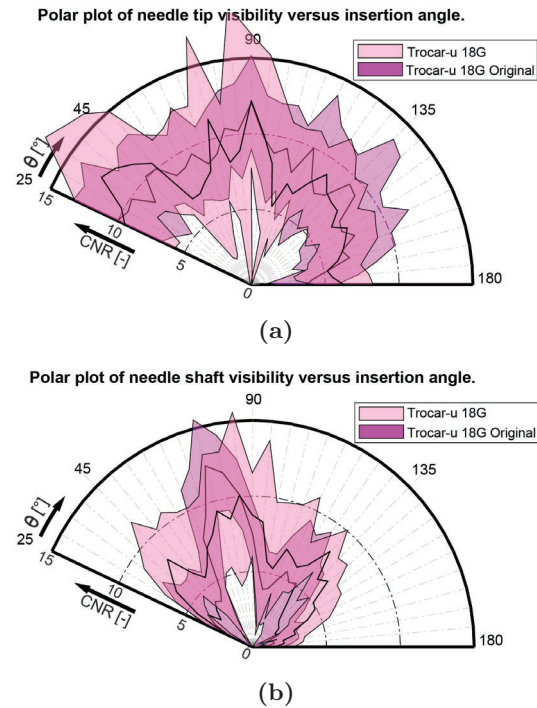
As a result, Matlab plots the visibility of the tip and the shaft. These plots are made with the contrast to noise ratio (CNR) as radial coordinates against the insertion angle ( $\theta$ ) as angular coordinates. The median from the measurements are shown as a darker line in the plots. The colored areas around the median represents the median  $\pm$  the standard deviation contours.

#### 4.2.2 | Results

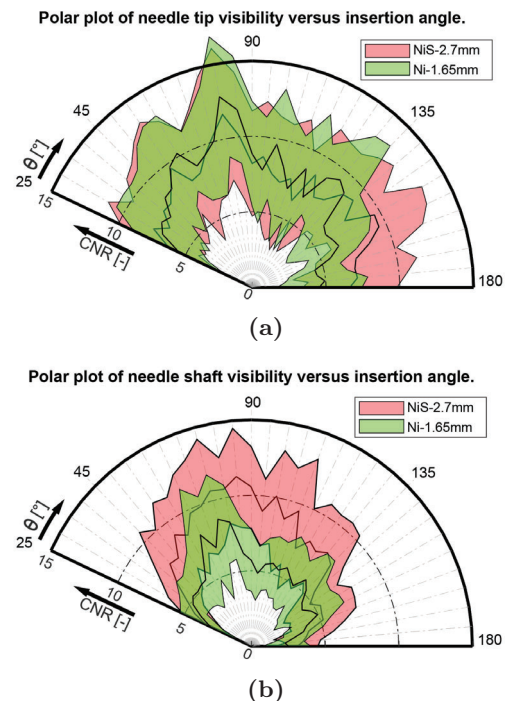
Figure 4.13 shows the visibility results from 18G trocar needle from the article (Original) and from this experiment. Both results, for the tip and the shaft, looks similar. The peaks in the plots are almost at the same angles where the 18G trocar needle is the best visible around  $90^\circ$ .

In Figure 4.14 the visibility results for the nitinol tip and shaft are shown for the steerable styllet with rigid cannula (Ni-1.65mm) and the steerable styllet with cannula and sheath (NiS-2.7mm). The nitinol trocar tip is the best visible around  $90^\circ$  and the sheath around the styllet gives a positive effect for the visibility of the shaft since the CNR values are higher.

The visibility of the tip of the steerable styllet (Ni-1.65mm) looks similar to the 18G trocar needle. Both are visible in a wide range with a peak around  $90^\circ$ . The visibility of the shaft scores lower then the shaft of the 18G trocar needle.



**Figure 4.13:** The results for the 18G trocar needle. In (a) the results for the visibility of the tip, with the results from this experiment and the original one from the article of Van de Berg et al. [81], in (b) the results for the visibility of the shaft.



**Figure 4.14:** The results for the visibility of the steerable styllet with rigid cannula (Ni-1.65mm) and for the styllet with rigid cannula and sheath (NiS-2.7mm). In (a) the results for the visibility of the tip, in (b) the results for the visibility of the shaft.

### 4.2.3 | Discussion

Some small differences between the results for the 18G trocar needle are visible in the results, especially the wider range of the visibility of the shaft. These differences may be due to the fact that the PVA sample was a bit different. Matlab looks at the contrast to noise ratio in the recorded videos of the image of the probe, if a PVA sample is used that is less homogeneous, it will produce more noise during ultrasound measurements which will influence the outcome.

Looking at the results for the steerable stylet, the visibility of the tip contains a lot of similarities. This was also expected since the tip is exactly the same, only the shaft contains a sheath. Looking at the results for the visibility of the shaft it appears that the sheath have a positive effect on the visibility. Comparing the results for the shaft with the results from the article, the steerable stylet with flexor sheath scores one of the best in a wide range. The flexor sheaths of Cook Medical© contains a radiopaque band, incorporated within the sheath material [82]. This radiopaque band helps to reflect the sound waves pulsed by the ultrasound device wherefore the visibility of the shaft increases.

The visibility of the steerable tip scores in general very well compared to the results of the other tips in the article. The steerable stylet is visible in a wide range with high peaks. In the article, stylets with a conical tip, a bevel tip, and a diamond tip are tested where the bevel and diamond tip scores the best for the tip visibility. This outcome is due to the fact that these tips contain flat surfaces which are able to reflect the ultrasound better. Since the steerable stylet is made with a trocar tip, with 3 flat surfaces, it is well-visible over a wider range.

### 4.2.4 | Conclusion

First of all, it is possible to reproduce the visibility experiments to get insight in the visibility of needles since the 18G trocar needle results are similar then the original ones from the article. In the article the trocar and Chiba needles scores the best for the tip visibility and the EDM-treated shafts for the shaft visibility. The tip visibility of the steerable stylet is similar to the 18G trocar needle. The shaft visibility of the steerable stylet with sheath is similar to the EDM-treated shafts. Without sheath the shaft scores low but is visible in a wide range due to the cut-outs in the joint mechanism. In general, tip shapes with flat surfaces, kerfed-patterns in the shaft or a Flexor Ansel Guiding sheath improves the visibility with ultrasound. For now, the steerable stylet without sheath scores still above average compared to the results of the other needles in the article of Van de Berg et al. [81]. The visibility could be improved by integrate a radiopaque band into the design of the steerable TIPS stylet.

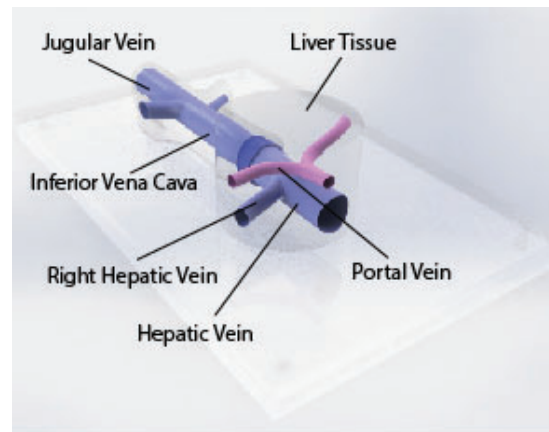
### 4.3 | Liver Model

For testing the steerable stylet, a PVA liver model was made to see if the steerable stylet is able to perform the TIPS procedure and if it eventually will reduce the complexity of the intrahepatic puncture. The liver model only contains the veins which are of interest during a TIPS procedure with some "tissue" around.

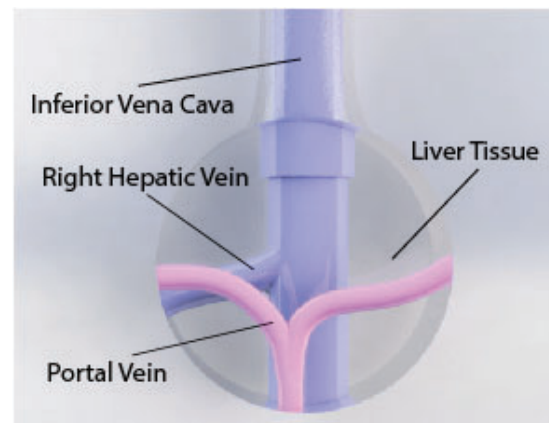
The liver model is made of PVA. Besides mixing the PVA grains with water, as described in the article of De Jong et al. [16], cooling fluid is added to the mixture since closed molds are used for making the samples. With only water, the PVA mixture will expand too much during the freeze-thaw cycles so the molds would break apart. Appendix D described a more detailed system description, which materials are used and how the test model is made.

The main goals of this liver model is to test if the steerable stylet is able to do the intrahepatic puncture during the TIPS procedure, and if it is able to steer while it is in the PVA sample. The TIPS procedure will be performed as realistic as possible, it is tested in combination with the stiffening cannula. To check if the steerable stylet is able to steer in the PVA sample both setups, with and without cannula are tested. In future, other new instruments can be tested on the model and/or new IRs can train the procedure before doing ex-vivo or in-vivo procedures.

The test model represents the navigation path through the veins, from the jugular vein to the portal vein. The IR is able to guide the catheters, cannula and stylet through the jugular vein, inferior vena cava into the RHV. From here, the IR have to perform the intrahepatic puncture to enter the PV. Figure 4.15 shows a CAD model of the liver model. In blue the jugular vein and HV, in pink the PV. A top view of the liver part is shown in Figure 4.16. Since the "tissue" is made transparent in this figures the inner veins are visible. In the final model these veins will not be visible from the outside of the model since the PVA will not be transparent. The IR has to use ultrasound or CT scans to locate the veins and the instruments. The sound waves transmitted by the ultrasound device travels into the liver model until they hit a boundary. Some of the sound waves will be reflected to the ultrasound device where others travels further. By filling the veins with water the sound waves will be better reflected then in air, wherefore the veins becomes better visible when the whole liver model is in water.



**Figure 4.15:** A schematic overview of the liver model, the model is made transparent to see the internal veins.



**Figure 4.16:** Top view of the liver part in the test model. The hepatic vein (blue) and the portal vein (pink) are clearly visible in the liver.

#### 4.3.1 | Evaluation Method

To evaluate the test model, an appointment was made with an IR at the Erasmus Hospital in Rotterdam. Here, the IR has done the TIPS procedure with an original RUPS access set and with the adapted stiffening cannula with the steerable stylet. The entire set-up was placed in a large bin filled with water to ensure all veins were filled with water, making them better visible with ultrasound. Figure 4.17 shows pictures of the IR and the liver model, the photos were taken during the evaluation procedures.

In total, the procedure was performed with 3 different access sets:

- OC OS: Original Cannula + Original Stylet;
- AC OS: Adjusted Cannula + Original Stylet;
- AC SS: Adjusted Cannula + Steerable Stylet.

The adjusted cannula (AC) is the stiffening cannula which was bend back from a pre-bent angle

of  $\pm 35^\circ$  to  $\pm 18^\circ$ . This was necessary because the steerable stylet was not able to push through the pre-bent angle of the original stiffening cannula. A fourth option as access set with the Original Cannula + Steerable Stylet was therefore not taking into account in the evaluation.

During the procedure, the time was measured to bring the stylet from the jugular vein into the PV by puncturing the stylet from the RHV through the tissue into the PV. With the knowledge of both access sets, the steerable stylet could be evaluated with a questionnaire after the procedures. In the end, procedure steps are done to remove the stylet from the rigid cannula and tests are done to push the stylet through a PVA sample while steering to see if the transmission could deliver enough force. To conclude of the steerable stylet could reduce the complexity of the intrahepatic puncture it must be visible with ultrasound, able to steer into the direction of the PV, better resistant against deflection and reduce the procedure time by entering the PV with one attempt.



(a) The IR performs the intrahepatic puncture step with the steerable stylet in the liver model. The image of the ultrasound probe is visible on the monitor.



(b) A close up from the Liver Model in water. The steerable stylet is first placed in the RHV with the use of the stiffening cannula. Afterwards, the steerable stylet will be pushed through the tissue from the RHV to the PV.

**Figure 4.17:** Pictures taken during the evaluation of the steerable stylet, tested on the liver model.

### 4.3.2 | Results

The procedure was performed with 3 different access sets described in the Methods section. During the evaluation the IR first tried to enter the RHV with the different access sets. If it was possible, the time was measured to bring the stylet from outside the liver model, into the jugular vein until the PV was entered. The results are summarized in Table 4.4 with some comments of the IR.

After the procedures with the different sets the IR answered a questionnaire to evaluate the experiences of the steerable stylet. The results of this questionnaire are shown in Table 4.5.

As last, the steerable stylet was able to steer while it was punctured into the PVA sample with and without cannula. In the Erasmus Hospital a study was started to make stiffer PVA samples wherefore the test also could be done with two other stiffer samples. In this samples the stylet was still able to steer with and without cannula. The transmission could transfer enough power exerted by the hand to the joint mechanism to perform steering movements inside the liver tissue. Curved puncturing paths were obtained from the ultrasound device.

**Table 4.4:** Time results from the TIPS procedures in the Liver Model.

#	Set	Time [min]	Reached the PV	Comment
1	OC OS	2:10	Yes	-
2	AC OS	-	No	The angle of the adapted cannula is too small. Not able to turn the cannula in the direction of the PV.
3	AC SS	5:00	No	The RHV can be reached with steering the tip of the stylet. The stylet can not steer far enough to puncture afterwards into the PV.

### 4.3.3 | Discussion

The first thing that stood out for the IR was the steering angle of the stylet, it was able to steer, but the angle was too small. Also the adapted stiffening cannula brought more problems than previously thought. With the new angle of  $\pm 18^\circ$  in the tip the IR was not able to get the cannula inside the RHV, what is a necessary step in the TIPS procedure. Although, the IR was able to place the steerable stylet in the RHV by placing the stiffening cannula as far as possible in the direction of the RHV and then push the stylet through with a steering movement. Since the stylet was already

**Table 4.5:** Results from the questionnaire after the TIPS procedures with different access sets.

Questions	Strongly Agree	Agree	Neutral	Disagree	Strongly Disagree
<b>Steer ability</b>					
Is it easy to control the steering movement of the stylet?		x			
Is the lever as actuator easy to use?		x			
Is it easier to enter the PV with the steerable tip?				x	
Is the stylet able to steer when it is in PVA?		x			
<b>Visibility</b>					
Is the steerable stylet visible?	x				
Is the steerable stylet better visible then the original one?		x			
<b>Stylet Design</b>					
Is the stylet easy to remove from the rigid cannula?		x			
Can the syringe be easily connected to the stylet?		x			
Is the stiffer steerable stylet positive for the procedure?		x			
<b>Liver Model (test model)</b>					
Is the test model a good representation to test and train the TIPS procedure?			x		
Is the PVA sample a good representation of sick liver tissue?				x	

steered to one direction to enter the RHV, it was too hard to rotate the whole set (stiffening cannula + steerable stylet) to orientate the stylet in the direction of the PV.

For better test and training sessions the model must be slightly adjusted. In the liver model the PVA was now too soft according to the IR. The mixture was made with 8% wt PVA grains which is already way more than the 4% wt for healthy liver tissue according to De Jong et al.[16]. During the mixture step for this sample, where the PVA is heated up to 90° Celsius, the bottom layer was burned in the borosilicate glass. This can be due to the fact that 8% wt PVA grains are not able to dissolve enough in the mixture of water and cooling liquid, that the mixture was heated too fast, or that the mixture rotated not fast enough. An additional result could be that some PVA grains were burned and the sample had less weight percentage PVA grains then additionally thought.

Besides the stiffness problems of the sample, the IR concluded that the diameters of the veins were correct, only that the PV was located a bit too much superior (in the direction of the head). To make a better liver model the liver mold must be adjusted to place the PV more inferior (direction to the legs).

#### 4.3.4 | Conclusion

First of all, the IR was very enthusiastic about the steerable stylet. A mechanical steerable tip with such long and thin shaft was something new. The stylet was easy to use and to control, it was well visible with ultrasound, able to steer when it was already in tissue and removing the stylet from the rigid cannula also worked well. Unfortunately, the steerable stylet was not sufficiently adjusted to the application. It was hard to get the stylet into the RHV with the adjusted cannula. Besides this, the original stiffening cannula could not be used with the steerable stylet since the rigid cannula was too stiff. The only set what was now able to enter the portal vein in the liver model was the original RUPS access set.

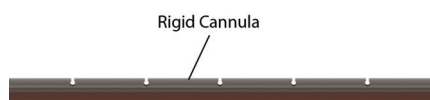
Next to the stylet, the liver model is a good representation to test or train the TIPS procedure. The closed molts in combination with the PVA mixture with cooling liquid are an outcome to create models with veins inside. By placing the setup in a bin with water, it was possible to test and train the procedure with ultrasound. The liver model can be made more complete by optimizing the veins to the exact location and do more research on the stiffness of sick liver tissue. If those issues are solved such liver model can be used to train the procedure or to test new instruments.

## 5 | Discussion

In this graduation project mechanical experiments, a visibility test and test procedures on a liver model are done to determine if the steerable stylet could reduce the complexity of the TIPS procedure. For the mechanical characteristics the maximum steering angle, joint stiffness characteristics and the force exerted by the tip while steering were measured. Besides the mechanical experiments, the stylet is also subjected to a visibility experiment with ultrasound and test procedures were performed in a liver model made of PVA. During these experiments and test procedures an adapted stiffening cannula was used since the angle in the original pre-bent stiffening cannula, item 3 in Figure 1.9 was too sharp ( $\pm 35^\circ$ ) wherefore the steerable stylet with rigid cannula was not able to push through.

### 5.1 | The TIPS Stylet

Since the rigid cannula was too stiff to push through the original stiffening cannula, some adjustments in the rigid cannula are tried during the design process to make it more flexible without changing the material. A number of grooves were made in the area where it had to overcome the angle in the stiffening cannula. Figure 5.1 shows a schematic overview of the grooves in the cannula. A round surface at the end of each groove was chosen wherefore the tensile and pushing stresses could be absorbed in a bigger area. Since the rigid cannula had to fulfill the function of the 5Fr catheter (Figure 1.9, item 2), it was sealed with a flexible thin sleeve. This makes the rigid cannula airtight so it could be pulled vacuum when the syringe was connected after the intrahepatic puncture.



**Figure 5.1:** The adapted rigid cannula with grooves in it to make it more flexible in the area where it has to bend in the stiffening cannula.

After the prototype was made a few test were done. A groove got stuck behind the stiffening cannula causing the rigid cannula to break at that point. Before the experiments with the prototype were executed, the rigid cannula was replaced by a new one without the kerfed pattern. This made the rigid cannula more stiff wherefore it became not able to push through the stiffening cannula. To fulfill all experiments with and without stiffening cannula, the angle of the stiffening cannula has been bend back from  $\pm 35^\circ$  to  $\pm 18^\circ$ . During the tests in

the liver model it became clear that the adapted stiffening cannula was not able to enter the RHV. Better results for these tests, and therefore for the TIPS procedure, will be obtained when the original stiffening cannula can be used in combination with the steerable stylet. To achieve this the rigid cannula must be redesigned to make it more flexible but still robust.

### 5.2 | Experiments

Looking into the results for all three mechanical experiments, it stands out that the orientation of the fixation does not show big differences in the measurements. Although, the stiffening cannula shows some influence on the mechanical characteristics which was already expected before the experiments were performed since the pre-bent angle of  $\pm 18^\circ$  could influence the push and pull translation in the transmission. In all three experiments the results with stiffening cannula were closer together relative to the results for the stylet without cannula.

Comparing the results in experiment 1 with cannula, the push transmission with fixation to the right (Exp1. EC12) and the pull transmission with fixation to the left (Exp1. EC23) were able to steer further. Both results followed the curvature of the pre-bent stiffening cannula. This outcome could be explained by a small pre-tension in the transmission due to the angle in the stiffening cannula. The outer radius of the transmission in the angle will be a bit longer and the inner radius a bit compressed. The steering angle towards the angle of the stiffening cannula will have an advantage since the transmission is already a little bit in a steering movement. With a small pre-tension in the transmission the results for experiment 2 and 3 with cannula were expected to be higher than the results without cannula. Due to the pre-tension it would be harder to push the stylet away in experiment 2 and since the pre-tension would give an advantage in the steering angle, more force on the force sensor was expected in experiment 3.

For the joint stiffness characteristics in experiment 2, all measurements without cannula, even for the original stylet, are higher. More force was needed to push the tip away. In other words, the stiffening cannula causes the stylet to become less stiff. The same happened with the results in experiment 3. The forces exerted by the tip for the pull transmission without cannula (EC21) resulted in the highest force where the results in combination with the stiffening cannula became closer together with both orientations, but lower.

Since both expectations did not come out, the results with stiffening cannula were lower for experiment 2 and 3, the higher steering angles in experiment 1 must be caused by something else. It became clear that the experimental setups were not properly constructed. All experiments without cannula were done in a proper way, the last point where the stylet was clamped was at the position where the stiffening cannula normally ends. For the experiments with cannula the last clamp was not placed at the end of the stiffening cannula but a bit towards the handle. This gives more freedom to deflect when the experiments are executed. During the pushing movements in experiment 2, the joint mechanism will first deflect in its steering plane, in combination with the stiffening cannula the stylet had a longer length where it could deflect, and even the stiffening cannula could deflect a bit till the point where the clamp was placed. Since the clamp is placed more towards the handle for the experiments with stiffening cannula, this explains the results where less force was needed to push the stylet 3mm away. In experiment 3 the same deflection problem occur. By steering the stylet towards the force sensor, deflection will occur till the point where the last clamp is placed. Since the length of the tip till the last clamp differs in both setups it can be explained wherefore the stylet without cannula can deliver more force towards the force sensor then the stylet with cannula since more deflection was occurred.

Comparing results from experiment 1 with experiment 2 with the same experimental conditions, it became clear that more force was needed in experiment 2 for the stylets with a small steering angle. Less friction will occur by pushing away the stylet within the steering area. Higher forces will be needed when the stylet is pushed further than its steering area, this outcome was expected since the joint mechanisms is more flexible then the nitinol stylet and rigid cannula. Comparing the results from experiment 1 with experiment 3 with the same experimental condition, the conditions without cannula shows similarities. The pull transmission could make a bigger steering angle and deliver more force towards the force sensor while steering, where the pull transmission scores in both experiments lower. The results in combination with the stiffening cannula shows big differences which can be explained again by the different distances between the tip and the last clamp in both experimental setups. During the maximum steering angle experiments the stiffening cannula will deflect in a positive way towards the steering movement for the experimental condi-

tions EC12 and EC23. During the maximum force exerted by the tip experiments with the stiffening cannula (EC12 and EC23), the cannula will deflect in a negative way wherefore the maximum measured force becomes lower then expected obtaining the results from experiment 1.

### 5.3 | Visibility

For this project the visibility tests were done with the steerable ablation needle assuming that the tip and joint mechanism were exactly the same. The joint mechanism was made with wire EDM where the nitinol staff was aligned by a person. Besides this, the groove for the key in the tip and the trocar tip itself are made by conditional milling. Even though this machining techniques are very accurate, it cannot be assumed that the mechanism and the tip of the ablation needle exactly match to the steerable stylet. Still the visibility tests were done with the ablation needle since the setup was not made for the long shaft of the steerable stylet. During the visibility experiments positive outcomes were found for the flat surfaces in the tip, the kerfed patterns in the shaft and the use of a sheath with a radiopaque band inside. In the current access set for the TIPS procedure, a flexor sheath around the shaft can not be used since it will not fit through the stiffening cannula. Incorporating a small piece of radiopaque band at the distal end, in the stylet or rigid cannula, can increase the visibility even more.

### 5.4 | Liver Model

The liver model was a good testing model. Since the test model was made of separated parts, the liver part could easily replaced after several puncturing attempts to avoid the stylet to puncture in previous paths. The PVA sample was now too soft which could be caused by too little %wt of grains or burning same grains in the borosilicate glass during the heating step. The sample can be made more stiff by adding more percentage weight PVA grains, or by doing more freeze-thaw cycles. For the option for adding more percentage weight grains some research must be done to find out how much % wt is able to solve in the mixture of water and cooling liquid. The other option is to do more freeze-thaw cycles with the sample. In the article of de Jong et al. [16] a maximum of 3 freeze-thaw cycles were performed which is copied by making the liver model for the liver model. A research can be done to conclude how stiff the PVA can be made by doing more freeze-thaw cycles.



## 5.5 | Recommendations

More research is always recommended, especially when it comes to medical steering instruments. With this graduation project, a considerable step has been taken in the right direction regarding a mechanical steering mechanisms for instruments with a long thin shaft. The following list contains recommendations for further research and/or changes in the design to make the steerable stylet applicable for the TIPS procedure:

- Redesign the rigid cannula so it becomes more flexible and can be pushed through the angle of  $\pm 35^\circ$  in the original stiffening cannula. What would happen if a flexible tube is used like the 5Fr catheter from the original access set? A small rigid cannula can be added in the tip where the key of the fixation is welded. Expected is that the stylet is still able to steer but that a kink may form in the inner radius of the flexible tube if there is too much force exerted on the transmission. Therefore it will lose some strength in the transmission and joint mechanism but will be more flexible so that the original stiffening cannula can be used.
- Another option to redesign the rigid cannula is to modify the stiffening cannula with also a small steering mechanism. The steerable stylet can first be pushed through the stiffening cannula in a straight configuration until the tip will reach the end of the cannula. The stiffening cannula can be steered into the RHV after which the steerable stylet can be pushed further through and steer into the direction of the PV.
- A research to the amount of holes in the nitinol tip. For now, there is chosen for 5 holes, motivated by the ablation needle designed by N.J. van de Berg. What is the influence of these holes on the steering angle? It is expected that the joint mechanism becomes more flexible. A bigger steering angle can be achieved but the transmission and joint mechanism would deliver less force during the force exerted by the tip experiments.
- In the prototype the distance from tip till the fixation between the rigid cannula and stylet is motivated from the steerable ablation needle. What happen to the steering angle if the fixation is halfway the rigid cannula? It is expected that the rigid cannula with stylet becomes more flexible and the stylet will lose some strength in the transmission. Is there an ultimate distance between the tip and fixation were the style with rigid cannula is flexible enough to push through the original stiffening cannula but is still stiff enough to resist the lateral forces?
- A research can be done to the possibilities to sterilize the steerable stylet after the procedure. Since the steerable stylet is made of nitinol it is possible to use it multiple times without any cracks in the material of the joint mechanism if all subparts can be sterilized.
- A redesign of the mold of the liver part in the liver model. The position of the portal vein must be made more ventrally. For making the liver model as realistic as possible more research must be done on the positions of the veins.
- A research on the possibilities of PVA. The liver model with 8%wt PVA grains was still too soft. A study to PVA is recommended to answer the question if PVA can be made stiff enough to represent sick liver tissue. What is the maximum %wt PVA grains that a mixture can dissolve? And if the maximum %wt PVA grains are known, what are the maximum freeze/thaw cycles wherefore the PVA becomes stiffer?

## 6 | Conclusion

The goal of this thesis was to design a steerable stylet to reduce the complexity of the intrahepatic puncture step during a TIPS procedure. The aim was to provide a good visible steerable stylet which was able to resist deflection and steer when the tip is in contact with tissue. It became a challenge to make a transmission and joint mechanism from the proximal to the distal end with the same shaft length and small diameter as the original access set. A steerable ablation needle is used as motivation for a lot of design criteria since it had a mechanical transmission, same diameter, and was able to make planar steering movements of  $\pm 10^\circ$  to both sides with a shaft length of  $\pm 15$  centimeters. With a few modifications to the design, a steerable stylet for the tips procedure has been made.

### 6.1 | Liver Model

A representative liver model was needed to do test procedures with the steerable stylet. A liver model was also desired for training purposes to train the procedure before doing ex-vivo or in-vivo procedures. The liver model made for the test procedure in this graduation project is a good start but will be better with some modifications. The used mold for the liver part must be adjusted so the location of the PV become more ventrally. The used PVA samples in this model were too soft. In the Erasmus MC hospital a research is started on different PVA samples to find the right percentages to achieve the same characteristics as liver tissue with cirrhosis.

### 6.2 | The TIPS Stylet

The prototype, with a long shaft ( $\pm 60$  centimeter) from actuator till joint mechanism, is able to steer with only a few components in the steering mechanism with a mechanical transmission. The stylet and rigid cannula in the prototype are both made of the super elastic material nitinol. Nitinol is more expensive than stainless steel but can deal with the stresses in the joint mechanism during steering movements which will give the steerable stylet a longer lifetime. The compliant joint mechanism and the trocar tip are well-visible in a wide range. The shaft became well-visible due to the joint mechanism with some cut-outs and the tip owes its visibility to the used trocar tip with three flat surfaces. In addition, the steerable stylet became stiffer than the original stylet wherefore it is better resistant against deflection and was able to steer, with and without cannula, inside PVA samples. The mechanical transmission was strong enough to deliver the power given by the actuator, exerted by the IR, through the long thin shaft to

the joint mechanism. Unfortunately, the maximum steering angle is smaller than proposed and the rigid cannula was too stiff to push through the pre-bent angle in the stiffening cannula. To fulfill all experiments and test procedures in the liver model, an adapted stiffening cannula with an angle of  $\pm 18^\circ$  was used.

Since the steering angle of the stylet was too small, and the rigid cannula too stiff, the stylet will not reduce the complexity of the TIPS procedure yet. During the test procedures it became clear that the angle of the adapted stiffening cannula was too small to enter the RHV wherefore the TIPS procedure could not be fulfilled. But still, despite these problems, there is potential to make mechanical transmissions for steerable instruments with long thin shafts. With further research and development, this steering mechanism must be able to steer the proposed amount of degrees without any extra components, is well visible with ultrasound, good resistant against lateral forces and able to steer while it is in tissue. This is something where the department of interventional radiology is waiting for and would definitely reduce the deflection, the procedure time and the uncertainty to enter the portal vein during a TIPS procedure wherefore the hit rate will increase.

## Bibliography

- [1] Julie Hallet, Olivier Mailloux, Mony Chhiv, Roger C. Grégoire, and Jean Pierre Gagné. The integration of minimally invasive surgery in surgical practice in a Canadian setting: Results from 2 consecutive province-wide practice surveys of general surgeons over a 5-year period. *Canadian Journal of Surgery*, 2015.
- [2] Kuan Ming Chiu. Minimally invasive cardiac surgery, 2013.
- [3] Robert E. Glasgow, Kathy A. Adamson, and Sean J. Mulvihill. The benefits of a dedicated minimally invasive surgery program to academic general surgery practice. *Journal of Gastrointestinal Surgery*, 2004.
- [4] Interventional Radiology MIOT Hospitals Chennai India.
- [5] Jonas J.B. Lim and Arthur G. Erdman. A review of mechanism used in laparoscopic surgical instruments. *Mechanism and Machine Theory*, 38(11):1133–1147, 2003.
- [6] Transjugular liver access An illustrated guide. Technical report, 2013.
- [7] Fulvio Calise and Luciano Casciola. *Minimally invasive surgery of the Liver*. 2013.
- [8] Dr. K.H. Brandt and Dr. M.N. van der Heyde. Herkenning en behandelning van portale hypertensie. *Ned. T. Geneesk.* 118, 25:960–970, 1974.
- [9] Shivanand Patil, Santosh Jadhav, Natraj Shetty, Jayashree Kharge, Beerasha Puttegowda, Rangraj Ramalingam, and Manjunath Nanjappa Cholenhally. Assessment of inferior vena cava diameter by echocardiography in normal Indian population: A prospective observational study. *Indian Heart Journal*, 68:S26–S30, 2016.
- [10] Jeanne M LaBerge. Anatomy relevant to TIPS. *Techniques in Vascular and Interventional Radiology*, 1(2):51–67, 1998.
- [11] Renan Uflacker. Anatomic Considerations Related to the TIPS Procedure. *Plenary Session-Liver Failure and Portal Hypertension*.
- [12] Sidika Deniz Micozkadioglu and Alper Nabi Erkan. Internal jugular vein anomaly: A lateral branch of the internal jugular vein in the neck. *Egyptian Journal of Ear, Nose, Throat and Allied Sciences*, 12(1):77–79, 2011.
- [13] The inferior vena cava — Anatomy of the inferior vena cava - Anatomy-Medicine.COM.
- [14] Yanping Cao, Guo Yang Li, Xiao Zhang, and Yan Lin Liu. Tissue-mimicking materials for elastography phantoms: A review. *Extreme Mechanics Letters*, 17(October):62–70, 2017.
- [15] Timothy J. Hall, Mehmet Bilgen, Michael F. Insana, and Thomas A. Krouskop. Phantoms Materials for Elastography. Technical Report 6, 1997.
- [16] Tonke L. de Jong, Loes H. Pluymen, Dennis J. van Gerwen, Gert Jan Kleinrensink, Jenny Dankelman, and John J. van den Dobbelsteen. PVA matches human liver in needle-tissue interaction. *Journal of the Mechanical Behavior of Biomedical Materials*, 69(January):223–228, 2017.
- [17] Naresh V. Datla, Bardia Konh, Joe J.Y. Koo, Daniel J.W. Choi, Yan Yu, Adam P. Dicker, Tarun K. Podder, Kurosh Darvish, and Parsaoran Hutapea. Polyacrylamide phantom for self-actuating needle–tissue interaction studies. *Medical Engineering and Physics*, 2013.
- [18] Mariya Lazebnik, Ernest L Madsen, Gary R Frank, and Susan C Hagness. Tissue-mimicking phantom materials for narrowband and ultrawideband microwave applications. *MEDICINE AND BIOLOGY Phys. Med. Biol.*, 50:4245–4258, 2005.
- [19] Irena Zivkovic, Redouan Mahou, Klaus Scheffler, and Christine Wandrey. CANDIDATE FOR TISSUE MIMICKING MATERIAL MADE OF AN EPOXY MATRIX LOADED WITH ALGINATE MICROSPHERES. *Progress In Electromagnetics Research C*, 2013.
- [20] Silvio L. Vieira, Theo Z. Pavan, Jorge E. Junior, and Antonio A O Carneiro. Paraffin-Gel Tissue-Mimicking Material for Ultrasound-Guided Needle Biopsy Phantom. *Ultrasound in Medicine and Biology*, 2013.
- [21] John P Cunha and Jay W Marks. Cirrhosis of the liver definition and facts. *World Journal of Hepatology*, 4(3):81, 2012.
- [22] Cirrhosis - Symptoms and causes - Mayo Clinic.
- [23] Johannes Wiegand and Thomas Berg. The Etiology, Diagnosis and Prevention of Liver Cirrhosis. *Deutsches Aerzteblatt Online*, 110(6):85–91, feb 2013.
- [24] Mona H Ismail and Massimo Pinzani. Reversal of liver fibrosis. *Saudi journal of gastroenterology : official journal of the Saudi Gastroenterology Association*, 15(1):72–9, jan 2009.
- [25] C.F. Cuijpers. Tips for TIPS. 2015.
- [26] Frederick S. Keller and Josef Rösch. The Transjugular Intrahepatic Portosystemic Shunt: Technique and Instruments. *Techniques in Vascular and Interventional Radiology*, 19(1):2–9, mar 2016.
- [27] M. Senzolo, P. Burra, E. Cholongitas, F. Lodato, L. Marelli, P. Manousou, D. Patch, G.C. Sturniolo, and A.K. Burroughs. The transjugular route: The key hole to the liver world. *Digestive and Liver Disease*, 39(2):105–116, feb 2007.
- [28] A R Owen, A J Stanley, A Vijayanathan, and J G Moss. The transjugular intrahepatic portosystemic shunt (TIPS).
- [29] Mengfei Zhao, Zhendong Yue, Hongwei Zhao, Lei Wang, Zhenhua Fan, Fuliang He, Jiannan Yao, Xiaogun Dong, and Fuquan Liu. Techniques of TIPS in the treatment of liver cirrhosis combined with incompletely occlusive main portal vein thrombosis. *Scientific Reports*, 2016.

- [30] Peter Ferenci. Hepatic encephalopathy. *Gastroenterology report*, 5(2):138–147, may 2017.
- [31] Andres T Blei. Diagnosis and treatment of hepatic encephalopathy. 2000.
- [32] Hauke S Heinzow, Philipp Lenz, Michael Köhler, Frank Reinecke, Hansjörg Ullerich, Wolfram Domschke, Dirk Domagk, Tobias Meister, and Roberto Testa. Clinical outcome and predictors of survival after TIPS insertion in patients with liver cirrhosis. *World J Gastroenterol*, 18(37):5211–5218, 2012.
- [33] S W Han, Y E Joo, H S Kim, S K Choi, J S Rew, J K Kim, and S J Kim. Clinical results of the transjugular intrahepatic portosystemic shunt (TIPS) for the treatment of variceal bleeding. *The Korean journal of internal medicine*, 15(3):179–86, 12 2000.
- [34] Filip Jelínek, Ewout a. Arkenbout, Paul W. J. Henselmans, Rob Pessers, and Paul Breedveld. Classification of Joints Used in Steerable Instruments for Minimally Invasive Surgery—A Review of the State of the Art. *Journal of Medical Devices*, 9(1):010801, 2015.
- [35] David Kelly. Texture Encoded Realistic Joint Limits. Technical report.
- [36] D.A. Parrott, B.T. Krupp, C.L. Gillum, C.J. Matice, and L.P. Mingione. Articulating laparoscopic surgical instruments, May 3 2012. WO Patent App. PCT/US2011/057,677.
- [37] M. S. Banik, D. R. Boulais, L. A. Couvillon, A. C. C. Chin, F. J. Anderson, F. T. Macnamara, S. D. Fantone, D. J. Braunstein, M. Orband, D. G., Saber, R. M. Hunter, I. W., Coppola, P. A., Kirouac, A. P., Clark, R. J., Wiesman, and A. E. R. Mason, T. J., Mehta, N. R., and Greaves. Articulation Joint, 2004.
- [38] Jimmie B. Allred and Richard Bingham. Endoscope steering section, 1987.
- [39] David Karl Stroup and Arthur Deptala. Wrist assembly for articulating laparoscopic surgical instruments, 2013.
- [40] S. Marczyk, R. Pribanic, D. Farascioni, E.J. Taylor, and P. Hathaway. Endoscopic vessel sealer and divider having a flexible articulating shaft, October 17 2013. US Patent App. 13/914,656.
- [41] Pavel Menn. Articulating steerable clip applicator for laparoscopic procedures, 4 2011.
- [42] V. Saadat, C. Rothe, R. Ewers, T. Maahs, and K. Michlitsch. Endoluminal tool deployment system, August 10 2006. US Patent App. 11/400,120.
- [43] Harb N. Boury. Selectively Manipulable Catheter, 1999.
- [44] Kevin T. Stone, Troy M. Walter, and Ryan A. Kaiser. Steerable Suture Passing Device, 2016.
- [45] Frank Dewaele, Cyriel Mabilde, and Bart Blanckaert. Steerable tube, 3 2013.
- [46] P. Breedveld and J.S. Scheltes. Instrument for fine-mechanical or surgical applications, September 25 2008. US Patent App. 10/597,186.
- [47] F Dirksen and R Lammering. On mechanical properties of planar flexure hinges of compliant mechanisms.
- [48] Robert J. Webster and Bryan A. Jones. Design and Kinematic Modeling of Constant Curvature Continuum Robots: A Review. *The International Journal of Robotics Research*, 29(13):1661–1683, nov 2010.
- [49] Nick J. van de Berg, Jenny Dankelman, and John J. van den Dobbela. Design of an actively controlled steerable needle with tendon actuation and FBG-based shape sensing. *Medical Engineering and Physics*, 2015.
- [50] Marta Scali, Tim P Pusch, Paul Breedveld, and Dimitra Dodou. Needle-like instruments for steering through solid organs: A review of the scientific and patent literature. *Proceedings of the Institution of Mechanical Engineers, Part H: Journal of Engineering in Medicine*, 2017.
- [51] MaterialsHypodermic Needle Materials - Connecticut Hypodermics Inc.
- [52] Rob Bohn. What’s the difference between 304 and 316 stainless steel? - Stainless Steel Enclosures — NEMA Enclosures, 2012.
- [53] Alloy 625 equivalent Inconel 625 Manufacturer Supplier Exporter.
- [54] N.B Morgan. Medical shape memory alloy applications—the market and its products. *Materials Science and Engineering: A*, 378(1):16–23, 2004.
- [55] C D J Barras and K A Myers. Nitinol – Its Use in Vascular Surgery and Other Applications. *Eur J Vasc Endovasc Surg*, 19:564–569, 2000.
- [56] T Duerig, A Pelton, and D Stöckel. An overview of nitinol medical applications. *Materials Science and Engineering: A*, 273:149–160, 1999.
- [57] Nick J Van De Berg, Juan A Sánchez-Margallo, Arjan P Van Dijke, Thomas Langø, and John J Van Den Dobbela. A methodical quantification of needle visibility and echogenicity in ultrasound images. Technical report.
- [58] Niki Abolhassani, Rajni Patel, and Mehrdad Moallem. Needle insertion into soft tissue: A survey. *Medical Engineering & Physics*, 29(4):413–431, 2007.
- [59] P. J. Swaney, J. Burgner, H. B. Gilbert, and R. J. Webster. A Flexure-Based Steerable Needle: High Curvature With Reduced Tissue Damage. *IEEE Transactions on Biomedical Engineering*, 60(4):906–909, apr 2013.
- [60] D.P. van Duijn. Steering Mechanisms for Interventional Needles. 2017.
- [61] Lawrence Kerver, Brian Tang, Friedrich Ho, and Ben Nordell. Apparatus for articulating the wrist of a laparoscopic grasping instrument, 2009.

- [62] D.E. Hegeman, D.J. Danitz, C.D. Hinman, and L.J. Alvord. Tool with articulation lock, April 19 2012. US Patent App. 13/334,628.
- [63] D.J. Danitz and A. Gold. Articulating endoscopes, October 14 2010. US Patent App. 12/766,825.
- [64] J.T. Malkowski, R. Cabrera, R. Fortier, A. Ziegler, A. Cruz, G.A. Stellon, and S. Evans. Articulating surgical device, July 28 2011. US Patent App. 13/047,930.
- [65] Troy K. Adebar, Joseph D. Greer, Paul F. Laeseke, Gloria L. Hwang and Allison M. Okamura. Methods for Improving the Curvature of Steerable Needles in Biological Tissue. *IEEE TRANSACTIONS ON BIOMEDICAL ENGINEERING*, 63, 2016.
- [66] W.T. Lin and C.C. Chan. Four-directional tip deflection device for endoscope, February 11 2010. US Patent App. 12/537,490.
- [67] DaVinci. EndoWrist® /Single-Site® Instrument & Accessory Catalog. 2014.
- [68] S. Mitchell, R.C. Ewers, and T.D. Maahs. Endoluminal surgical tool with small bend radius steering section, September 20 2012. US Patent App. 13/483,371.
- [69] Jumpei Arata, Shinya Kogiso, Masamichi Sakaguchi, Ryu Nakadate, Susumu Oguri, Munenori Uemura, Cho Byunghyun, Tomohiko Akahoshi, Tetsuo Ikeda, and Makoto Hashizume. Articulated minimally invasive surgical instrument based on compliant mechanism. *International Journal of Computer Assisted Radiology and Surgery*, 10(11):1837–1843, nov 2015.
- [70] Steerable Guidewires. Revolutionizing Access FAtHoM tM. Technical report, 2017.
- [71] K. Stone, T. Walters, and R. Kaiser. Steerable suture passing device, February 15 2007. US Patent App. 11/501,171.
- [72] J. Kortenbach, S. Gottlieb, K. Smith, C. Slater, and T. Bales. Rotatable and deflectable biopsy forceps, October 16 2003. US Patent App. 10/437,143.
- [73] T.G. Cooper and S.C. Anderson. Flexible wrist for surgical tool, April 18 2013. US Patent App. 13/692,024.
- [74] W.T. Lin. Two-way endoscope steering mechanism and four-way endoscope steering mechanism, June 20 2013. US Patent App. 13/328,005.
- [75] W. Lee, A. Chamorro, and W. Lee. Surgical instrument, October 4 2011. US Patent 8,029,531.
- [76] A.J. Miller. Steerable endoluminal devices and methods, May 17 2012. US Patent App. 13/288,918.
- [77] John Speich and Michael Goldfarb. A Compliant-Mechanism-Based Three Degree-of-Freedom Manipulator for Small-Scale Manipulation. *Robotica*.
- [78] Nick J. van de Berg. Unpublished work/personal communication. 2018.
- [79] Takeshi Soyama, Daisuke Yoshida, Yusuke Sakuhara, Ryo Morita, Daisuke Abo, and Kohsuke Kudo. The Steerable Microcatheter: A New Device for Selective Catheterisation. *Cardio-Vascular and Interventional Radiology*, 2017.
- [80] Unique tip configurations allow for intraprocedural flexibility and efficiency. Technical report, 2017.
- [81] Nick J Van De Berg, Juan A Sánchez-Margallo, Arjan P Van Dijke, Thomas Langø, and John J Van Den Dobbelen. A methodical quantification of needle visibility and echogenicity in ultrasound images. Technical report.
- [82] Optimizing access throughout the body. Technical report.



Graduation Project:

A STEERABLE STYLET FOR THE  
TRANSJUGULAR INTRAHEPATIC  
PORTOSYSTEMIC SHUNT PROCEDURE



APPENDICES

D.P. VAN DUIJN  
#4003616



## A | TIPS: The Procedure Step-by-Step

#	Steps	Instrument	Visibility
1	To determine whether a TIPS procedure must be performed, the radiologist will first conclude if there is actual portal hypertension. This is done by measuring the pressure in the inferior vena cava and the portal vein.		
2	The portal vein will be entered by a supportive 21G needle which is punctured through the skin, along the ribs, into the liver. The interventional radiologist is guided by ultrasound to see if the needle has entered the portal vein.	21G Needle	Ultrasound
3	A guidewire is pushed through the 21G needle into the liver.	Guidewire	
4	The 21G needle is retracted, a 4Fr catheter is pushed over the guidewire into the portal vein.	4Fr Catheter	
5	Through the 4Fr catheter an agriographic catheter (with small holes in the front) is placed into the liver. By pushing contrast fluid through the catheter, it will be spread in the portal vein and its branches. With the help of a CT scan and the contrast fluid, the filled veins will be highlighted on the CT scans.	4Fr Catheter Agriographic Catheter	Fluoroscopy CT Scan
6	Afterwards, the jugular vein is punctured from the right side of the neck with a 17G needle. A small wire with a 10Fr sheet around are already inside the needle.	17G Needle Guidewire 10Fr Sheet	
7	The needle will be pushed through the jugular vein and the superior vena cava into the inferior vena cava.	17G Needle Guidewire 10Fr Sheet	
8	Now, pressure measurements will be performed by the radiologist in the portal vein and the inferior vena cava. This difference between both veins is measured with the portosystemic pressure gradient (PSPG).		
9	If the pressure gradient exceeds 6 mm HG, portal hypertension is an issue. Internal bleeding will occur around a pressure gradient of 10 mm HG. To decide whether the interventional radiologist will perform a TIPS procedure he will briefly consult with his colleagues about the PSPG value and the health of the patient.		
10	Through the 10Fr catheter, which is still in the inferior vena cava, an agriographic catheter (Torcon NB catheter) is pushed with a small angle in front (30 degrees). With the help of this angle the interventional radiologists can place the tip of the catheter in the right hepatic vein.	10Fr Catheter Torcon NB Catheter	Ultrasound
11	Again contrast fluid will be pushed through the agriographic catheter wherefore also the hepatic veins becomes visible on the CT scans.		Ultrasound CT Scans
12	A 10Fr catheter is pushed over the agriographic catheter into the right hepatic vein. If the 10Fr catheter is in place, the agriographic catheter is retracted from the body.	10Fr Catheter	Ultrasound

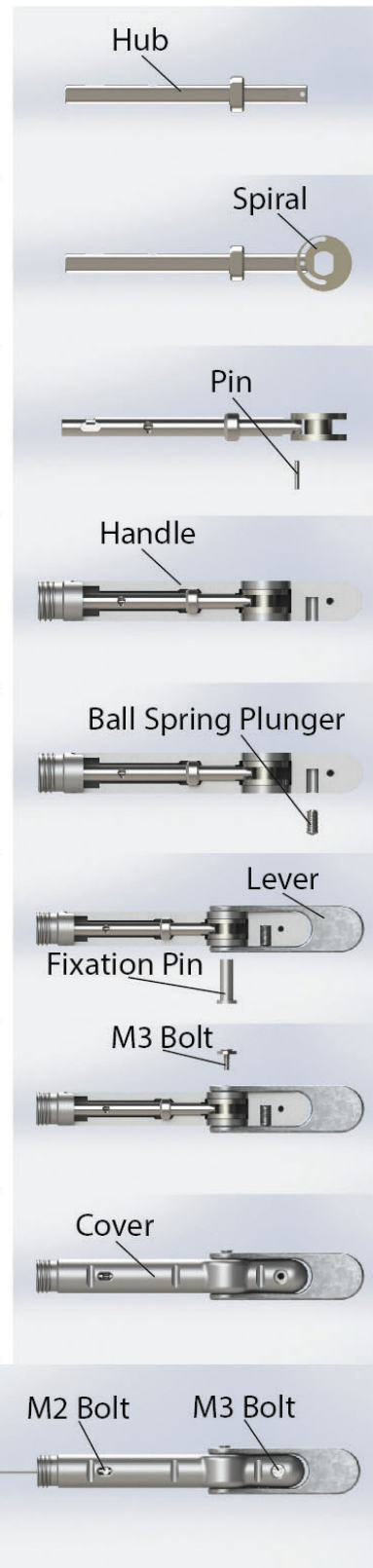


13	<p>The 14G stiffening cannula, also with an angle in front, is pushed through the 10Fr catheter which is still located in the right hepatic vein. When the stiffening cannula enters the right hepatic vein, it is rotated ventrally (to the front) so the tip is orientated in the direction of the portal vein. The interventional radiologist can make an estimation how far the stiffening cannula must rotate ventrally with the help of the CT scans and on his experience.</p>	<p>10Fr Catheter 14G Stiffening Cannula</p>	CT Scans
14	<p>A stylet, with a 5Fr van Andel catheter is pushed through the 14G stiffening cannula into the right hepatic vein. Since this stiffening cannula is orientated to the portal vein, the stylet can directly pushed into the liver tissue. The radiologist tries to enter the portal vein by pushing the stylet and rotating the 14G stiffening cannula. This puncturing step is called the <b>intrahepatic puncture</b>.</p>	<p>Stylet 5Fr van Andel Catheter 14G Stiffening Cannula</p>	CT Scans
15	<p>If the stylet with the 5Fr van Andel catheter is in the portal vein, the stylet is retracted from the body. The 5Fr van Andel catheter stays through the liver tissue in the portal vein. On the outside of the body, a syringe (with some contrast fluid) is connected to the van Andel catheter. By pulling out the syringe, a vacuum is created in the van Andel catheter. If blood is visible in the syringe, the radiologist knows that the stylet is in the portal vein. If not, the radiologists have to do the intrahepatic puncture step again. If blood is visible, the blood is pushed back with the contrast fluid. A double check with fluoroscopy is done to check if the stylet is in the portal vein.</p>	<p>5Fr van Andel Catheter Syringe</p>	<p>CT Scans Fluoroscopy</p>
16	<p>Through the van Andel catheter a guidewire is pushed from outside the body, through the hepatic vein into the portal vein. If the guidewire is in the portal vein the van Andel catheter is retracted from the body.</p>	<p>5Fr van Andel Catheter Guidewire</p>	
17	<p>Again, the Torcon NB catheter goes into the patient, over the guidewire all the way to the portal vein. If the interventional radiologists is not able to push the Torcon NB catheter through the liver tissue, they first use a small balloon which is placed inside the punctured path. By blowing the balloon a bit, the path will be expanded.</p>	<p>Torcon NB catheter Guidewire</p>	
18	<p>If the Torcon NB catheter is placed through the hepatic vein into the portal vein, all the other instruments are retracted from the patients body. Through this catheter a shunt and its device can be placed in the puncturing path between the hepatic and portal vein.</p>	<p>Self Expandable Shunt</p>	CT Scans
19	<p>The shunt device is retracted where the shunt will stay in place. By placing a balloon in the shunt, the shunt can be expanded by blowing the balloon.</p>		
20	<p>The last step is to check if the pressure gradient is reduced. The interventional radiologists measures again the pressure in the inferior vena cava and the portal vein. If the pressure is reduced the shunt already does his work.</p>		

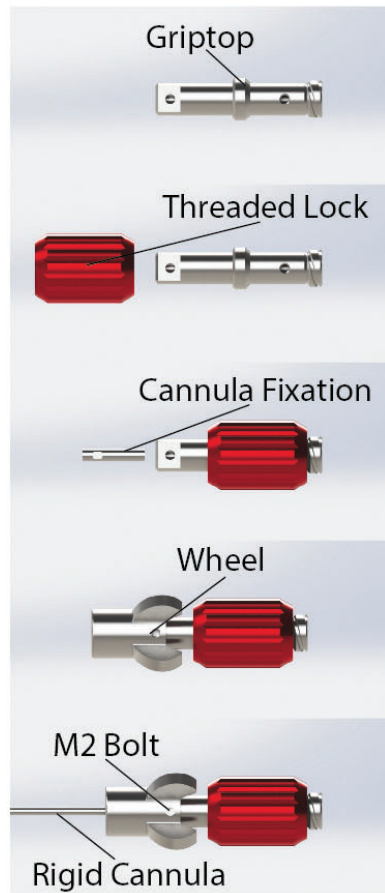
## B | How to: Assembling the TIPS Stylet

The entire TIPS needle with steerable stylet is assembled as indicated in the following steps:

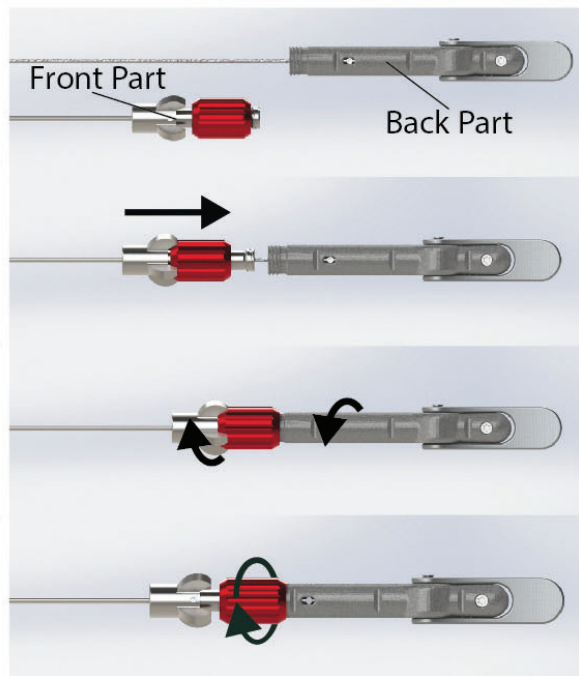
1. Assembling the steerable stylet starts with the Hub. The Hub is the part that will take care of the transmission.
2. The Spiral must be slide on the Hub. The assymmetric groove have to be aligned with the hole in the Hub.
3. The Spiral is attached to the Hub with a Pin.
4. The transmission mechanism (Spiral + Hub) can be placed in the Handle.
5. The Ball Spring Plunger can be screwed into the Handle.
6. The Lever can be attached to the Handle by sliding it over the Handle and fix it with the Fixation Pin.
7. A M3 Bolt with a ring must be tightened in the other side of the Fixation Pin to secure the Lever.
8. The first part of the steerable stylet can be closed by placing the Cover on the Handle part.
9. The Cover can be fixed with a M3 Bolt. The Stylet can be placed and tightened with a M2 Bolt.



10. The front part of the stylet can be made separate. This part begins with the Griptop.
11. The Threaded Lock must slide over the Griptop as far as possible.
12. The Cannula Fixation must be pressed into the Griptop. The flat surface must match the hole in the Griptop.
13. The Wheel can now slide over the Griptop. The hole in the Wheel must match the hole in the Griptop.
14. The Rigid Cannula must be pushed as far as possible in the Fixation Cannula. All parts are secured with one M2 Bolt.



15. Both parts, Front and Back, can now easily be connected to each other.
16. The Front Part can slide over the Stylet, where the Griptop slide partly in the Back Part.
17. By turning both parts 90 degrees apart they are locked into each other.
18. The parts will be secured by tighten the Threaded Lock.



**Figure B.1:** The following steps explains how the steerable stylet for the TIPS procedure can be assembled.

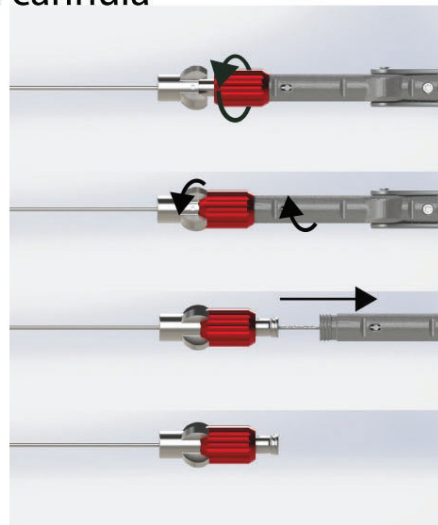
## C | How to: Remove Stylet from Rigid Cannula

During the TIPS procedure a syringe is connected to a 5Fr catheter after the intrahepatic puncture. With this syringe a vacuum is created to conclude whether the IR is actually in the portal vein. In the new design there was no space anymore for the 5Fr catheter since the rigid cannula is necessary for the steering mechanism to work.

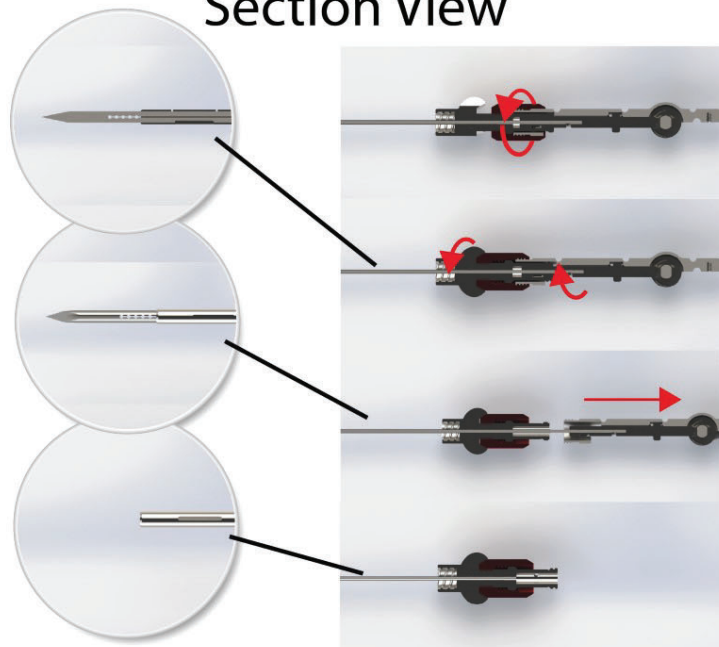
After the intrahepatic puncture, the stylet can be taken out of the body where the rigid cannula remains to connect the syringe. The following steps explain how to separate these two parts of the stylet after the intrahepatic puncture.

### Remove Stylet from cannula

1. The first step to remove the stylet from the cannula is to loosen the threaded lock.
2. The threaded lock can be slid off the thread. The front part can be turned 90 degrees in relation to the rear part.
3. The rear part can be removed by pulling it backwards.
4. The front part with cannula is still in place. A syringe can be connected to the luer lock.



### Section View



**Figure C.1:** The following steps must be performed by the IR after the intrahepatic puncture. After the stylet has been removed, a syringe can be connected with a luer lock to conclude if they are really in the portal vein.

## D | Test Model for the TIPS Procedure

### Purpose

This setup is designed to make it possible for radiologists to test, but also train, with the original and the new designed steerable TIPS stylet. In order to make a realistic model, the related veins for the TIPS procedure, as described in chapter 1.2.1, are properly constructed. Besides this, the used material mimics imaging and stiffness characteristics of liver tissue.

### Materials and Description

Two important properties for the material choice are the Echogenic (visibility) and mechanical (stiffness) properties. During the TIPS procedure the interventional radiologist locates the stiffening cannula and stylet with ultrasound, it is important that the material in the test model does not make any conflicts with this image modality otherwise the stylet and stiffening cannula becomes not good visible. Deflection of the stylet is a problem which arise during the intrahepatic puncture with the original stylet, to test the resistance against this deflection of the steerable stylet the stiffness of the tissue in the test model must meet the characteristics of a liver with cirrhosis.

From Chapter 1.3 the best suitable options are the water-based tissue models. The oil-based and oil-in-hydrogel options are too flexible for making the test model. These materials will have problems with the hollow veins in the model. From the water-based models, Poly Vinyl Alcohol (PVA) meets the requirements for echogenic and mechanical properties. PVA is a synthetic polymer with comparable ultrasound imaging properties and the ability to change in stiffness by making the mixture with other ratios and/or varying the amount of freeze-thaw processes.

PVA will not recover from the puncturing paths, therefore the liver model can be used for a few test procedures. In order to use the liver model multiple times, the liver part must be made replaceable.

#### Materials

- An acrylic base plate;
- An acrylic plate with a cut-out section for the setup;
- 4 M6 nuts and bolts;
- A 3D printed mold for the connection vein and liver;
- Selvol Polyvinyl Alcohol, Selvol 165;
- Silica gel 60 (grain diameter: 0.015-0.040 mm);
- Cooling liquid;
- Water;
- A borosilicate Glass 2000ml;
- Hot and steering table, IKA<sup>®</sup> werke RETcontrol-visc (recommended);
- A small flat screwdriver (recommended);
- Pigment (optional).

#### Description

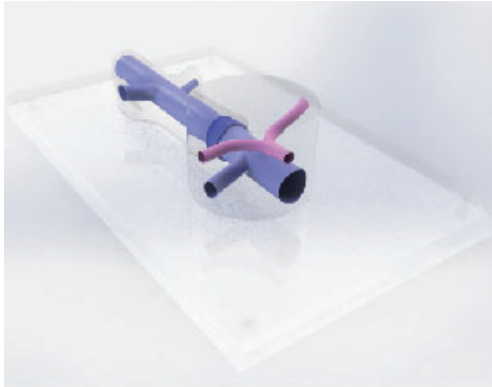
The test setup consists of 3 components: the base plate, connection vein from neck to liver, and the liver. The base plate ensures that the other two parts remain in place. The connection represents the jugular vein, superior and inferior vena cava connected together. During the TIPS procedure the interventional radiologist (IR) makes an incision in the neck and reaches the right hepatic vein in the liver by pushing the instruments through the jugular vein, superior and inferior vena cava. In Chapter 1.2.1 dimensions are given for the superior and inferior vena cava which are used to make this model as realistic as possible. The third component is the liver with the hepatic vein, the right hepatic vein, the right branch of the portal vein and a part of the portal vein inside.

In the article of de Jong et al.[16] a research is done to mimic human liver tissue using a mixture of

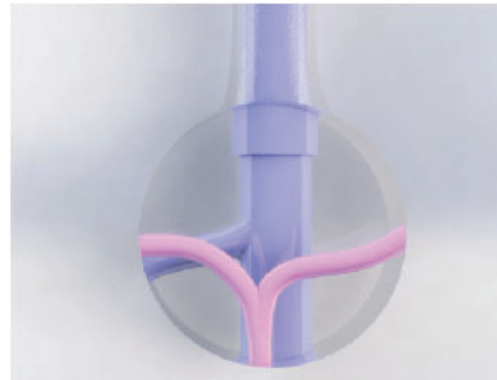
PVA. A liver with cirrhosis is stiffer due to the scarred tissue than a healthy liver. To mimic the human liver with cirrhosis, samples are made with more weight percentage PVA grains than needed for a healthy liver according to de Jong et al.

## Design

With the help of the train model of Cook Medical © and the information from literature described in Chapter 1.2.1, a final design for the liver model, represented by Figure D.1, is created. In the figures the model is made with transparent liver tissue to see the veins inside the model. In the real model the tissue is not transparent wherefore the IR must use ultrasound or CT scans to locate the instrument during the procedure.



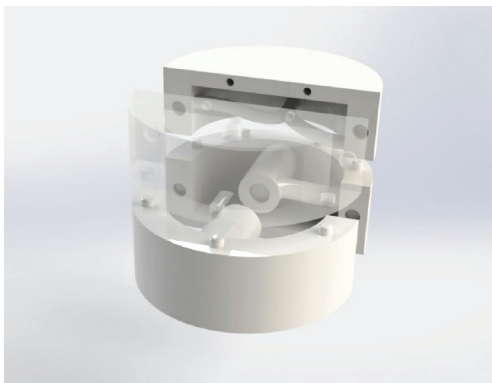
(a) Overview of a CAD model of the liver model.



(b) Top view of the design of the liver part.

**Figure D.1:** In (a) an overview of the design of the test model. In (b) a top view of the liver model where the hepatic vein (blue) and the portal vein (pink) are clearly visible in the liver.

To make the model with hollow veins, two molds are made. One mold for the liver and one for the connection vein. The molds are produced with a 3D printer and contain multiple components. Both samples are made by casting the molds with the PVA mixture. After the casting process the molds can be disassembled. This can be done without damaging any parts of the mold wherefore the molds can be used multiple times. Even if a part of a mold breaks down, it is easily reproduced since it is all made with a 3D printer.



(a) Mold to produce a PVA sample of the liver with the hepatic and portal vein.



(b) Mold to produce a PVA sample of the jugular vein, superior and inferior vena cava.

**Figure D.2:** Representation of the models for the liver mold (a) and the connection mold (b). Both molds consist of several parts. After the casting process the mold can be disassembled without any damage to the PVA sample and the mold.

The liver model design is built up from the liver and connection part as two separate components. These two components stay together on the base plate since this plate has a cut-out of the shapes connected

together. During test procedures, both components will be punctured. The connection vein will be punctured at the top, which will represent the incision in the neck to enter the jugular vein where the liver part will be punctured between the hepatic and portal vein (the intrahepatic puncture). After several attempts a hole will arise in the connection part and multiple puncturing paths will be in the liver part. The hole in the connection vein has no further influence for testing the intrahepatic puncture step in the TIPS procedure with the steerable stylet. The connection vein is only made to simulate the procedure as realistic as possible, replacing this sample after several attempts is not necessary. The puncturing paths in the liver part, on the other hand, will influence the test procedures. The stylet will quickly follow an existing path between the hepatic and portal vein. To keep the test procedure as realistic as possible the liver model must be replaced after a few test procedures.

Since the connection vein and the liver model are separate parts only the liver model have to be replaced after some test procedures. Since there is the opportunity to remake the liver sample with other characteristics, the TIPS procedure can be tested with different liver characteristics.

## Methods

### PVA Mixture

A mixture of PVA grains with liquid is used to make the liver and connection vein. Since both molds are closed molds, and the PVA mixture will have a few freeze-thaw cycles, cooling liquid is used in the mixture besides the water. This will prevent that the mixture expand too much during the freezing process which can damage the mold.

#### Amount of mixture required:

- Liver Mold: 0.6 L of Mixture;
- Connection Mold: 0.4 L of Mixture;

It is recommended to make some more of the PVA mixture that is required. Since the molds contains several parts, it is possible that the PVA mixture will flow through the cracks out of the mold. To fill this up, some extra mixture is needed. If a lot of PVA leaks, it is possible to smear the contact surfaces of the components with vaseline or by wrap foil and tape all around the mold.

#### Process steps:

By changing the weight percentages of the PVA grains and the freeze-thaw cycles the mixture can be made with different characteristics. More weight percentages grains or more freeze-thaw cycles makes the PVA mixture stiffer. The TIPS procedure is performed in a liver with cirrhosis, typical of this is that the liver tissue is stiffer. To achieve the best characteristics the mixture is made according to the article of de Jong et al. [16] only with some more weight percentages PVA grains to get the PVA sample stiffer.

The following ratios are used for the samples:

- 40% cooling liquid;
- 60% water;
- 8% wt Polyvinyl Alcohol grains;
- 1% wt Silica gel 60 grains;
- Pigment (optional);

To make the PVA mixture, all ingredients are put into a borosilicate glass. The mixture is heated to 90 degrees Celsius while stirring where a hot and steering table is recommended for this step. The mixture stood for 15 minutes on 90 degrees Celsius while stirring, the PVA grains need some time to melt nicely into the mixture. Steering is required otherwise the PVA will burn onto the bottom of the glass. If the PVA is nicely melt the mixture must cool down to, at least, 50 degrees Celsius before pour into the molds.

### Liver Mold

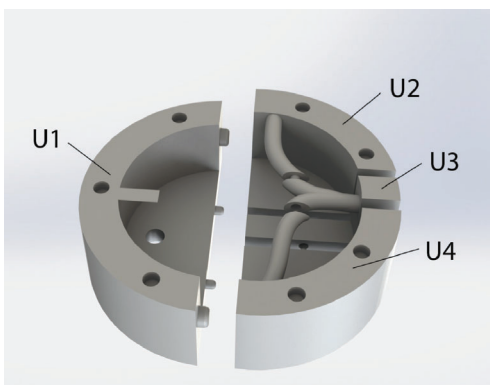
The mold can easily be divided into an upper and lower part as shown in Figure D.3. Both upper and lower parts are separated into more components which are all denoted in the figures.

#### Pour process steps:

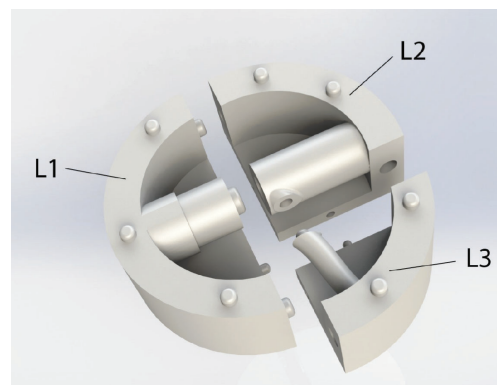
- Make the molds cold by putting them in a freezer for a hour;
- Meanwhile, the PVA mixture can be made as described above;
- After the mixture is cooled down to 50 degrees Celsius or less, the mixture can be poured into the molds;
- Fill the lower part with the PVA mixture first;
- Place the upper part on the lower part (possible in one way);
- Use the small hole in the upper part to fill the mold till the top with the PVA mixture;
- If necessary, refill the mold with PVA mixture. If the PVA mixture runs out through the cracks it is possible to close the mold with foil and tape;
- Place the mold in the freezer for 12 hours;
- Remove the mold from the freezer and allow the mixture to thaw,  $\pm 12$  hours;
- To make the PVA stiff enough, the freeze and thaw process must be done 3 times.

#### Remove mold process steps:

- Place a small flat screwdriver through the lower and upper part of the mold and push them slightly apart all around;
- Remove component U1 from U2 + U3 + U4;
- Remove L1 from the lower part;
- Place the flat screwdriver between L3 and U2 to push both components slightly apart, making just enough space so the pins of L3 are not in the holes of U2 anymore. L3 can now be removed;
- Push L2 and U4 apart with the screwdriver. With enough space the pins of L2 are not in the U4 holes anymore, L2 can then be removed;
- Now easily U2 and U4 can be removed;
- As last, component U3 can be removed.



(a) The lower part of the liver mold.



(b) The upper part of the liver mold.

**Figure D.3:** In (a) the lower part of the liver mold is shown, where it is in three components, L1, L2 and L3. In (b) the upper part is shown which is divided into four components, U1, U2, U3 and U4. All the components are denoted in the figures.



### Connection Vein Mold

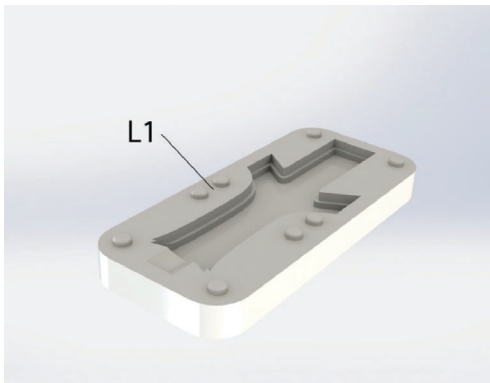
The connection vein mold also contains two main parts. Figure D.4 shows the upper and the lower part. The lower part is one piece, the upper part is divided into five different components. In Figure D.4 all components are denoted. Before starting the molding process the upper components can already be assembled together as shown in Figure D.4b.

#### Pour process steps:

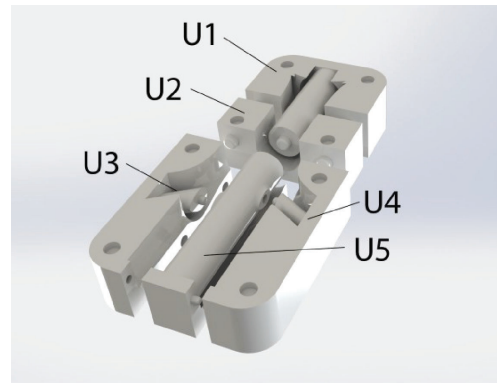
- Make the molds cold by putting them in a freezer for a hour;
- Make the PVA mixture as described above;
- After the mixture is cooled down to 50 degrees Celsius or less, the mixture can pour in the molds;
- Place the upper part on the lower part (possible in one way);
- Use the small hole in the upper part to fill the mold till the top with the PVA mixture;
- If necessary, refill the mold with PVA mixture. If the PVA mixture runs out through the cracks it is possible to close the mold with foil and tape;
- Place the mold in the freezer for 12 hours;
- Remove the mold from the freezer and allow the mixture to thaw,  $\pm 12$  hours;
- To make the PVA stiff enough the freeze and thaw process must be done 3 times.

#### Remove mold process steps:

- Place a small flat screwdriver through the lower and upper part of the mold to push them slightly apart all around;
- The lower part L1 can easily be removed from the upper components;
- Remove part U1 from the upper part. If necessary, use the screwdriver to push component U1 from U2;
- U2 can now be removed. If necessary use the screwdriver to push U2 from U3+U4+U5;
- The parts U3 and U4 can be removed from part U5;
- As last, component U5 can be removed.



(a) The lower part of the connection mold.

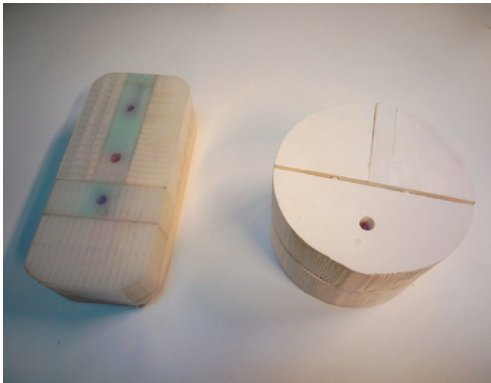


(b) The upper part of the jugular mold.

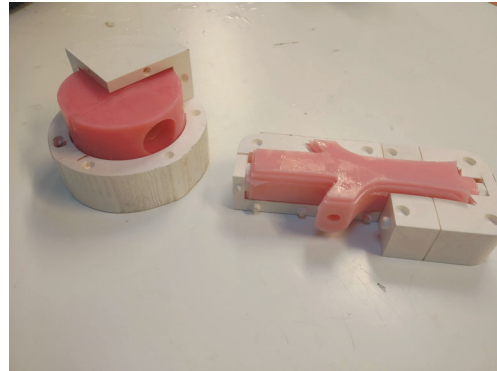
**Figure D.4:** In (a) the lower part and in (b) the upper part of the jugular mold is shown. The lower component is one part, the upper part is divided in five components, U1, U2, U3, U4 and U5. All the components are denoted in the Figures.

## Conclusion

Overall, this test setup is a good representation model to train the TIPS procedure with new interventional radiologists or test the procedure with new designed stylets, needles or catheters. Because the components are easy to replace, this setup can be used multiple times by remaking the PVA models. Since the models can be made with different characteristic by changing the amount of weight percentages PVA grains or the amount of freeze/thaw cycles, radiologist in training can practise the TIPS procedure with different "livers" to feel more comfortable before they perform a real TIPS procedure and new instruments can be tested in tissue with different stiffness characteristics.



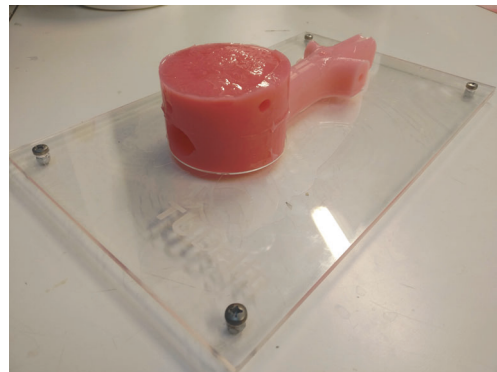
(a) The closed molds for the liver model and connection vein, both filled with the PVA mixture.



(b) Both where the molds are partly removed after the freeze-thaw cycles.



(c) The liver part of the test model, made of the PVA mixture with some red pigment.



(d) An overview of the test model.

**Figure D.5:** The results of making the PVA connection vein, the liver part and the test setup.

## E | Experimental Setup

### Measuring Steering Angles, Joint Stiffness and Maximum Transverse Forces

#### Purpose

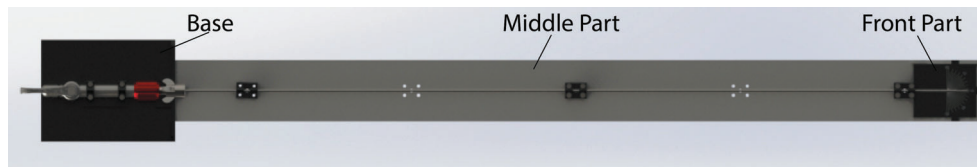
This experimental setup is made to measure the maximum steering angle, joint stiffness and maximum forces exerted by the tip of the new designed TIPS needle with steerable stylet. The base of the setup is made universal wherefore experiments can be done easily with, and without the pre-bent stiffening cannula in succession.

The purpose of these experiments is to see if the new stylet can meet the mechanical requirements. Is the steerable stylet able to reach the proposed steering angle? Can the new stylet match, compared to the original used stylet, the resistance against the transverse forces exerted on the stylet during the intrahepatic puncture, or is it even better? And finally, what are the maximum forces that the stylet can deliver during a steering movement, is it able to steer while puncturing through tissue? To answer the following questions an experimental setup is built where parts can be switched in order to do all the experiments with one single base.

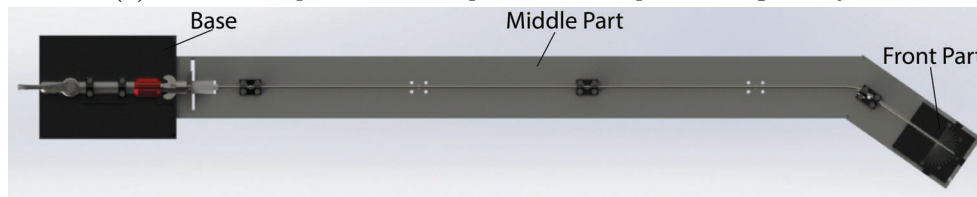
#### Materials

Figure E.1 represents schematic top views of both experimental setups. Both setups exist of three main components as denoted in the figure. Firstly, the base is represented by the black panels at the left where the handle of the stylet is clamped, the steering lever will still have enough freedom to rotate to both sides. The base is made with cut outs in the front wherefore the second component, the middle part, can be clamped into the base. The middle part is different for the experiments with and without stiffening cannula. Since this stiffening cannula has an angle of  $\pm 18$  degrees in the front, the middle part of this setup is also built with a 18 degree angle in front. For the experiments without cannula (only the stylet) a straight middle part is used. The last component in the experimental setup is the front part. This part decides which experiment can be performed. Since these front parts can easily be switched with other ones, it is possible to perform multiple experiments in succession with almost the same setup.

Figure E.1a represents the experimental setup for only the stylet with a straight middle part. Figure E.1b represents the experimental setup for the experiments with the stylet in combination with the pre-bent stiffening cannula. The used materials for the experimental setups are given in the given for each part separately.



(a) Schematic top view of the experimental setup for testing the stylet.



(b) Schematic top view of the experimental setup for testing the stylet in combination with the pre-bent stiffening cannula with an angle of  $\pm 18$  degrees.

**Figure E.1:** In (a) the experimental setup for the stylet. In (b) the experimental setup with the stiffening cannula and stylet.

## Design

All panels to build the parts for the experimental setup are made with a lasercutter. Parts can easily be changed and/or replaced by remaking the necessary parts. With the universal base for the handle, all the experiments can be done after each other by changing the middle part and/or the front part. By removing the middle part the stiffening cannula can be easily slide over the stylet. The other middle part can be placed and the stiffening cannula can be clamped, the experiments for the stylet in combination with the stiffening cannula can now be executed.

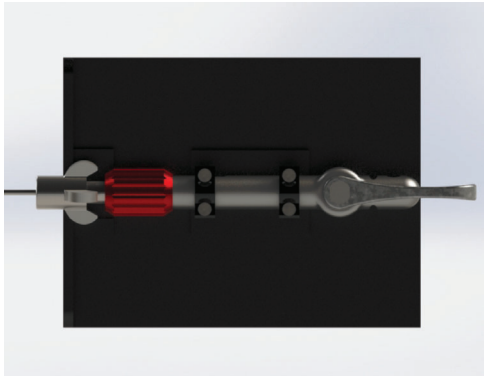
### Base

The base consist of multiple acrylic panels glued together. The handle of the needle has 6 small notches at the sides with a diameter of 5mm. Using this notches, the handle can be clamped easily with M2.5 bolts and nuts. 4 of the 6 notches are used to clamp the needle which is represented by Figure E.2a. The last two notches are not used since the lever must have the ability to steer to its maximum configurations. Figure E.2b shows the front of the base plate with the cut outs, protrusions made in the middle part fits exactly in the cut outs.

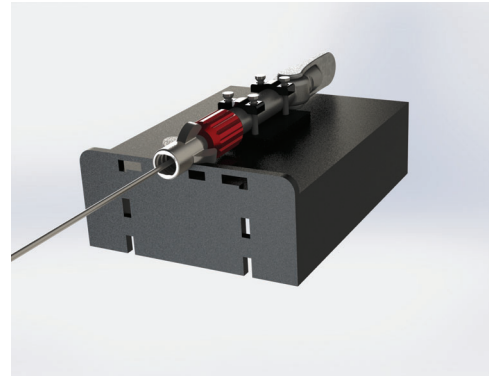
### Materials

The following materials are used to build the base of the experimental setup:

- 3mm acrylic plate;
- Lasercut drawings to cut the panels of the base;
- Lasercut drawings to make the mechanisms to clamp the handle to the base;
- Acrylic glue;
- 2 clamp mechanism;
- 4 x 2.5mm x 10 mm bolts and nuts.



(a) Top view of the base part of the experimental setup. The handle is clamped with 4 M2.5 bolts.



(b) Front view of the base part of the experimental setup. Different middle parts can be clamped into the cut outs.

**Figure E.2:** The base for the experimental setup, in (a) a top view, in (b) a front view.

### Middle part

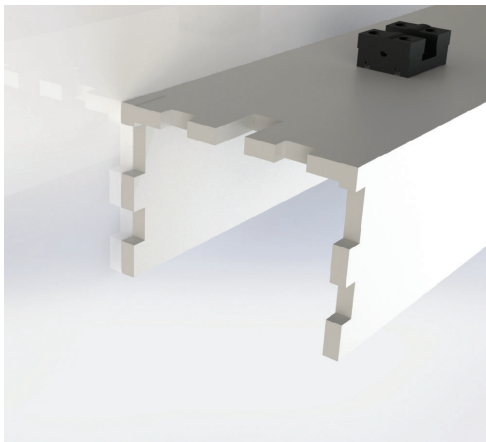
The middle part of the experimental setup is also build from acrylic panels. One side of the middle part, represent by Figure E.3a, have protrusions which fits exactly into the cut outs of the base. Experiments with and without the stiffening cannula can be done by changing the middle part. The middle part for the stiffening cannula contains an angle of  $\pm 18$  degrees in front which follows the shape of the stiffening cannula.

Both middle parts have 5 points on the top plate where clamping mechanisms can be attached. Figure E.3b shows the clamp mechanism. These mechanisms can clamp the stiffening cannula but also the stylet on itself. In Figure E.1 only three of the five clamp mechanisms are attached on the top plate. In the experimental setup for the stylet without stiffening cannula the last clamp is made at the same position where the stiffening cannula ends when the stylet is pushed through.

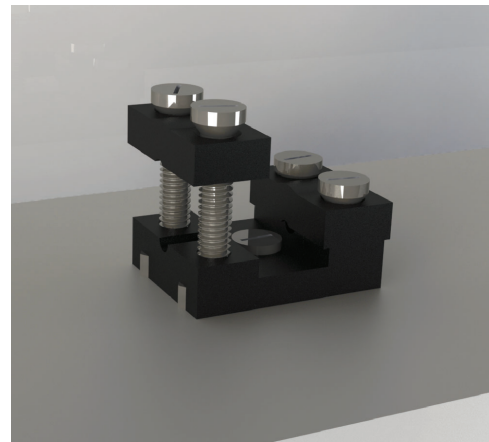
### Materials

The following materials are used to build the middle part of the experimental setup:

- 3mm acrylic plate;
- Lasercut drawings to cut the panels of the middle part;
- Lasercut drawings to make the mechanisms to clamp the stylet/stiffening cannula to the middle part;
- Acrylic glue;
- 10 clamp mechanisms (for both setups);
- 50 x 2.5mm x 10 mm bolts with nuts (for both setups).



(a) The protrusions in the middle part. These protrusions can attach the middle part to the base of the experimental setup.



(b) The clamp mechanisms used to clamp the stiffening cannula or the stylet. These mechanisms can be tighten by four M2.5 bolts.

**Figure E.3:** The middle part of the experimental setup, in (a) the protrusion to attach to the base, in (b) a clamp mechanism to clamp the stiffening cannula/needle.

### Front part

By only changing the front part, three different experiments can be done in succession for the stylet or the stylet in combination with the stiffening cannula. Figure E.4 shows a schematic overview of the three different front parts.

The front part for measuring the steering angle is a single acrylic plate with a protractor engraved. This plate is aligned so the steering angle is zero degrees if the lever is at his unsteered configuration as shown in Figure E.4a.

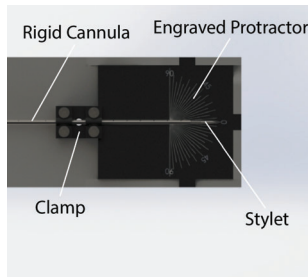
The front part for the joint stiffness characteristics consist of a acrylic base plate with slots. Two 5mm plates are glued together, the under plate has bigger slot where the M5 nuts fits in. The linear stage can be attached to the base plate by M5 x 10 mm bolts. Slots have been used so the linear stage can be moved a little to the left and right to perfectly align the linear stage to the tip of the stylet. Since the corner profile (white part on top of the linear stage in the Figure) contain two slots, one can be used to attach the profile to the linear stage and one to attach the Futek 2lb (9N) force sensor. To measure the forces while the tip of the stylet is pushed, the force sensor must contain a M3 bolt which make contact with the tip while it is in its unsteered configuration. An overview of the front plate is given in Figure E.4b.

The third front part contains acrylic plates and the force sensor. With this setup the forces are measured while the stylet presses (in a steering movement) against the Futek 2lb (9N) force sensor. The force sensor can slightly move to the left and to the right so it can be perfectly aligned. The 3mm bolt from the force sensor to the stylet can be adjusted so it makes contact with the stylet while the stylet is at its unsteered configuration. Figure E.4c represents the front part for measuring the maximum forces exerted by the tip.

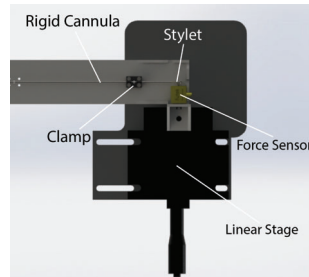
### Materials

The following materials are used to build the three front parts of the experimental setup:

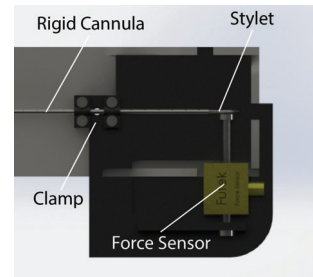
- 3mm and 5mm acrylic plate;
- Lasercut drawings to build the front part;
- Acrylic glue;
- A ThorLabs XR25C linear stage;
- A Futek 2lb (9N) force sensor;
- A corner profile with two perpendicular slots for a M5 and M3 bolt;
- 2 x M3 x 5 mm bolts;
- 5 x M5 x 10 mm bolts with nuts;
- 1 x M3 x 10 mm ring bolt;



(a) Front section to measure the steering angle of the new steerable stylet.



(b) Front section with a linear stage to find joint stiffness characteristics.



(c) Front section to measure the forces which the stylet can exert while steering.

**Figure E.4:** The three different front sections for the experiments, in (a) a protractor the measure the the angle for the steerable stylet. In (b) the front section with a force sensor in combination with a linear stage. In (c) the front section with a force sensor wherefore the forces during a steering movement can be measured.

## Experiments

Three experiments have been done with this experimental setup. The purpose, experimental setup, methods, discussion and conclusion for each experiment can be found in Chapter 4. All the experiments are performed for the stylet and the combination of the stylet with the stiffening cannula:

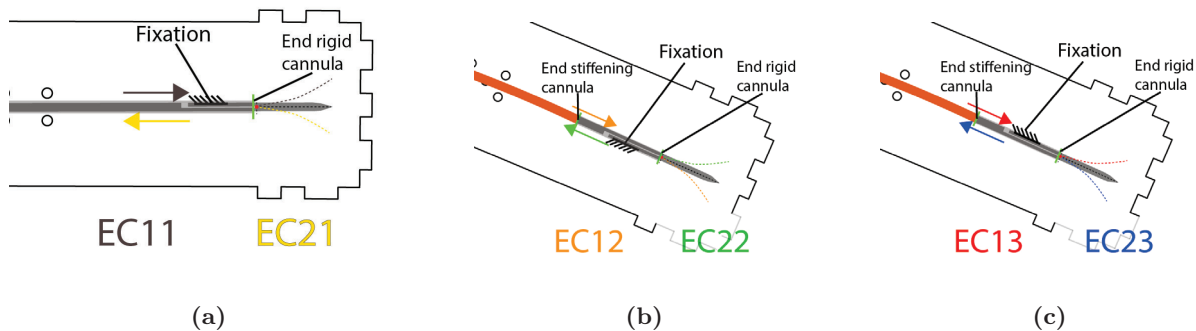
- TIPS Stylet - Maximum Steering Angle;
- TIPS Stylet - Joint Stiffness;
- TIPS Stylet - Force Exerted by Tip.

### Orientation

All experiments are done with two different orientations of the stylet to conclude if the orientation of the fixation will influence the measurements. In the experiments the fixation is orientated to the left and right side. The differences between the orientations are explained by schematic overviews in the figures below.

#### Experiment 1: Maximum Steering Angle

In the steering angle experiment for only the stylet the orientation will not make any influence since the stylet is able to steer in both directions where the steering movement is made with a push and a pull transmission. Still, the orientation is denoted to compare the results with the other experiments more easily. For the experiments with the stiffening cannula the angle in the pre-bent stiffening cannula can have influence on the steering characteristics of the stylet. To test this, the experiments are done with the fixation to the left and to the right. In Figure E.5 all three different setups are shown. The used colors in these picture corresponds to the results which are shown in Figure 4.7.



**Figure E.5:** Schematic overviews of the different experimental setups. In (a) the setup for the stylet without the cannula. In (b) the setup with cannula with the fixation to the right and in (c) the setup with the fixation to the left.

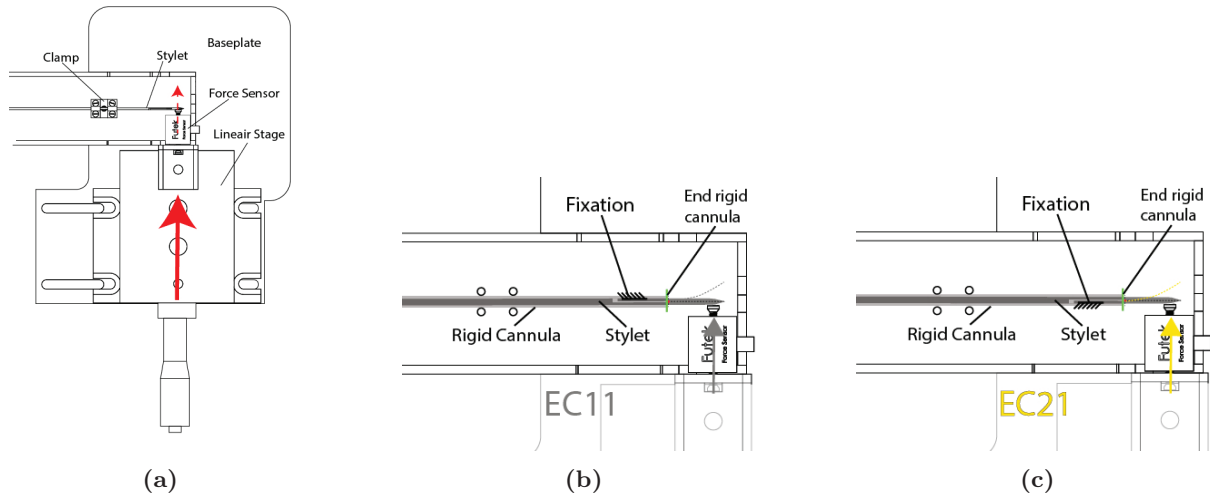
In Table E.1 all different experiments are summarized. Each experimental condition (EC) is randomly done 5 times ( $n = 5$ ). Experiments will be done with only the stylet (St) and with stylet and stiffening cannula (St + Can). During the experiments with cannula the fixation is orientated to the right (R) or left (L) side.

**Table E.1:** The experimental conditions for the maximum steering angle experiment.

$n = 5$	L	R	L
	St	St + Can	St + Can
Push	EC11	EC12	EC13
Pull	EC21	EC22	EC23

### Experiment 2: Joint Stiffness

In the second experiment the joint stiffness will be measured for the original stylet, the steerable stylet and the steerable stylet with cannula in both orientations. Figure E.6a shows a schematic overview of the experimental setup. The linear stage will push the tip of the stylet to one side (red arrow). Figure E.6b and E.6c shows both orientations which are used in the experiments with only the stylet, in Figure E.6b the fixation is to the left, in Figure E.6c is the fixation to the right side of the setup. The setups of the experiments with the stiffening cannula looks similar to these. The used colors in the figures corresponds to the colors in the results shown in Figure 4.8.



**Figure E.6:** Schematic overviews of the experimental setup and its orientations. In (a) the setup where the linear stage will push the stylet to one direction during the measurements. In (b) the setup for the stylet without cannula with the fixation to the left side and in (c) the setup for the stylet without the cannula with the fixation at the right side. The setups for the experiments with the stiffening cannula looks similar.

A summarize of the different experimental conditions are summarized in Table E.2. All experiments will be done 5 times for the steerable stylet (SS) and the steerable stylet with stiffening cannula (SSC) in both orientations. Besides this, the experiment is also done 5 times for the original stylet without (OS) and with stiffening cannula (OSC). For those experiments there is no difference in orientation since there is no fixation in the stylet.

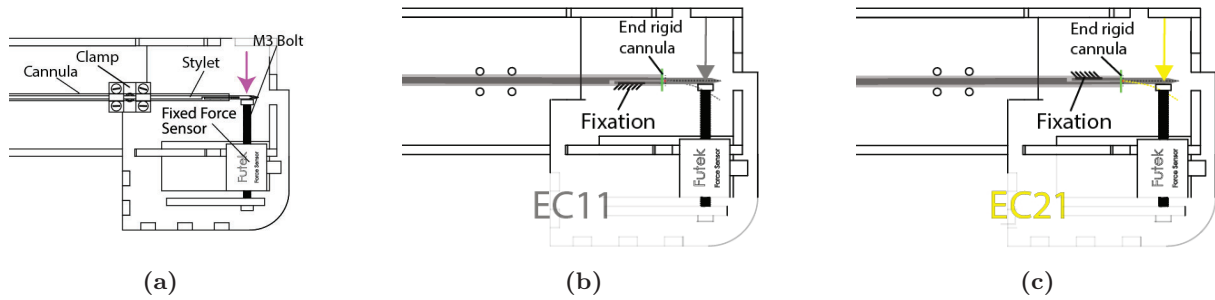
**Table E.2:** Experimental conditions for the joint stiffness experiment. Both original and steerable stylet are tested in combination with the stiffening cannula.

n = 5	SS	SSC	OS	OSC
L	EC11	EC13		
R	EC21	EC22		
-			EC33	EC34



### Experiment 3: Force Exerted By Tip

The third experiment will look at the maximum force what the stylet can deliver while making a steering movement. These experiments are performed with almost the same setups as the previous experiments. Now, the front part will contain a fixed Futek 2Lb (9N) force sensor. A bolt connected to the sensor can be adjusted to make contact with the tip of the stylet in an unsteered configuration. The forces are measured while the transmission makes a push movement (fixation to the right) and for the pull movement (fixation to the left). Both experiments are done for the stylet and the stylet with stiffening cannula. Figure E.7a shows a schematic overview of the front part where the stylet and fixed force sensor are mentioned. Figure E.7b and E.7c shows two different orientations for the experiments with only the stylet. Both orientations are also done in the experiments for the stylet with stiffening cannula. The used colors corresponds to the colors used in the results shown in Figure 4.9.



**Figure E.7:** Schematic overviews of the experimental setup and its orientations. In (a) the setup where the stylet will be pushed through the fixed force sensor. In (b) the setup for the stylet without the cannula with the fixation to the left side and in (c) with the fixation to the right side. The setups for the experiments with the stiffening cannula looks similar.

Table E.3 shows the different experimental conditions for the Force Exerted By Tip experiments. Experiments are done with the steerable stylet (SS) and the steerable stylet with stiffening cannula (SSC). The names of the experimental conditions corresponds to the names of the other experiments wherefore it is easier to compare the results between the different experiments afterwards.

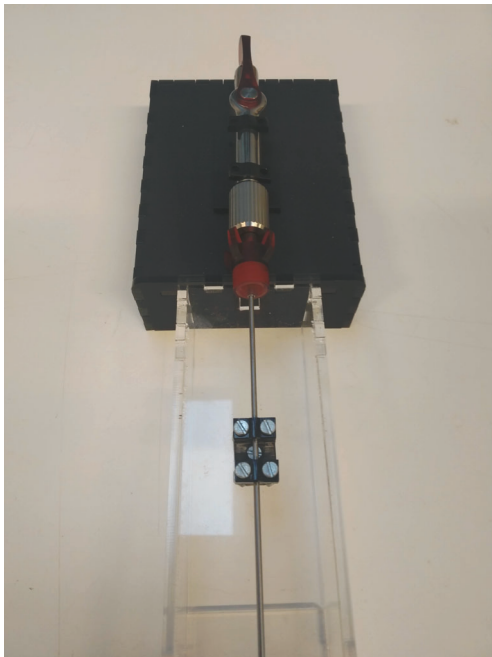
**Table E.3:** Experiments to define the forces exerted by the tip of the stylet.

<b>n = 5</b>	<b>SS</b>	<b>SSC</b>
<b>R</b>	EC11	EC12
<b>L</b>	EC21	EC23

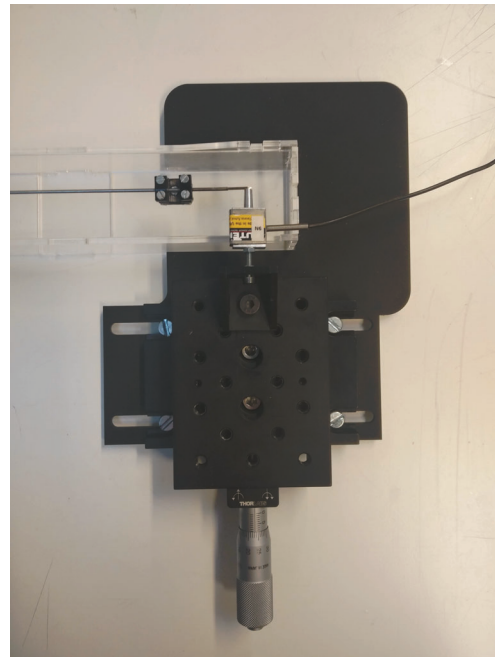
## Conclusion

With the universal base in this setup it is easy to evaluate the steerable stylet with the three different experiments, with and without the stiffening cannula. By doing the experiments with the two different orientations, the influence of the angle in the pre-bent stiffening cannula can be obtained and compared. From the first experiment a conclusion can be drawn about the steering ability in both push and pull translations in the transmission. In the second experiment, the joint stiffness experiment, a conclusion can be made about the stiffness of the steerable stylet compared to the original stylet to answer the question if the steerable stylet is better resistant against the lateral forces and therefore deflection. With the third experiment a conclusion can be made about the strength of the transmission and the joint mechanism. Is the transmission strong enough to steer the tip even when pressure is applied in the form of lateral forces. In other words, is the steerable stylet able to steer while the tip is already in tissue.

With this experimental setup the mechanical characteristics for the steerable stylet could be measured. Since the middle part and the front part can be disconnected from the base, it is even possible to do in the future more experiments with the same base.



(a) The base (black) and middle part (transparent) with the stylet attached to it.



(b) Front section with a linear stage and force sensor to find the joint stiffness characteristics.

## F | Data from Experiments

### Experimental Setup: Force Sensor

For the Displacement-Force experiment and Maximum Force experiment a Futek 2lb (9N) force sensor is used. The force sensor is connected to a computer. The voltage of the sensor can be read with a LabJack controller and the software LJStreamM on the computer. The more force the sensor receives, the higher the voltage. To do accurate measurements, the force sensor has been calibrated first. This is done by hanging weights of 0 to 300 grams in steps of 50 grams on the force sensor. The voltage of the sensor is read after each step. This measurements are done three times. Since the only force on the hanging weight is the gravity, the factor voltage-force can be calculated. In Figure F.1 the data set to calibrate the force sensor is shown. Here the force of the hanging weights are calculated by:

$$Force[N] = Weight[kg] \cdot 9,81[m/s^2] \quad (F.1)$$

For the voltage the  $\Delta$  voltage is measured by looking between the difference between the two successive steps. From the three measurements the average voltage  $V$ ,  $\Delta V$ , and the cumulative voltage  $C_v$  is calculated

The voltage-force factor is calculated with:

$$Factor[N/v] = Force[N]/C_v[v] \quad (F.2)$$

From all the factors in the last column the average value is taken to use as the final factor for the experiments.

22-11-2018		Calibration Futek 2lb (9N) Force Sensor									
Gram	Force [N]	Measurement 1		Measurement 2		Measurement 3		Average			Factor
		Voltage [v]	$\Delta V$ [v]	Voltage [v]	$\Delta V$ [v]	Voltage [v]	$\Delta V$ [v]	Voltage [v]	$\Delta V$ [v]	$C_v$ [v]	Fac [N/v] = F[N] / V[v]
0	0	-0,0986	0,5726	-0,097	0,572	-0,0972	0,5722	-0,0976	0,5723	0,0000	0,0000
50	0,4905	0,474	0,576	0,475	0,574	0,475	0,575	0,4747	0,5750	0,5723	0,8571
100	0,981	1,05	0,574	1,049	0,576	1,05	0,574	1,0497	0,5747	1,1473	0,8551
150	1,4715	1,624	0,573	1,625	0,575	1,624	0,576	1,6243	0,5747	1,7219	0,8546
200	1,962	2,197	0,578	2,2	0,575	2,2	0,575	2,1990	0,5760	2,2966	0,8543
250	2,4525	2,775	0,575	2,775	0,575	2,775	0,585	2,7750	0,5783	2,8726	0,8538
300	2,943	3,35		3,35		3,36		3,3533		3,4509	0,8528
										<b>FACTOR</b>	<b>0,8546</b>

**Figure F.1:** All measured data during the calibration of the Futek 2lb (9N) force sensor.

### Experiment 1: Maximum Steering Angle

All data to find the maximum steering angle of the stylet are shown in Figure F.2. All photos with the 0° line, the 90° line and the line from the rotation point to the tip of the stylet are shown. From this lines first the angle between the 0° line and 90° line was measured to reduce the margin of error. Afterwards, the angle between the 0° line and the line through the rotation point to the tip were measured and adjusted with the following equation:

$$\text{Angle [degrees]} = \text{Measured Angle} / (\text{Real 90 degrees angle}/90) \tag{F.3}$$

All vector lines are drawn in Adobe Illustrator after which the angles are measured in Solidworks. The final results are shown in a bar chart in Chapter4.1.1.

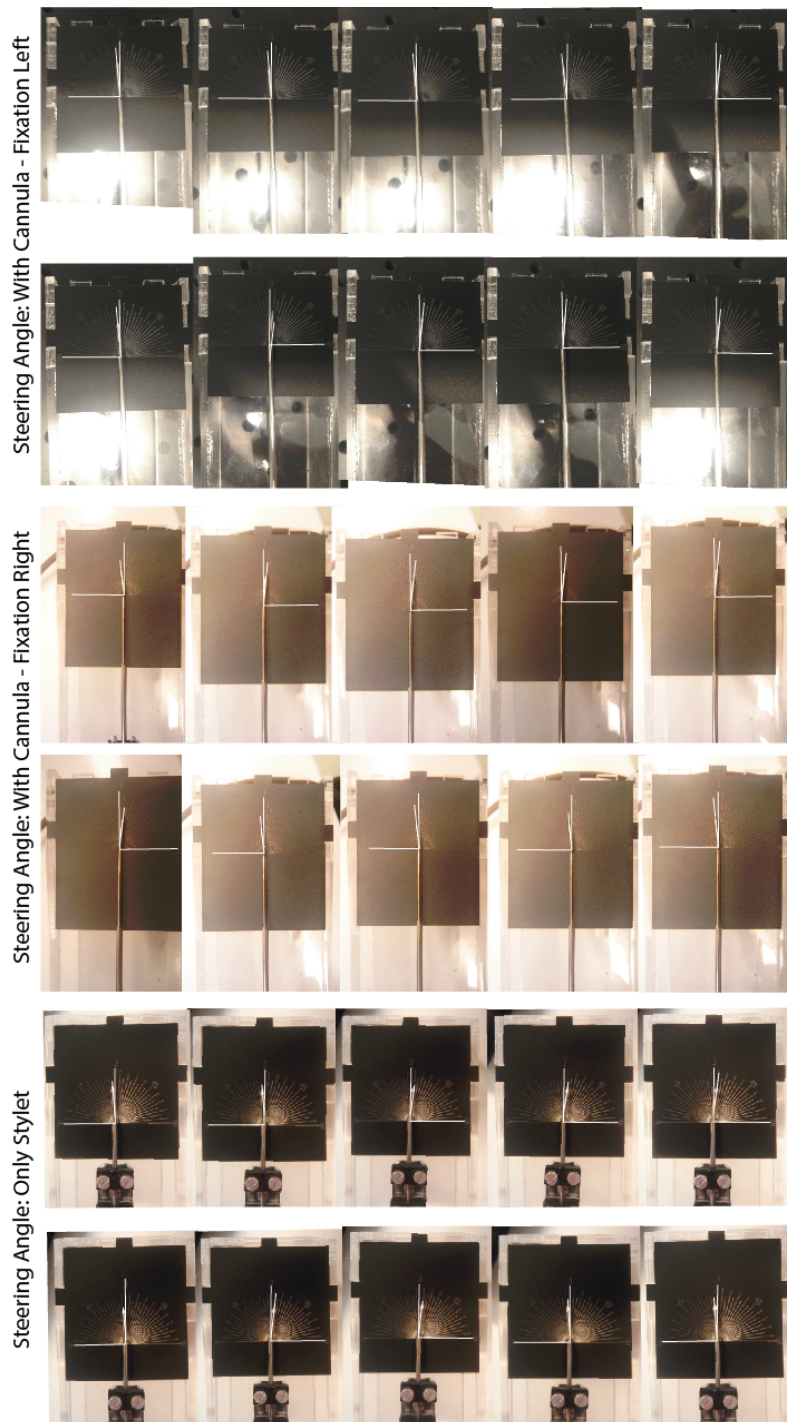


Figure F.2: All measured data during the steering angle experiment.

**Experiment 1**  
11-12-2018

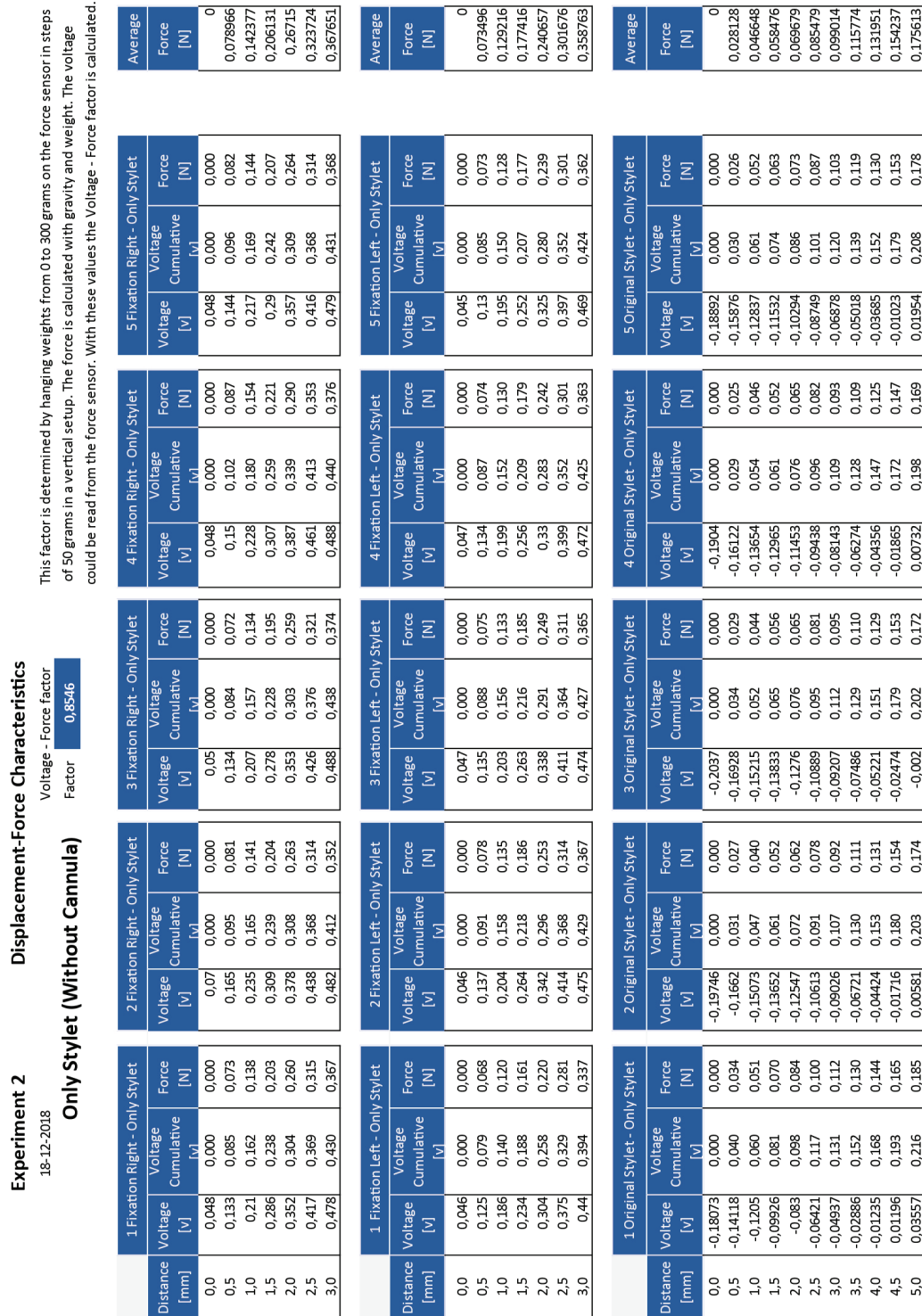
**Steering Angle Stylet**

Push Transmission - Only Stylet															
Measurement #	1			2			3			4			5		
	Real 90 degree Angle [degrees]	Measured [degrees]	Angle [degrees]	Real 90 degree Angle [degrees]	Measured [degrees]	Angle [degrees]	Real 90 degree Angle [degrees]	Measured [degrees]	Angle [degrees]	Real 90 degree Angle [degrees]	Measured [degrees]	Angle [degrees]	Real 90 degree Angle [degrees]	Measured [degrees]	Angle [degrees]
Start	0	0	0	0	0	0	0	0	0	0	0	0	0	0	0
Angle [degrees]	90,54	4,15	4,13	90,11	4,30	4,29	91,08	4,18	4,13	90,00	3,59	3,59	91,35	5,02	4,95
Pull Transmission - Only Stylet															
Start	0	0	0	0	0	0	88,89	7,2	7,29	89,68	7,15	7,18	89,83	0	0
Angle [degrees]	89,4	6,47	6,51	90,19	6,53	6,52									6,88
Fixation Right - Push Transmission - With Cannula															
Measurement #	1			2			3			4			5		
	Real 90 degree Angle [degrees]	Measured [degrees]	Angle [degrees]	Real 90 degree Angle [degrees]	Measured [degrees]	Angle [degrees]	Real 90 degree Angle [degrees]	Measured [degrees]	Angle [degrees]	Real 90 degree Angle [degrees]	Measured [degrees]	Angle [degrees]	Real 90 degree Angle [degrees]	Measured [degrees]	Angle [degrees]
Start	0	0	0	0	0	0	0	0	0	0	0	0	0	0	0
Angle [degrees]	90,05	7,71	7,71	89,66	5,73	5,75	90,46	7,28	7,24	90,69	6,45	6,40	90,16	6,05	6,04
Fixation Right - Pull Transmission - With Cannula															
Start	0	0	0	0	0	0	88,87	5,56	5,63	89,4	5,09	5,12	89,46	0	0
Angle [degrees]	89,46	6,87	6,91	89,59	5,42	5,44									5,75
Fixation Left - Push Transmission - With Cannula															
Measurement #	1			2			3			4			5		
	Real 90 degree Angle [degrees]	Measured [degrees]	Angle [degrees]	Real 90 degree Angle [degrees]	Measured [degrees]	Angle [degrees]	Real 90 degree Angle [degrees]	Measured [degrees]	Angle [degrees]	Real 90 degree Angle [degrees]	Measured [degrees]	Angle [degrees]	Real 90 degree Angle [degrees]	Measured [degrees]	Angle [degrees]
Start	0	0	0	0	0	0	0	0	0	0	0	0	0	0	0
Angle [degrees]	88,8	4,85	4,92	90,11	4,87	4,86	89,96	4,92	4,92	88,79	4,98	5,05	90,94	7,22	7,15
Fixation Left - Pull Transmission - With Cannula															
Start	0	0	0	0	0	0	0	0	0	0	0	0	0	0	0
Angle [degrees]	88,9	6,35	6,43	90,42	6,19	6,16	90,46	5,62	5,59	91,16	6,21	6,13	90,17	6,31	6,30

**Figure F.3:** All measured data during the steering angle experiment.

## Experiment 2: Joint Stiffness

The data sets for the displacement - force characteristics of the stylet are shown in the figures below. Figure F.4 shows the measurements for the original non-steerable stylet without cannula, the measurements for the steerable stylet without cannula with the fixation orientated to the left and right. Figure F.5 shows the measurements for the original stylet and the steerable stylet with the cannula. Where for all measurements the fixation is both orientated to the left and right.



**Experiment 2**  
18-12-2018

**Displacement-Force Characteristics**

Voltage - Force factor  
Factor **0.8546**

**With Cannula**

This factor is determined by hanging weights from 0 to 300 grams on the force sensor in steps of 50 grams in a vertical setup. The force is calculated with gravity and weight. The voltage could be read from the force sensor. With these values the Voltage - Force factor is calculated.

Distance [mm]	1 Fixation Right - With Cannula		2 Fixation Right - With Cannula		3 Fixation Right - With Cannula		4 Fixation Right - With Cannula		5 Fixation Right - With Cannula		Average Force [N]
	Voltage [v]	Cumulative [v]	Voltage [v]	Force [N]	Voltage [v]	Force [N]	Voltage [v]	Force [N]	Voltage [v]	Force [N]	
0.0	0.05	0.000	0.059	0.000	0.054	0.000	0.051	0.000	0.056	0.000	0
0.5	0.111	0.061	0.122	0.063	0.116	0.062	0.115	0.064	0.12	0.064	0.053669
1.0	0.172	0.122	0.178	0.119	0.171	0.117	0.169	0.118	0.174	0.118	0.101527
1.5	0.23	0.180	0.235	0.176	0.221	0.167	0.217	0.166	0.223	0.167	0.146308
2.0	0.28	0.230	0.291	0.232	0.275	0.221	0.268	0.217	0.275	0.219	0.191261
2.5	0.33	0.280	0.35	0.291	0.326	0.272	0.327	0.276	0.333	0.277	0.238606
3.0	0.39	0.340	0.41	0.351	0.405	0.351	0.4	0.349	0.401	0.345	0.296719

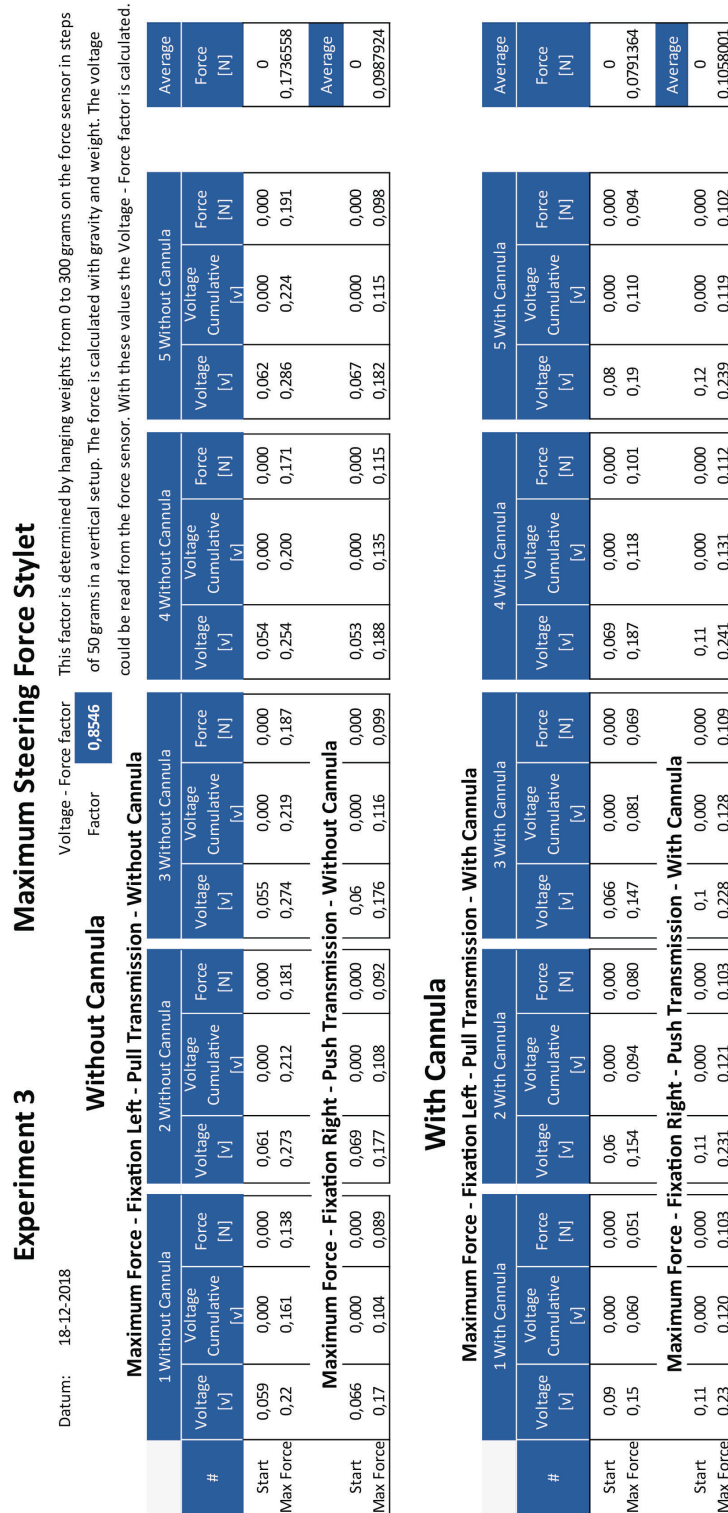
Distance [mm]	1 Fixation Left - With Cannula		2 Fixation Left - With Cannula		3 Fixation Left - With Cannula		4 Fixation Left - With Cannula		5 Fixation Left - With Cannula		Average Force [N]
	Voltage [v]	Cumulative [v]	Voltage [v]	Force [N]	Voltage [v]	Force [N]	Voltage [v]	Force [N]	Voltage [v]	Force [N]	
0.0	0.056	0.000	0.054	0.000	0.056	0.000	0.056	0.000	0.056	0.000	0
0.5	0.107	0.051	0.114	0.060	0.119	0.063	0.12	0.064	0.118	0.062	0.051276
1.0	0.167	0.111	0.182	0.128	0.176	0.120	0.175	0.119	0.177	0.121	0.102382
1.5	0.223	0.167	0.237	0.183	0.228	0.172	0.228	0.172	0.229	0.173	0.148189
2.0	0.281	0.225	0.297	0.243	0.287	0.231	0.279	0.223	0.286	0.230	0.196901
2.5	0.327	0.271	0.343	0.289	0.337	0.281	0.324	0.268	0.343	0.287	0.238606
3.0	0.388	0.332	0.401	0.347	0.392	0.336	0.393	0.337	0.403	0.347	0.290395

Distance [mm]	1 Original Stylet - With Cannula		2 Original Stylet - With Cannula		3 Original Stylet - With Cannula		4 Original Stylet - With Cannula		5 Original Stylet - With Cannula		Average Force [N]
	Voltage [v]	Cumulative [v]	Voltage [v]	Force [N]	Voltage [v]	Force [N]	Voltage [v]	Force [N]	Voltage [v]	Force [N]	
0.0	-0.16353	0.000	-0.1632	0.000	-0.16944	0.000	-0.16447	0.000	-0.16062	0.000	0
0.5	-0.14886	0.015	-0.14481	0.018	-0.15499	0.014	-0.15389	0.011	-0.15336	0.007	0.011169
1.0	-0.12851	0.035	-0.134	0.029	-0.14355	0.026	-0.14664	0.018	-0.14552	0.015	0.021031
1.5	-0.11199	0.052	-0.12444	0.039	-0.13052	0.039	-0.14047	0.024	-0.13857	0.022	0.029957
2.0	-0.10816	0.055	-0.11489	0.048	-0.12109	0.048	-0.13247	0.032	-0.13108	0.030	0.036504
2.5	-0.0997	0.064	-0.10558	0.058	-0.11166	0.058	-0.11823	0.046	-0.11971	0.041	0.045532
3.0	-0.08385	0.080	-0.09508	0.068	-0.10313	0.066	-0.10681	0.058	-0.10905	0.052	0.055266
3.5	-0.07762	0.086	-0.08503	0.078	-0.09224	0.077	-0.09998	0.064	-0.09934	0.061	0.062738
4.0	-0.06897	0.095	-0.074	0.089	-0.08273	0.087	-0.08792	0.077	-0.09042	0.070	0.071312
4.5	-0.0466	0.117	-0.06358	0.100	-0.07092	0.099	-0.07892	0.086	-0.08183	0.079	0.081941
5.0	-0.03921	0.124	-0.05293	0.110	-0.05908	0.110	-0.06174	0.103	-0.07407	0.087	0.091311

**Figure F.5:** All measured data for the displacement-force experiments where the original stylet and the steerable stylet where in combination with the stiffening cannula.

### Experiment 3: Force Exerted By Tip

The experiment for the maximum forces is only done with the steerable stylet since push movements against the force sensor are required by making a steering movement which was not possible with the original stylet. Figure F.6 shows the data sets for the maximum force measured with the fixation orientated to the left and to the right, with and without cannula.







A STEERABLE STYLET FOR THE TRANSJUGULAR  
INTRAHEPATIC PORTOSYSTEMIC  
SHUNT PROCEDURE

D.P. VAN DUIJN [#4003616]

